ICAR

INTERNATIONAL CENTER FOR AGGREGATES RESEARCH

EVALUATION OF SUPERPAVE FINE AGGREGATE ANGULARITY SPECIFICATION

RESEARCH REPORT ICAR – 201-1

Sponsored by the
Aggregates Foundation
for Technology, Research and Education

Technical Report Documentation Page

1. Report No.	2. Government Accession No.	3. Recipient's Catalog No.
ICAR/201-1		

4. Title and Subtitle
EVALUATION OF SUPERPAVE FINE AGGREGATE ANGULARITY SPECIFICATION

5. Report Date
June 2001

6. Performing Organization Code

7. Author(s)
Arif Chowdhury, Joe Button, Vipin Kohale, and David Jahn

8. Performing Organization Report No.
Report No. 201-1

9. Performing Organization Name and Address
Texas Transportation Institute
The Texas A&M University System
College Station, Texas 77843-3135

10. Work Unit No. (TRAIS)

11. Contract or Grant No.
Project No. 404011

12. Sponsoring Agency Name and Address
Aggregates Foundation for Technology, Research, and Education
2101 Wison Blvd, Suite 100
Arlington, VA 22201-3062

13. Type of Report and Period Covered
Final:
June 2001

14. Sponsoring Agency Code

15. Supplementary Notes
Research performed in cooperation with International Center for Aggregates Research and Aggregates Foundation for Technology, Research, and Education.
Research Project Title: Evaluation of Superpave Aggregate Specifications

16. Abstract

The validity of the Superpave fine aggregate angularity (FAA) requirement is questioned by both the owner agencies and the paving and aggregate industries. The FAA test is based on the assumption that more fractured faces will result in higher void content in the loosely compacted sample; however, this assumption is not always true. Some agencies have found that cubical shaped particles, even with 100 percent fractured faces, may not meet the FAA requirement for high-volume traffic. State agencies are concerned that local materials, previously considered acceptable and which have provided good field performance, cannot meet the Superpave requirements.

Researchers evaluated angularity of 23 fine aggregates representing most types of paving aggregates used in the USA using seven different procedures: FAA test, direct shear test, compacted aggregate resistance (CAR) test, three different image analyses, and visual inspection. The three image analyses techniques included Hough Transform at University of Arkansas at Little Rock (UALR), unified image analysis at Washington State University (WSU), and VDG-40 videograder at Virginia Transportation Research Council (VTRC). A small study was performed to evaluate relative rutting resistance of HMA containing fines with different particle shape parameters using the Asphalt Pavement Analyzer (APA).

The FAA test method does not consistently identify angular, cubical aggregates as high quality materials. There is a fair correlation between the CAR stability value and angle of internal friction (AIF) from the direct shear test. No correlation was found between FAA and CAR stability or between FAA and AIF. Fairly good correlations were found between FAA and all three image analysis methods. Some cubical crushed aggregates with FAA values less than 45 gave very high values of CAR stability, AIF, and 'angularity' from imaging techniques. Moreover, the three image analysis methods exhibited good correlation among themselves. A statistical analysis of the SHRP-LTPP (Strategic Highway Research Program-Long-Term Pavement Performance) database revealed no significant evidence relationship between FAA and rutting. This lack of relationship is not surprising since many uncontrolled factors contribute to pavement rutting. The APA study revealed that FAA is not sensitive to rut resistance of HMA mixtures.

Image analysis methods appear promising for measuring fine aggregate angularity. Until a suitable replacement method(s) for FAA can be identified, the authors recommend that the FAA criteria be lowered from 45 to 43 for 100 percent crushed aggregate. Analysis of the FAA versus rutting data should be examined later as the amount of data in the SHRP-LTTP database is expanded.

17. Key Words
fine aggregate angularity, CAR test, Hough Transformation, Unified image analysis, VDG-40,

18. Distribution Statement
No restrictions. This document is available to the public through NTIS:
National Technical Information Service
5285 Port Royal Road, Springfield, Virginia 22161

19. Security Classif.(of this report)	20. Security Classif.(of this page)	21. No. of Pages	22. Price
Unclassified	Unclassified		

Form DOT F 1700.7 (8-72) **Reproduction of completed page authorized**

EVALUATION OF SUPERPAVE FINE AGGREGATE ANGULARITY SPECIFICATION

by

Arif Chowdhury
Engineering Research Associate
Texas Transportation Institute

Joe W. Button
Senior Research Engineer
Texas Transportation Institute

Vipin Kohale
Graduate Research Assistant
Texas Transportation Institute

and

David W. Jahn
Director of Product Development
Martin Marietta Technologies

Report No. 201-1
Project No. ICAR 201
Research Project Title: Evaluation of Superpave Aggregate Specifications

Sponsored by the

International Center for Aggregate Research

May 2001

TEXAS TRANSPORTATION INSTITUTE
The Texas A&M University System
College Station, Texas 77843-3135

DISCLAIMER

The contents of this report reflect the views of the authors, who are responsible for the facts and the accuracy of the data presented herein. The contents do not necessarily reflect the official view or policies of the International Center of Aggregate Research (ICAR), Texas Transportation Institute (TTI), or Texas A&M University. The report does not constitute a standard, specification, or regulation, nor is it intended for construction, bidding, or permit purposes.

ACKNOWLEDGMENTS

Financial support of this research project by the Aggregates Foundation for Technology, Research, and Education (AFTRE) is gratefully acknowledged.

Mr. David Jahn of Martin Marietta Technologies served as the primary technical contact for the AFTRE. His guidance and advice were instrumental in developing and completing this project. Mr. Richard C. Meininger also provided valuable advice to the researchers.

Special thanks are extended to Vulcan Materials Company, Martin Marietta Technologies, and Fordyce Materials Company for providing several hundred pounds of aggregates at no cost to the project. Several agencies provided testing of fine aggregates at no cost to the project; these include: University of Arkansas at Little Rock, Washington State University, Virginia Transportation Research Council, and Horiba Instruments, Incorporated. Accomplishing this work would have been impossible without the participation of these agencies.

Twenty-three state Departments of Transportation (DOT) sent fine aggregate samples for testing. The researchers appreciate their help.

TABLE OF CONTENTS

CHAPTER		Page
LIST OF FIGURES		vii
LIST OF TABLES		xi
I	INTRODUCTION	1
	BACKGROUND	1
	STATEMENT OF PROBLEM	2
	OBJECTIVES	4
II	LITERATURE REVIEW	7
	BACKGROUND	7
	CHARACTERIZATION OF MATERIAL PROPERTIES	9
	NAA Flow Test Method	9
	Flow Rate Method	11
	ASTM Method D-3398	12
	Direct Shear Test	13
	Compacted Aggregate Resistance (CAR)	13
	New Zealand Test	14
	Fractal Method	14
	Hough Transform	15
	Image Analysis at Washington State University	15
	Image Analysis Using VDG-40 Videograder	15
	WipShape	16
	Commercially Available Software/Hardware	16
	Other Methods	16

TABLE OF CONTENTS
(Continued)

CHAPTER		Page
III	EXPERIMENTAL PLAN	19
	EVALUATION OF FINE AGGREGATE ANGULARITY TEST	19
	Material Selection and Acquisition	20
	Fine Aggregate Angularity Test	20
	Direct Shear Test	22
	Compacted Aggregate Resistance Test	23
	Visual Evaluations of Aggregate Shape and Angularity	24
	Image Analysis by Hough Transform Method	25
	Image Analysis by Washington State University Method	33
	Image Analysis Using VDG-40 Videograder	37
	Surface Area Analyzer for Measuring Angularity	41
	FAA VERSUS PERFORMANCE IN THE SHRP-LTPP DATABASE	42
	EFFECTS OF FINE AGGREGATES ON RUTTING RESISTANCE	42
	Superpave Volumetric Mix Design	42
IV	RESULTS AND DISCUSSION	45
	LABORATORY TEST RESULTS	45
	FAA Test	45
	Direct Shear Test	47
	Compacted Aggregate Resistance Test	48
	Hough Transform Method	51
	Image Analysis at WSU	53
	Image Analysis at VTRC	56
	Comparison Between the Different Image Analyses	59
	Comparison of FAA with Other Test Results	62
	Visual Inspection	72
	Surface Area Analysis	76

TABLE OF CONTENTS

(Continued)

CHAPTER **Page**

FAA VERSUS PERFORMANCE IN THE SHRP-LTPP DATABASE..........................78
RUTTING RESISTANCE EVALUATION WITH APA 86
Specimen Preparation and Testing...88
APA Rut Depth and Measures of Angularity 89
V CONCLUSIONS AND RECOMMENDATIONS 93
CONCLUSIONS...94
RECOMMENDATIONS...96
REFERENCES 99
APPENDIX A - FINE AGGREGATE DATABASE...105
APPENDIX B - TYPICAL TEST OUTPUT 113
APPENDIX C - CAR TEST PROCEDURE AND SUPPLEMENTAL CAR
TEST RESULTS...121

LIST OF FIGURES

FIGURE		Page
1	Fine Aggregate Angularity Test Setup	21
2	Shear Box for Direct Shear Test	22
3	Direct Shear Test Machine	23
4	Compacted Aggregate Resistance Test Setup	24
5	Microscope Used for Visual Inspection	25
6	Hough Transform Data Collection Hardware	27
7	Particle Outline and Convex Hull for T-index Calculation	28
8	Particle Outline (Left) and Its Hough Transform (Right)	30
9	Fast Fourier Transform of S Function	31
10	Neural Network Processing Unit	33
11	Illustration of the Effect of Erosion-Dilation and Fractal Operations	35
12	VDG-40 Videograder	38
13	Principle of the VDG-40 Videograder	39
14	Principle of Image Capturing and Processing	40
15	CAR Stability at Different Moisture Contents	50
16	Log of CAR Value Versus Surface Parameter (WSU)	55
17	Relation Between Log of CAR Value and Fractal Length (WSU)	55
18	Relation Between Log of CAR Value and Form Factor (WSU)	56
19	Log of CAR Value Versus Slenderness Ratio (VTRC)	58
20	Log of CAR Value Versus Flatness Factor (VTRC)	58
21	K-index (Hough Transform) Versus Surface Parameter (WSU)	59

LIST OF FIGURES (Continued)

FIGURE Page

22 K-index (Hough Transform) Versus Fractal Length (WSU) 60

23 K-index (Hough Transform) Versus Form Factor (WSU) 60

24 K-index (Hough Transform) Versus Slenderness Ratio (VTRC) 61

25 Relation Between Logarithmic Value of CAR Stability and FAA 62

26 Relation Between Angle of Internal Friction and FAA 63

27 Relation Between Logarithmic Value of CAR Stability and Angle of Internal Friction ... 63

28 CAR Values of Selected Aggregates 65

29 K-index Versus FAA Value 66

30 Relation Between K-index and Logarithmic Value of CAR Stability 67

31 Relation Between K-index and Angle of Internal Friction 68

32 FAA Value Versus Surface Parameter (WSU) 69

33 FAA Value Versus Fractal Length (WSU) 69

34 Relationship Between FAA Value and Form Factor (WSU) 70

35 FAA Value Versus Slenderness Ratio (VTRC) 70

36 Correlation Between Water Absorption and Surface Area 77

37 Average Rutting of All 160 Points and Corresponding FAA Value 79

38 Residual Plot for Rutting Versus FAA 79

39 Average Rutting Depth Versus FAA for Asphalt Content Less than or Equal to 5.5 % 82

LIST OF FIGURES (Continued)

FIGURE Page

40 Average Rutting Depth Versus FAA for Asphalt Content Greater than 5.5 % 82

41 Average Rutting for Aggregate Passing #200 Sieve is Equal to or Less than 4 % 84

42 Average Rutting for Aggregate Passing #200 Sieve is Greater than 4 %..........................84

43 Average Rutting for Aggregate Passing #4 Sieve is Equal to or Less than 56 % 85

44 Average Rutting for Aggregate Passing #4 Sieve is Greater than 56 %............................85

45 Aggregate Gradation Used in Mix Design..87

46 Rut Depth Measured by APA for Different Mixtures 88

47 APA Rut Depth Versus FAA..89

48 APA Rut Depth Versus Angle of Internal Friction..90

49 APA Rut Depth Versus CAR Value 90

50 APA Rut Depth Versus WSU Fractal Length..92

51 APA Rut Depth Versus VTRC Slenderness Ratio 92

B1 A Typical Shearing Stress vs Normal Stress Chart for Angle of Internal Friction Calculation 114

B2 A Typical CAR Test Output 115

B3 A Typical Chart for Calculating Median of K-indices 118

B4 A Typical Output VDG-40 Flat & Elongated Worksheet 119

B5 A Typical Output VDG-40 Aggregate Gradation Worksheet 120

C1 CAR Values of Different Fine Aggregate Materials 127

C2 Sensitivity of CAR Stability to Varying Amounts of Natural Rounded Sand.................128

C3 Sensitivity of CAR Stability to Changes in Gradation 129

C4 Sensitivity of CAR Stability to Changes in Gradation 130

C5 The CAR Test can Differentiate Between like FAA Values 131

LIST OF TABLES

TABLE Page

1 Superpave Fine Aggregate Angularity Requirements 2
2 Fine Aggregate Angularity Test Data 46
3 Direct Shear Test Data 48
4 Compacted Aggregate Resistance Test Data. 49
5 Hough Transform Results 52
6 WSU Image Analysis Test Results 53
7 VTRC Image Analysis Test Results 57
8 Ranking of Each Sample in Descending Order 71
9 Visual Inspection Results..73
10 Summary of All Tests Results 74
11 Surface Area and Water Absorption Data 77
12 ANOVA for All Rutting and FAA Data Points 80
13 ANOVA of FAA Values Versus Rutting Data for Asphalt Content Less Than or Equal to 5.5%. 81
14 ANOVA of FAA Vales Versus Rutting Data for Asphalt Content Greater Than 5.5% 81
15 Aggregate Angularity Measurement of Fine Aggregates 86
16 Mixture Design Properties for Different Mixtures 87
A1 Description of All Fine Aggregates Collected..107
B1 A Typical Hough Transform Output for K-index Calculation 116

CHAPTER I

INTRODUCTION

BACKGROUND

From 1987 to 1993, the Strategic Highway Research Program (SHRP) implemented a very ambitious research program to improve the streets and highways in the USA. SHRP administered a $50 million research effort on asphalt binder and hot mix asphalt (HMA) pavements. Superpave^{TM} was the final product of the SHRP research effort. Superpave is a state-of-the-art performance-based HMA mixture design and analysis system that specifies acceptance criteria for asphalt, aggregate, and the asphalt-aggregate mixture. The SHRP research effort mainly concentrated on properties and testing of asphalt binder. Little time and money was devoted to the study of the contribution of aggregates to pavement performance (*1*). Although several new binder tests were developed by SHRP, no new test methods were developed for specifying aggregate for the HMA mixture. Yet, SHRP researchers were required to produce aggregate specifications and, under the circumstances, they did a very good job on this task. However, some aspects of the Superpave aggregate specifications are not universally accepted by the industry. For example, the validity of the fine aggregate angularity (FAA) test procedure and criteria are questioned by both the owner agencies (Departments of Transportation) and the pavement and aggregate industries.

STATEMENT OF THE PROBLEM

Superpave adopted the National Aggregate Association (NAA) Flow Test, Method A, to determine the fine aggregate angularity (FAA). This test is an indirect method for estimating fine aggregate angularity and texture. This standard procedure is designated as ASTM C-1252 Method A or AASHTO T-304. The goal of this requirement is to ensure that the fine aggregate has adequate internal friction to provide rut-resistance to an HMA mixture (*2*). In this test method, fine aggregate smaller than #8 sieve size (2.36-mm) with a particular gradation is allowed to flow into a calibrated cylinder from a standard funnel. Voids in the uncompacted fine aggregate in the cylinder, expressed as a percentage, are referred to as the fine aggregate angularity. The FAA requirement varies depending on the traffic level and the proximity of the layer to the pavement surface. Table 1 gives the FAA requirements for Superpave (*2*).

TABLE 1 Superpave Fine Aggregate Angularity Requirements

Traffic, millions of ESALs*	**FAA Requirement at Given Depth from Surface**	
	< 100 mm	> 100 mm
< 0.3	-	-
0.3 to < 3	40	40
3 to < 10	45	40
10 to < 30	45	40
. 30	45	45
Note: The criteria are presented as a minimum percentage air voids in the loosely compacted fine aggregate. * Equivalent Single Axle Load		

The FAA test is based on the assumption that more fractured faces will result in higher void content in the loosely compacted sample; however, this assumption is not always true. The aggregate industry has found that cubical shaped particles, especially from impact type crushers and even with 100 percent fractured faces, usually will not meet the FAA requirement for high-volume traffic (*1, 3*). Cubical particles may behave similarly to rounded aggregate in the FAA test procedure, thus fitting close together to form a dense configuration when poured into the cylinder. As a result, the uncompacted voids of cubical angular particles often range between 43 and 46 percent (*1*). Some flaky and/or elongated particles, even with low angularity, will have significantly higher uncompacted voids because the sharp points of the elongated particles prevent them from reaching a dense configuration (*4*). Some rounded natural sands with demonstrated poor field performance in HMA may yield uncompacted voids as high as 43 percent (*1*).

Cubical and blocky particles (fitting closely together in a mixture) have highly desirable properties from the structural viewpoint. It is widely believed that cubical particles offer the ideal particle shape for HMA mixtures. Unfortunately, the current Superpave FAA method cannot consistently distinguish between cubical aggregates which perform well and rounded aggregates that perform poorly (*1*).

Some evidence suggests that fine aggregates above the minimum FAA exhibit poor performance and some fine aggregates below the minimum FAA exhibit good performance (*5, 6*). Experience has shown that there are some 100 percent crushed fine aggregates fail to meet the FAA criteria (*5*). State agencies are concerned that local materials previously considered acceptable, and which have provided good field performance, now cannot meet the Superpave requirements. Some researchers also question the validity of the levels defined by Superpave on actual performance (*7*).

AASHTO T-304 or ASTM C-1252, Method A, appears to lose the ability to discriminate angularity among aggregates when the uncompacted voids are more than 43 percent (*8*). FAA alone is not a good predictor of fine aggregate shear strength; rather, it is most strongly related to particle surface texture (*6*). Very high FAA values may actually be due to the high percentage of elongated and sharp-pointed particles, but there is no upper limit of the FAA requirement to control elongated particles. Elongated fine aggregates may be subject to breakage during mixing and compaction. This breakage may increase the amount of fines in the mixture, thus affecting the void of mineral aggregates (VMA) and, hence, the performance of the mix. Contractors can compensate for the breakage by adjusting the aggregate blend.

The FAA test method presents a dilemma by acquiring a standard gradation that is different from that actually used in the HMA. The relationship to performance of the HMA may be questionable as gradation plays an important role. If the method requires testing of the grading used in the HMA (ASTM C-1252, Method C), grading affects the FAA results in a nonuniform manner. That is, one grading of the fine aggregate may pass the specification but another may fail.

OBJECTIVES

The objective of this study is to evaluate the ability of the current method (AASHTO T-304 or ASTM C-1252, Method A) to measure angularity of fine aggregate and to determine if it can distinguish aggregates with good and poor performance in HMA. A secondary objective is to compare FAA test results with other measures of particle angularity. The ultimate goal of this study is to develop and recommend improvements in the test protocol and/or the specification for the FAA test or to recommend an improved procedure to replace the Superpave FAA test. A limited study was also performed to evaluate the effects of fine aggregate with different angularities on resistance to rutting in HMA as measured using an Asphalt Pavement Analyzer (APA).

CHAPTER II

LITERATURE REVIEW

BACKGROUND

HMA pavements have experienced premature rutting due to increases in the magnitude of traffic loads and volume. Truck tire pressure, axle load, and volume of traffic have increased considerably in recent years. Average truck tire pressure is about 100 psi (689 kPa) (*9*) and can be as high as 130 psi (896 kPa) (*10*). Progressive movement of materials, either in the asphalt pavement layer or in the base or even in the subgrade, yields rutting in vehicle wheelpaths. Under repeated loading, this movement of materials occurs through consolidation or plastic flow (*11*). Inappropriate selection of aggregate and binder quality and quantity for HMA are major contributors to rutting of HMA pavements. Use of poorly graded aggregates having smooth, subrounded particles and a high percentage of rounded sand has contributed to the loss of shearing resistance of asphalt concrete mixtures (*12*).

In HMA mixtures, aggregate particles usually comprise 94 to 96 percent by weight of the total mix. Normally, approximately 40 percent by weight of HMA is fine aggregate (passing 4.75 mm or No. #4 sieve). The quality and quantity of sand-size aggregates play a very important role in the permanent deformation performance of HMA mixtures. The major fine aggregate properties that influence the rutting potential of HMA are (*13*):

- particle shape or angularity,
- particle surface texture, and
- particle porosity.

Rounded, nonporous, smooth-textured particles tend to produce rut-susceptible HMA mixtures. Angular, slightly porous, rough-textured particles should maximize the resistance of

HMA mixtures to rutting. These latter aggregate properties also improve resistance to fatigue cracking and wet-weather skidding (*14*). Bayomy and Guirgus used rounded gravel aggregate with a thin coating of portland cement mortar (*15*). The cement coating provided a more angular shape, a rougher texture, and a more porous surface to the aggregates. Aggregate particles were coated with portland cement, allowed to cure, and then used in the preparation of asphalt concrete mixtures. HMA specimens were prepared using both coated and uncoated aggregates. Both types of specimens were tested for rutting, stripping, and raveling susceptibility. Researchers found specimens with cement-coated aggregates showed more resistance to rutting and fatigue cracking than specimens prepared with uncoated aggregate. The above mentioned test supports the idea that the angular and rough aggregates are beneficial for both rutting and fatigue resistance. The advantage of angular aggregate in HMA is well documented (*13*, *16*, *17*).

The geometric irregularity of both coarse and fine aggregate has a major effect on mechanical behavior and physical properties of HMA mixtures (*18*). This geometric irregularity can be attributed to the aggregate particle shape, angularity, and surface texture. Bucher (*18*) reported an increase of stiffness and a significant increase of resistance to permanent deformation of HMA with the increase of unrodded particle index, I_{ua} of fine aggregate. According to Bucher unrodded particle index is an indication of fine aggregate angularity (*18*). He also reported a significant increase in fatigue life of HMA with the increase of unroded particle index of coarse aggregate.

According to Kandhal et al. (*19*), the shape and texture of fine aggregate are more important than those of coarse aggregate in improving the stability of HMA and increasing its resistance to permanent deformation. Perdomo and Button found that the rounded shape and smooth texture of fine aggregate were significant contributors to rutting in Texas HMA pavements (*13*).

In 1988, a Federal Highway Administration (FHWA) memo (*20*) stated, “Since most natural sands are rounded and often contain a high percentage of undesirable materials, the amount of natural sand, as a general rule, should be limited to 15 percent to 20 percent for high volume pavements and 20 percent to 25 percent for medium and low volume pavements.” However, since the guidelines were quite general and since the quality of natural sand varies widely from state to state, the FHWA recommendation has not been uniformly applied nationwide.

CHARACTERIZATION OF MATERIAL PROPERTIES

Superpave requires that fine aggregate angularity be measured according to ASTM C 1252, Method A or AASHTO T-304, as a consensus property. Further, voids in uncompacted fine aggregate measured using this method must be at least 45 percent to qualify for a mixture designed for heavy traffic (*9*).

NAA Flow Test Method

ASTM C-1252 (or AASHTO T-304) is an indirect method of measuring FAA and is sometimes referred to as the National Aggregate Association (NAA) Flow Test. The test was originally developed to determine the ‘finishability’ of portland cement concrete (*1*). In this method, FAA is defined as the percent of air voids present in loosely compacted aggregates smaller than 2.36 mm when a sample of dry fine aggregate is allowed to flow into a small calibrated cylinder through a standard funnel. The diameter of the funnel orifice is 12.5 mm (0.5 inch) and the tip of the funnel is located 114 mm (4.5 inch) above the top of the cylinder. The concept of this procedure is that higher uncompacted void content implies more freshly fractured faces and more highly textured particle faces.

Voids present in loosely compacted aggregate (uncompacted voids) are calculated as the difference between the volume of the calibrated cylinder and the absolute volume of the fine aggregate collected in the cylinder. The volume of the cylinder is 100 ml. Absolute volume of collected fine aggregate is calculated using the bulk specific gravity. The bulk specific gravity of fine aggregate is determined using ASTM Standard Method C-128 (or AASHTO T-84). The uncompacted voids are calculated using the following formula (*21*):

$$U = \frac{V - (F / G_{sb})}{V} * 100$$

here: U = uncompacted voids in the fine aggregate, %
V = volume of a calibrated cylinder, ml
F = mass of fine aggregate in the cylinder, gm, and
G_{sb} = bulk dry specific gravity of fine aggregate.

The test procedure describes three methods: Method A, B, and C. Method A uses a specific, defined gradation; Method B uses three separate aggregate size fractions; and Method C uses the as-received gradation passing the 4.75 mm (No. 4) sieve. Method A is used for the Superpave specification. The gradation used in Method A is as follows:

Individual Size Fraction	Mass, gm
2.36 mm (No. 8) to 1.18 mm (No. 16)	44
1.18 mm (No. 16) to 0.60 mm (No. 30)	57
0.60 mm (No. 30) to 0.30 mm (No. 50)	72
0.30 mm (No. 50) to 0.075 mm (No. 100)	17
	Total 190 gm

Determination of bulk dry specific gravity of fine aggregate is very important in the calculation of uncompacted void content. A change in bulk specific gravity, G_{sb}, by 0.05 will change the calculated void content by approximately one percentage point (*22*). The specific gravity of the particular aggregate gradation tested must be used in the calculation of uncompacted voids.

The following sections describe other test methods considered indirect measures of fine aggregate angularity.

Flow Rate Method

The flow rate method (*23*) was originally developed by the Bureau of Public Roads, presently known as FHWA. In this method, an aggregate sample of definite weight and size fraction is poured through a standard funnel. The time required for a specified quantity of sand to flow through the funnel is measured. Flow rate is calculated by dividing the volume of the sample in cm^3 by the flow time in second. The volume of sand is determined by dividing the mass of the sand that flows through the funnel by its bulk dry specific gravity. A shape-texture index (STI) is calculated by dividing the flow rate for a standard set of round balls by the flow rate of the sand.

Since the flow rate for a standard set of round balls is constant, the STI of fine aggregate sand is proportional to its flow rate (*23*). No national standard has been adopted for this test. Variations of the aggregate size fraction and the amount of the sample by different users of this method have been reported (*23*). Because of these variations, the empirical nature of the procedure, and its similarity to FAA, this test was not used in this study.

ASTM Method D-3398

ASTM D-3398 determines an index, I_a, related to aggregate particle shape and texture. Washed samples of four different size fractions are compacted individually using two different standard compaction procedures. The size fractions are:

2.36 mm (No. 8) to 1.18 mm (No. 16)
1.18 mm (No. 16) to 0.60 mm (No. 30)
0.60 mm (No. 30) to 0.30 mm (No. 50)
0.30 mm (No. 50) to 0.075 mm (No. 100)

A sample of each size fraction is then compacted in three layers in a calibrated mold using 10 drops per layer of a standard tamping rod in a standard manner. The percentage of voids, V_{10}, at this stage is calculated as the difference between the volume of the mold and the absolute volume of fine aggregate. The absolute volume of fine aggregate is calculated by dividing the mass of fine aggregate by the bulk dry specific gravity of that size fraction. A similar procedure, where a fresh sample is compacted in three layers using 50 drops per layer, is followed to calculate V_{50}. I_a is calculated by the following empirical formula.

$$I_a = 1.25\,V_{10} - 0.25V_{50} - 32.0$$

The shape index, I_a, for the original fine aggregate is determined by calculating the weighted average of I_a of all size fractions in the original gradation. The principle of this test method is basically the same as that of the NAA method. Kandhal et al. (*19*) reported a high correlation ($R^2 = 0.97$) between the results obtained by the NAA method and those from ASTM D-3398. Determination of the bulk specific gravity of all size fractions is required for this test method. This method is very time consuming, laborious, and expensive and, therefore, not a suitable replacement for the FAA test.

Direct Shear Test

Resistance to shear of a cohesionless soil or fine aggregate is derived from friction between grains and the interlocking of grains. This resistance is expressed by the angle of internal friction (AIF) or simply the angle of friction, Φ. A standard direct shear apparatus for soil (ASTM D 3080) is used to measure Φ. The sample used for this test is usually air dry so that no pore pressure develops during the test. The sample is placed in a direct shear box. This box is either rounded or square and is split horizontally into two parts. Either the upper or lower half is held stationary while a force is applied to the other half. Shear tests are performed using at least three different normal stresses. Normal stresses are applied to consolidate the sample. Shear stress is gradually increased until it reaches a maximum for each normal load. Ultimately, the sample fails in shear along a predefined horizontal plane. A graph of applied normal stress versus maximum shear stress is constructed. The slope of this line is the angle of internal friction.

The angle of internal friction is an indication of particle interlocking and, hence, shape and texture (*23*). Although this is considered a fundamental test, it is an indirect measure of aggregate particle shape and texture.

Compacted Aggregate Resistance

The compacted aggregate resistance (CAR) test method (*5*) was developed to evaluate shear resistance of compacted fine aggregate as blended for the HMA. Individual fine aggregate components may also be evaluated. In this method, an as-received aggregate sample passing the No. 8 sieve is oven dried at 230 ± 9°F (110 ± 5°C) to a constant weight. Then the sample is cooled to ambient temperature and thoroughly mixed with 1.75 percent water by weight. The sample is placed in a 4-inch (102-mm) diameter Marshall mold to prepare an approximately 2.5-

inch (63.5-mm) high compacted sample. To simplify testing, the base plate is normally attached to the mold. A sample is compacted using 50 blows of a Marshall hammer on only one face.

The stability value or CAR value is measured by applying an unconfined compressive load using a Marshall HMA testing machine. The compacted sample, while still in the mold, is placed in the Marshall test machine in the upright position. A load, at a rate of 2 inch/minute (50.8 mm/min), is transmitted through a 1.5-inch (37.5-mm) diameter flat-faced steel cylinder on the plane surface of the compacted sample. This test is also an indirect but performance-related method for measuring fine aggregate angularity. Researchers believe that this test is performance-related because the compacted specimen is subjected to shearing load. This test method has similarity with the California Bearing Ratio test (AASHTO T-193).

New Zealand Test

The New Zealand test method is similar to ASTM C-1252 and the flow rate method. A sample of fine aggregate smaller than 7.94 mm is poured through a standard funnel. Both the uncompacted void content and time required for 1000 gm of the sample to flow through the funnel are measured. These two values are reported as indirect measures of particle shape and texture.

Fractals Method

Perdomo & Button and Yegonni & Button measured aggregate particle shape and texture using a fractals-based method (*13, 12*). Fractals are a family of complex mathematical functions that can describe shape and texture of natural phenomena. Black and white digitized images of aggregate particles obtained from either photographs or video frames are analyzed by a computer program using a mathematical algorithm that computes a fractal dimension. A greater fractal dimension indicates greater angularity and/or surface texture. Significant work is needed on this fractal procedure before it can be used for routine measurement of aggregate angularity. It does, however, provide a direct method of measuring angularity and surface texture.

Hough Transform

Wilson et al. (*24*) used a video-based computer-controlled imaging system to measure fine aggregate angularity. In this method, 2-dimensional images of individual aggregate particles are characterized by shape attributes. Hough transformation, a mathematical technique, is employed as the algorithm for image analysis. The detailed theory and procedure are described in Chapter III. The Hough Transform provides a method of directly measuring fine aggregate angularity. This technique for characterizing aggregate particle shape and texture is still in the developmental stage. Improvements are necessary to make it commercially viable for routine measurement of aggregate angularity and texture.

Image Analysis at Washington State University

This method of quantifying fine aggregate shape and texture was developed by Dr. Eyad Masad at Washington State University (*25, 26*). The WSU method uses two-dimensional images of fine aggregates to quantify the shape and texture of the particles. The following chapter illustrates this method.

Image Analysis Using VDG-40 Videograder

LCPC VDG-40 videograder was developed in France to determine particle size distribution; the producers are developing algorithms to quantify particle shape, angularity, and possibly texture (*27*). Details of this method are described in the following chapter.

WipShape

WipShape is a 3-D-based shape analyzer that makes objective measurements quickly. The hardware and software are being developed by WipWare, Inc. and the University of Missouri-Rolla (*28*). WipShape appears worth more evaluation.

Commercially Available Software/Hardware

There are several commercially available software packages designed to perform image analysis; two packages include ImagePro® and MetaMorph®. The ImagePro® software is a readily available software package capable of analyzing shapes of two-dimensional digitized images. The software quantifies maximum and minimum dimensions, perimeter, area, etc. of multiple particles. It automatically computes parameters such as aspect ratio, and perimeter/area ratio of particle images. These parameters are related to shape, angularity, and texture of particles. A few small research efforts are underway to evaluate ImagePro for use in quantifying aggregate angularity (Texas DOT and North Carolina DOT). During discussions with researchers ImagePro® representatives indicated they have a software package that may do a better job of measuring aggregate angularity and surface texture than ImagePro. The name of the new product is MetaMorph®.

Other Methods

There are also several other image analysis methods listed below. The researchers think these other methods, even though they are in research stage, have the potential to be studied more.

Image Analyzer

Yudhbir and Abedinzadeh used an image analyzer to quantify angularity and shape of fine aggregate (*29*). They used an image analyzer that is commonly used by powder metallurgists. In this method, angularity is quantified in terms of the average number of tangents obtained from the image analyzer studies.

PenPad Digitizer

Barksdale et al. developed this digitizing at Georgia Institute of Technology to measure aggregate shape, surface area, and roughness (*4*).

CHAPTER III

EXPERIMENTAL PLAN

EVALUATION OF FINE AGGREGATE ANGULARITY TEST

The objective of this study is to compare FAA test results with other indirect and direct or empirical and fundamental measures of aggregate angularity. The ultimate goal of this study is to develop improvements in the FAA test protocol and specification and/or recommend a better procedure to replace the FAA test. A plan was adopted to collect fine aggregate materials from most state DOTs and compare results from the FAA test with other test methods. The other methods included direct shear test, compacted aggregate resistance test, Hough transform method, WSU procedure, and VDG-40. The reason for choosing these tests was that the researchers sought a quick, repeatable, and, if possible, a direct and performance-related test method. A surface analysis was performed (unsuccessfully) since there should be a relationship between angularity and surface area. Visual examination was also performed to obtain a subjective rating of the aggregate specimen.

Image analysis techniques are very versatile tools for quantifying object geometry. These techniques have been used for quantifying shape, texture, and size distribution of different types and sizes of particles. Scientists in metallurgy, mineralogy, and health science have used image analysis to characterize particles has been used for some time. With advancements in microscopy and faster computer hardware and software, image analysis appears promising for civil engineers, as well. This technique is finding a practical application in the field of HMA for aggregate shape analysis. In digital image processing, video pictures of aggregate particles are digitized. Various mathematical techniques are then applied to these digital forms to quantify the shape, size, and even texture of aggregate particles.

For this project, researchers sent fine aggregate samples were sent to three different agencies to evaluate their innovative image analysis methods. These agencies include the University of Arkansas at Little Rock (UALR); Washington State University (WSU) at Pullman; and Virginia Transportation Research Council (VTRC) at Charlottesville. The three image analysis methods are briefly described in subsequent subsections.

Material Selection and Acquisition

The Materials engineer of each state DOT was requested to send four fine aggregates (two typically demonstrating good performance and two normally exhibiting poor performance) for inclusion in the testing program. Additional data, such as gradation, specific gravity, other typical specification test data and performance estimates were requested. The researchers received 92 fine aggregate samples from 23 states. Some state DOTs sent test results such as specific gravity, gradation, and abrasion value and subjective performance evaluations of their fine aggregates in HMA mixtures. These 92 fine aggregate samples came from different climatic regions and a wide range of mineralogical sources.

Each sample is designated by an alphanumeric symbol. The first two letters denote the name of the state of the sample's origin. The numeric part was assigned arbitrarily to facilitate brevity. Table 2 in Chapter III describes the sample designation, its source, and general description.

Fine Aggregate Angularity Test

Researchers conducted fine aggregate angularity tests (ASTM C-1252, Method A) on 47 samples from 14 states. These aggregates were specifically selected to cover a wide range of angularities as well as geologic sources. Both manufactured and natural fine aggregate samples were included in this test program. Duplicate FAA and specific gravity tests were performed on each sample to increase confidence in the uncompacted void content. For specific gravity determinations, the samples used were the “as-received” materials passing the sieve No. 4 (−4.75 mm). The average from two replicate tests was used to calculate uncompacted voids. If the difference between two results of bulk dry specific gravity was more than 0.032, both results were discarded and the tests were repeated. It is noteworthy that a change in specific gravity of 0.05 will change the calculated uncompacted voids by approximately one percentage point. The test setup is shown in Figure 1.

Twenty of the fine aggregates, representing a wide range of FAA values, were chosen for evaluating the direct shear test, compacted aggregate resistance test, and image analysis tests. Additionally, FAA and the other angularity tests were performed on the three fine aggregates used in the restricted zone analysis (another phase of this research project).

FIGURE 1 Fine Aggregate Angularity Test Setup

Direct Shear Test

Direct shear tests (ASTM D-3080) were conducted on 23 fine aggregate samples at three different normal loads to permit application of the Mohr-Coulomb theory. Air dry samples with the same gradation as that used for FAA tests (i.e., ASTM C-1252, Method A) were used for these tests. The three normal stresses used for this series of tests were: 350 psf (16.67 kN/m^2), 987 psf (47.23 kN/m^2), and 1633 psf (78.18 kN/m^2). T. W. Lambe suggested similar normal stresses for the direct shear testing of sand sample *(30)*. The applied rate of strain was 0.05 inch/min (1.27 mm/min). Replicate direct shear tests were performed on each 1

sample and the average angle of internal friction were reported. Figure 2 depicts the shear box used in this work. The test setup is shown in Figure 3.

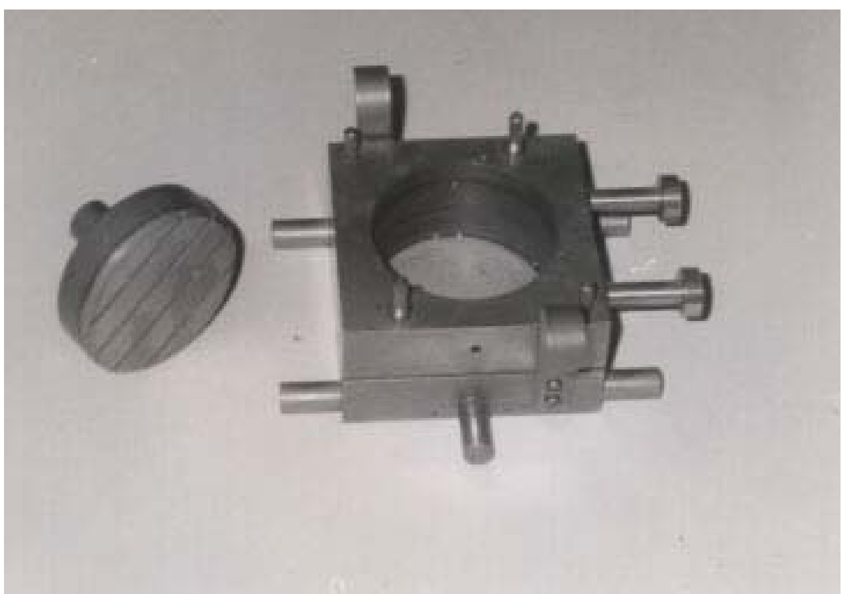

FIGURE 2 Shear Box for Direct Shear Test

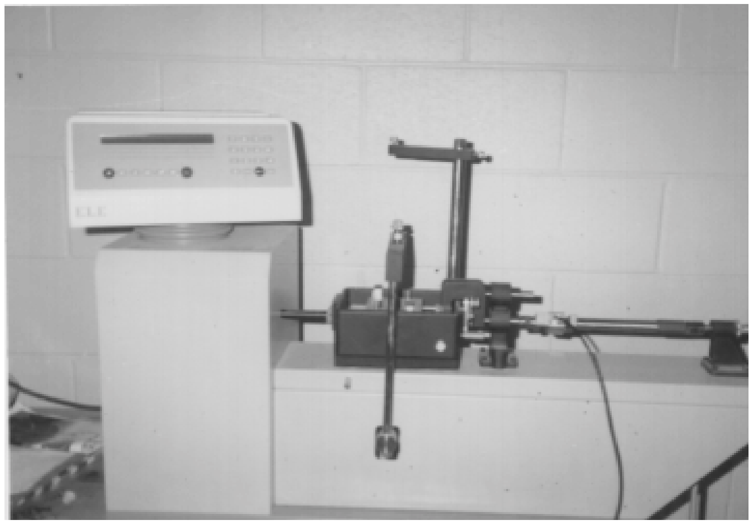

FIGURE 3 Direct Shear Test Machine

Compacted Aggregate Resistance Test

Researchers performed CAR tests on the same 23 fine aggregates that were tested with the direct shear apparatus. Tests were performed on unwashed, “as-received” fine aggregate samples passing No. 8 (2.36-mm) sieve with a moisture content of 1.75 percent. Samples were compacted following the Marshall method using 50 blows applied to only one face of the specimen and tested using the Marshall stability tester.

In addition, researchers performed CAR tests on four fine aggregates at several moisture contents to examine the effect of moisture on the measured resistance values. These four samples were chosen from natural and manufactured sources to cover low to high values of angularity. The CAR test setup is shown in Figure 4.

FIGURE 4 Compacted Aggregate Resistance Test Setup

Visual Evaluations of Aggregate Shape and Angularity

Researchers performed visual examinations using an optical microscope (Nikon H III, shown in Figure 5) to obtain subjective evaluations of particle shape and texture for each fine aggregate. Both washed and unwashed samples were used for this test. The “standard” used to estimate shape and texture were photographs and descriptions presented by Monismith in his short course, *Asphalt Paving Mixtures* (*31*). The appearance of the fine aggregates was compared with those photographs and described as angular, subangular, subrounded, or rounded.

FIGURE 5 Microscope Used for Visual Inspection

Image Analysis by Hough Transform Method

Although the researchers refer to this technique as “Hough Transform”, it also employs other mathematical mechanisms (e.g., fast Fourier transformation and neural network). This method was recently developed at the Applied Science Department at University of Arkansas at Little Rock (UALR) (*8, 24, 31*). This is an automated method for measuring fine aggregate shape, angularity, and texture. Researchers from the Texas Transportation Institute visited UALR and evaluated the 23 samples using the department’s laboratory facilities. The procedure can be divided into three steps: automated data acquisition, image analysis, and classification using a neural network.

Automated Data Acquisition

Fine aggregate particles were spread over a glass transport (X-Y) table (Figure 6). Aggregate samples passing No. 4 sieve and retained on No.16 sieve were used. Three aggregates with smaller sizes were also tested. During a test, only one size of aggregate was used to facilitate focusing under magnification. Smaller particles were tested separately after adjustment of the camera lens and necessary calibration. A Hitachi KP-C553 ½ inch CCD color camera with a resolution of 682 X 492 pixel captured the images of individual particles as the X-Y table moved automatically in both the X and Y directions. The table moved 0.00025 inch (0.00635 mm) per step for a total of 6.0 inch (152.4 mm). For each type of aggregate, images of approximately 500 particles were captured. The number 500 is chosen to provide statistically valid results (*31*).

A Data Translation DT2871 video frame grabber installed in a PC was used to capture the video signals from the camera for image analysis. A Velmex unislide motor-driven positioning system and Velemx NF90 stepping motor controller automatically controls the movement of the of X-Y table (*8*). The different components of this hardware system are marked in Figure 6 as: (A) Video Camera (B) Glass Sample Plate (C) LED Back Light (D) X-Y Table (E) DC Back Light Power Supply (F) Stepper Motor Controller (G) Video Monitor (H) Computer Monitor (I) Computer. The data acquisition system operates with software called DAGPIC. Details of the data acquisition system are beyond the scope of this report.

FIGURE 6 Hough Transform Data Collection Hardware

Image Analysis

Mathematically, image analysis is a relatively complex process. This subsection describes the process.

A particle outline coordinate data file, created by DAGPIC, is analyzed with software called DAGGAER for shape characterization. The particle outlines are stored in a rectangular coordinate (x, y) system during the data acquisition process. Length and width of each particle image are measured using a “virtual” caliper. Aspect ratio (maximum image dimension/minimum image dimension) of each particle is then calculated. The centroid of each particle is calculated by averaging all x and y coordinates of each particle outline. Next, all the rectangular coordinates are transferred into polar (r, θ) coordinates without changing the centroid of the particle. All values of r are divided by the largest distance from the centroid to the edge, r_{max} , and fitted into a circle of unit radius and stored for further analysis.

T-index. A convex hull is formed using the X_{max}, X_{min}, Y_{max}, and Y_{min} of the particle outline (Figure 7). This convex hull is like an elastic band around the particle image (*31*). The T-index is calculated using the following formula,

$$T = 1 - (A_p / A_h)$$

where A_p = area of a particle outline

A_h = area of a convex hull

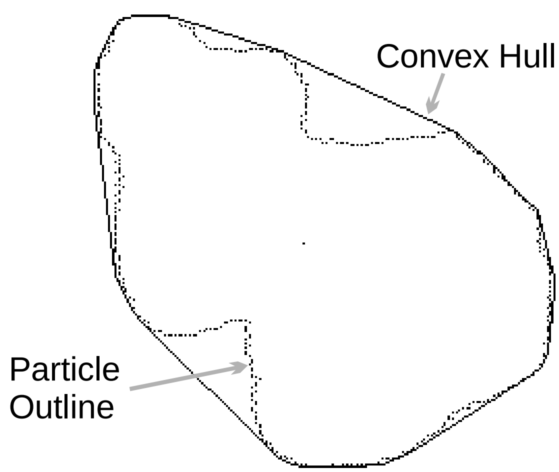

FIGURE 7 Particle Outline and Convex Hull for T-index Calculation

The T-index provides a quantitative estimate about the texture of the particle. T-index approaches zero for a smooth-sided particle and increases as the particle image becomes more irregular and/or the surface texture becomes rough. The maximum value of this index is 0.25;

above that, it is considered to be multiple touching particles and is discarded from subsequent calculations.

E-index. E-index is defined as the reciprocal of the aspect ratio of the particle outline. This index provides information about the shape of the particle image whether it is elongated or cubical. Higher the value of E-index means that the particle is more cubical or in the other way lower E-index suggests more elongated particle.

S-index. After applying several other mathematical steps of data preprocessing and refining, every coordinate on the particle outline is formed as a Hough Parameter Space Array (HPSA) (*29*). The Hough Transform algorithm is then applied to the HPSA. A sample output illustrating application of the Hough Transform algorithm is shown in Figure 8. The $S(\theta)$ function is calculated as a two-dimensional projection of the HPSA by an angle. The highest peak of the $S(\theta)$ function is termed A_{max}. A is the average of the $S(\theta)$ function.

$$\text{S-index or } S_i = 1 - (A / A_{max})$$

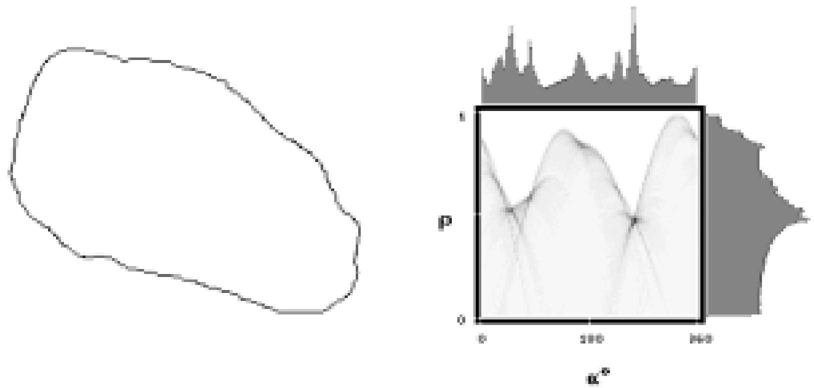

FIGURE 8 Particle Outline (Left) and Its Hough Transform (Right)

S_i is considered as 1.0 minus the average of the Hough line length divided by the longest Hough line length. When one or two lines dominate the particle perimeter, S_i will approach unity and, for rounded particles, S_i will approach zero. The S-index of an angular particle is typically greater than 0.6. This index basically measures the length of straight lines and the angle between them.

R-index. The R-index line density function, R(r), is calculated from a two dimensional Hough Transform, H(r, θ), using the following formula.

$$R(r) = \sum_{i} H(r, \theta_i)$$

The R-index describes how the straight line segments are distributed as a function of distance from the centroid of the object (*8*). The highest value among the R(r) functions is called R-index. The R-index represents the radial distance to the highest density of points from the centroid of the image outline. This index basically measures the roundness of the particle. The R-index of a circular object is near 1.0 and for a square object it is 0.707.

Harmonic Component of S(θ) Function. A series of harmonic components is achieved when the S(θ) function is entered into a Fast Fourier transform (FFT) function. These harmonic components provide improved shape discrimination (Figure 9). These are similar to the "slope density function" used by Li et al. (*33*). The second through sixteenth harmonic components are used as a set of inputs for the neural network classifier.

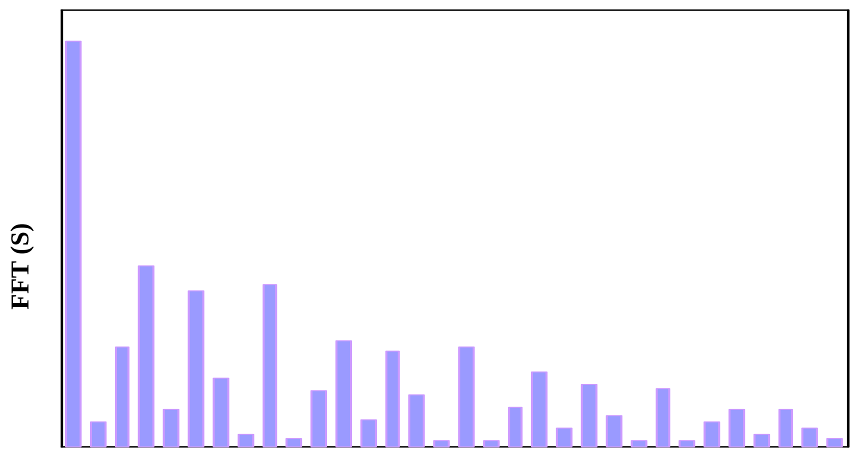

FIGURE 9 Fast Fourier Transform of S Function

Neural Network Classifier

The above four indices and other harmonic components are combined into a single number, or index, that describes the angularity of each particle. This combination is done through a neural network on the basis of an expert panel's scored example. Wilson et al.(*33*) describe the neural network as

> "a non-linear transformation of all the available information (indices and harmonic components) into a single linear estimate. Neural networks are not programmed, they are trained by example. Training is accomplished by applying data from an outline to the inputs of the neural network and comparing the computed output with desired results. When there is difference between the network output and the desired output, weighting factors within the network are adjusted to move the output toward desired value. This process is repeated thousand times using several hundred examples. Normally, the available examples are divided into a training set and a test set. One hundred and thirty-five expert examples were sorted by score and reprinted in sequence as a reference template. Then several hundred new outlines were assigned a score by finding the closest match among the 135 scored examples and giving the new outline the same score. The data set became the training set for the neural network. "

A neural network is a combination of various processing units connected together. This artificial neural network can also be described as an abstract simulation of a real nervous system (*34*). This system is a collection of neuron units. These units are connected with each other via axon connections. They are assembled in layers with multiple processing elements as inputs and outputs (*33*). Figure 10 is a pictorial description of a neural network.

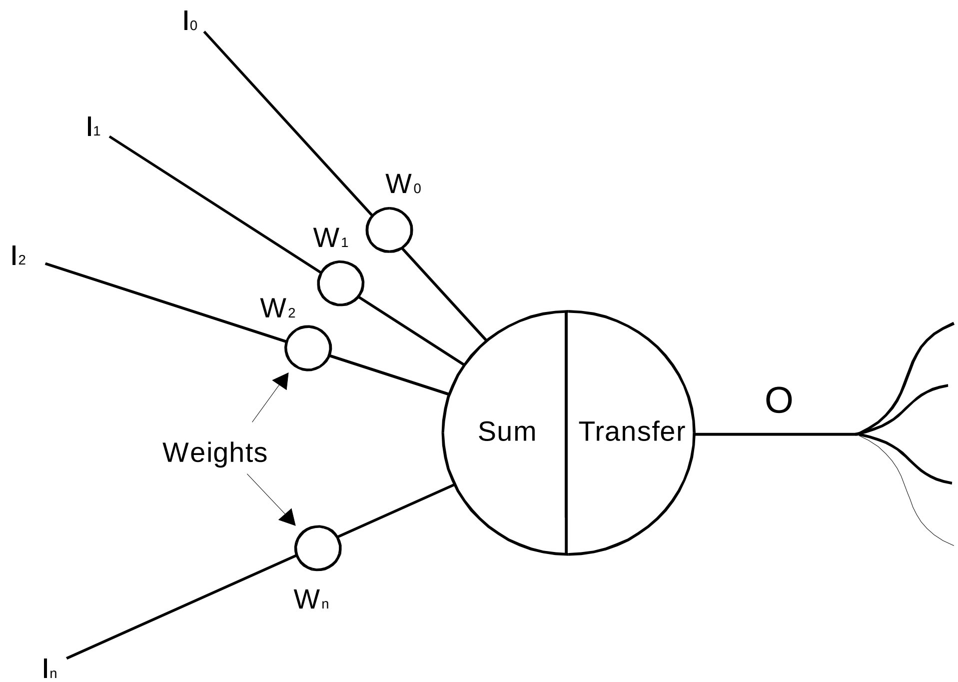

FIGURE 10 Neural Network Processing Unit

Image Analysis by Washington State University Method

WSU introduced this automated method of fine aggregate shape analysis (*25*). Our researchers sent 23 samples of fine aggregate to WSU for testing. Particles are painted black to obtain sharp, high quality images. Fine aggregate images are captured by an optical microscope. Depending on the purpose of analysis, shape or texture, images are captured at two different resolutions. High and low resolution images are captured for the analysis of texture and shape, respectively. This microscope is linked with an image analyzer. After some modification, particle images are converted to binary images. These binary images are subjected to three different mathematical techniques to quantify the shapes: surface erosion-dilation, fractal behavior, and form factor.

Surface Erosion-Dilation Technique

Each particle image is subjected to a number of erosions and followed by the same number of dilations. Erosion is a well known morphological process in image analysis (*25*). In this operation, pixels are removed from a binary image according to the number of neighboring pixels that have different color. Erosion tends to smooth and simplify the object image by removing pixels from the outer boundary and advancing toward the center. Dilation is the reverse of erosion. In dilation, a layer of pixels is added to the object to construct a simplified version of the original image. Erosion and subsequent dilation does not necessarily produce an image of original shape and size (*35*). During this process, the image loses some area. According to this technique, it is considered that the area lost after a certain number of erosions and dilations is proportional to the percent of objects smaller than a certain size and surface irregularity. Figure 11 illustrates the erosion and dilation process.

Masad (*25*) suggested a new term called surface parameter (SP). SP is the percentage of area lost during the erosion and dilation operations.

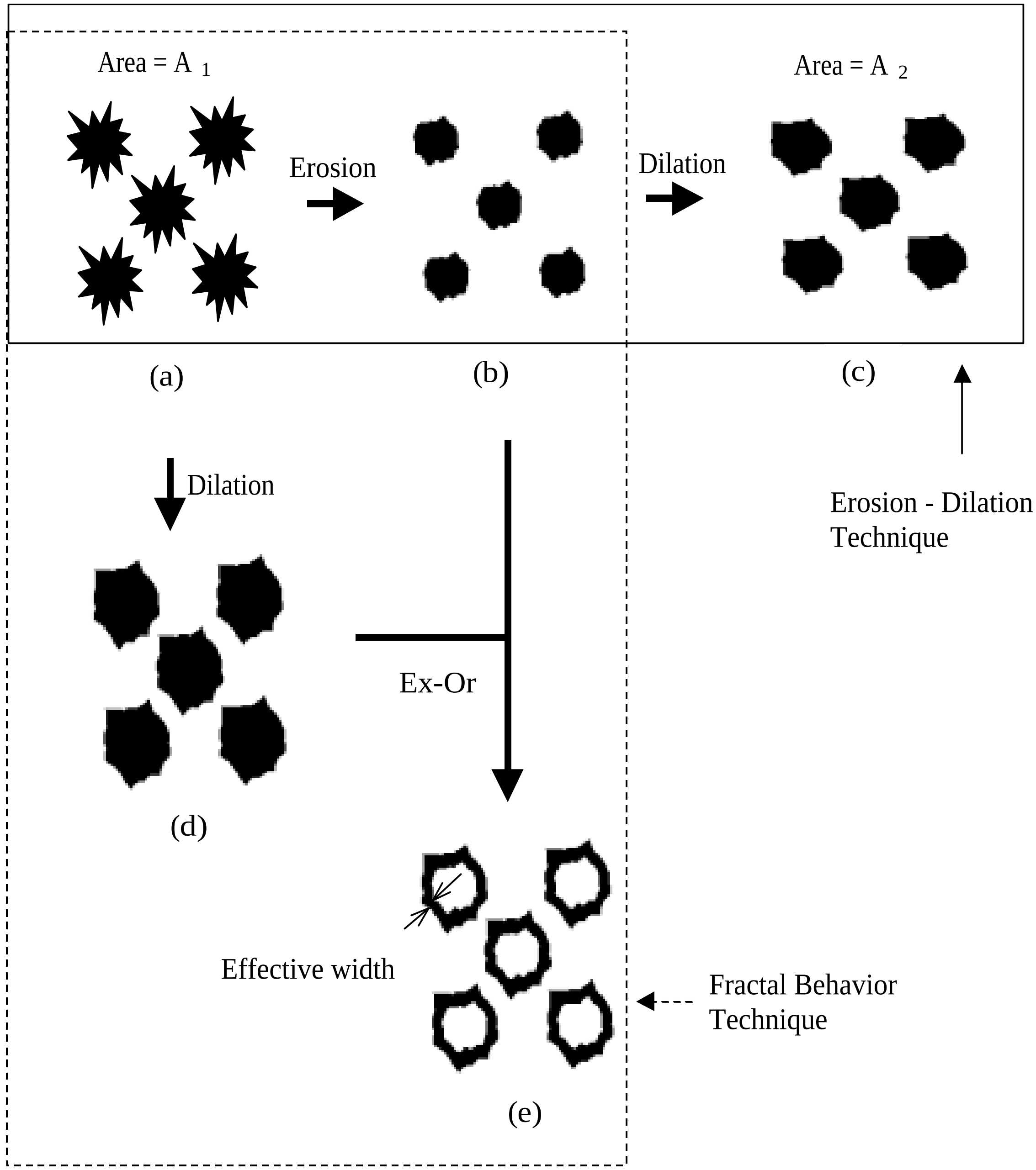

FIGURE 11 Illustration of the Effect of Erosion-Dilation and Fractal Operations

$$SP = \frac{A_1 - A_2}{A_1} \times 100\%$$

where A_1 = Original area before erosion-dilation

A_2 = Reduced area after erosion-dilation.

The surface parameter value increases with the increase of surface irregularity. SP, measured with images of high resolution and low resolution yields the surface texture and particle angularity, respectively.

Fractal Behavior Technique

Fractal behavior is simply defined as the self-similarity exhibited by an irregular boundary when captured at different magnifications (*25*). Smooth boundaries erode-dilate at a constant rate; whereas, irregular boundaries do not erode-dilate at a constant rate. In this process, a number of erosion and dilation operations are applied on the original image. The eroded and dilated images are again superimposed with the help of a logic operator (Ex-OR). Using the logic operator, the overlapping pixels are removed. The remaining pixels (those removed and added during erosion and dilation processes, respectively) form a boundary. The width of this boundary is proportional to the number of erosion-dilation cycles and, hence, surface irregularity (Figure 11). Several erosion-dilation cycles are applied, and the increase in effective width is measured.

Fractal length (FL) of the boundary is the slope of the line drawn by plotting the effective width versus number of erosion-dilation cycles on a log-log scale. Smooth boundaries show very flat slopes, and irregular boundaries show steep slopes. Fractal length increases with the increase of boundary angularity.

Form Factor Technique

Form factor (FF) is a parameter that describes the object's dimensions, especially surface irregularity. It is defined by the following mathematical formula (*26*):

$$FF = \frac{4\pi \times A}{P^2}$$

where, A = Area of the object image

P = Perimeter of the object image

The area is measured as the number of total pixels of the image and the perimeter is measured as the number of pixels that touch the background. It is evident that this measurement depends on resolution. Varying the resolution, one can determine the angularity or surface texture. The value of form factor for a perfect circular object is 1. The FF value decreases with the increase of surface irregularity.

Image Analysis Using VDG-40 Videograder

The VDG-40 videograder (Figure 12) is an optoelectronic device developed by the French LCPC (Laboratorie Central des Ponts et Chaussées). This equipment has been used in France for several years to make automated gradation measurements of aggregate particles. This device is now being used in the FHWA Turner-Fairbank Research Center and the Virginia Transportation Research Center (VTRC) for determining the shape of aggregate particles.

FIGURE 12 VDG-40 Videograder

Research to examine the VDG-40 as a potential replacement of the flat and elongated particle test (ASTM D-4791) is ongoing.

This equipment can be used to evaluate fine aggregate with minor modifications. Due to limited quantities, only 22 of the 23 fine aggregates were sent to Mr. Brian Prowell at VTRC for testing by the VDG-40 videograder.

The basic principle of this apparatus is shown in Figure 13. Aggregate particles are fed into the hopper. The vibrating separator deposits the particles in one layer so that there is no particle rotation or over lapping particles.

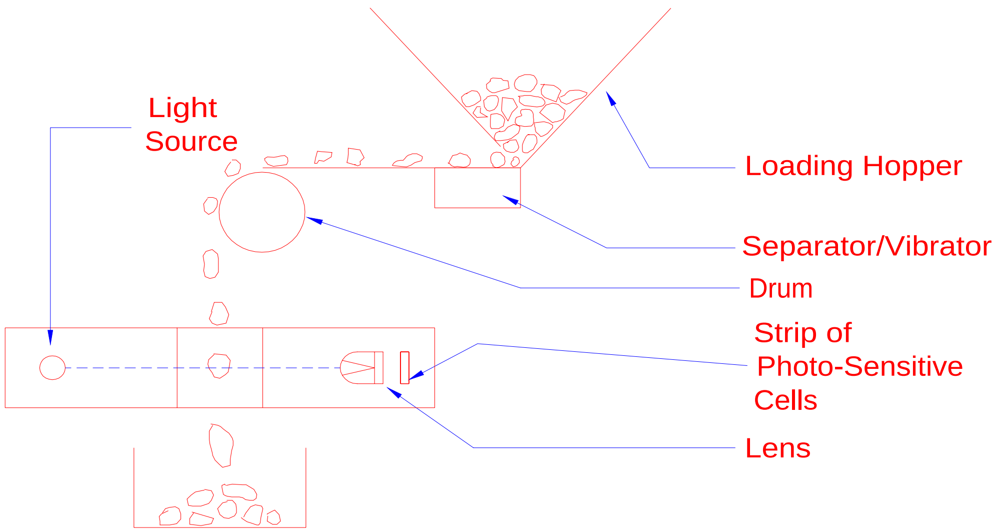

FIGURE 13 Principle of the VDG-40 Videograder

These particles fall between a linear light source and a charged-coupled device (CCD) camera. This camera grabs the image of the falling particles through its horizontal strip of in-line photo-sensitive cells. The image capturing principle is depicted in Figure 14. As the aggregate passes through the light path, some photo cells are masked by the aggregate. The coordinates of the aggregate's contours and the projected surface are stored in memory. The captured images are processed to measure principal dimensions using a software algorithm. This device measures three principal dimensions (L_1, e_1, and G_1) from the two-dimensional image. The definition of L_1, e_1, and G_1 are as follows (*36*):

$L_1 =$ The greatest distance between a pair of parallel planes tangential to the item

$e_1 =$ The smallest distance between a pair of parallel planes tangential to the item and orthogonal to the planes defining L_1

$G_1 =$ Spacing between a pair of parallel planes tangential to the item and orthogonal to L_1 and e_1

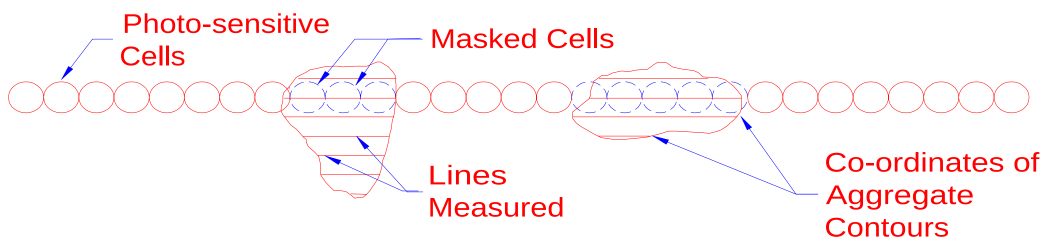

FIGURE 14 Principle of Image Capturing and Processing

In this process, two shape parameters are calculated using measured image dimensions. They are average elongation factor (AEF) and flattening factor (FF). The mathematical definition of AEF and FF are: (*36*)

$$AEF = \frac{\sum \frac{L_i}{G_i}}{n}$$

$$FF = \frac{\sum V_{ti}}{V_r}$$

where, n	=	number of particles in a given size
V_{ti}	=	theoretical volume of aggregate
V_r	=	real volume of aggregate = m/ρr
m	=	mass of sample
ρr	=	density of sample.

Surface Area Analyzer for Measuring Angularity

Six fine, washed aggregates were sent to Horiba Instruments, Inc., at its Irvine, California, laboratory for analysis using the Surface Area Analyzer (Model SA-9600). These aggregates, with the same gradation as those used in the FAA test, represented two each with high, medium, and low angularity. Both manufactured and natural aggregates were included in this test program. Researchers believed Horiba's device might provide useful information related to particle angularity and texture. Horiba's process measures specific surface area using adsorption and desorption of nitrogen gas. This process is a very quick and repeatable method for measuring surface area of small particles.

FAA VERSUS PERFORMANCE IN THE SHRP LTPP DATABASE

The Long-Term Pavement Performance (LTPP) program is a comprehensive program designed to meet a wide range of pavement information needs. This program was initiated by the Transportation Research Board (TRB) under the sponsorship of FHWA during early 1980s (*37*). The American Association of State Highway and Transportation Officials (AASHTO) cooperated with this program. Under this program, a wide range of information was collected in a database. The data collection process began in the late 1980s. The type of pavement data collected includes but is not limited to: various design features, traffic, environments, materials, construction quality, maintenance types, etc. The overall objective of the LTPP program is to assemble information that can be used to increase pavement service life by investigation of the various design, construction, and performance features (*37*). One of the main objectives is to establish a national long-term pavement database to support present and future needs. In the last 10 years, the program has collected enormous amounts of pavement data. The latest database software from LTPP is DataPave ‘97. It includes more than 2500 in-service test sections being monitored throughout North America over a 20-year period.

This subtask was conducted to analyze the relationship between FAA and rutting in actual HMA pavements. For the statistical analysis, the data for FAA and pavement rut depths were retrieved from the SHRP LTPP database. Data from both General Pavement Studies (GPS) and Specific Pavement Studies (SPS) test sections were utilized. Test sections were identified which contained both FAA and rutting data. Attempts were made to find relationships between FAA and rutting on the basis of other parameters like asphalt content, and aggregate gradation (percentage of passing #4 aggregate, and percentage of passing #200 filler content).

EFFECTS OF FINE AGGREGATES ON RUTTING RESISTANCE

Almost at the end of this study, a limited sub-study was initiated to examine the effect of fine aggregates on rutting resistance using the APA machine. The main objective of this part of study was to evaluate the different fine aggregate angularity measuring method using the rutting produced by APA. Six fine aggregates were selected for this study. They are: crushed river gravel (TX # 2) supplied by Fordyce, McAllen, Texas; crushed granite (GA # 5) supplied by Martin Marietta, Forsyth Quarry, Georgia; crushed limestone (TX # 1) supplied by Vulcan Materials, Brownwood, Texas; sub-rounded natural sand obtained from Brazos county, Texas; and Blend 1 & 2. Blend 1 consists of 85 percent GA # 5 and 15 percent natural sand. Blend 2 consists of 70 percent TX # 1 and 30 percent natural sand. These six aggregates were selected to obtain a wide range of FAA value.

Researchers performed Superpave volumetric mix design with these fine aggregates. The fine aggregate angularity were measured using FAA, CAR, direct shear test, image analysis by WSU, and image analysis by VTRC method.

Superpave Volumetric Mix Design

The gradation selected for this study was below the restricted zone. The same combined aggregate gradation was used for all six mixtures. Coarse limestone aggregate supplied by Vulcan Materials, Brownwood, Texas was used in all mixtures. Researchers selected a traffic level of 3-10 million ESALs for design purposes. For the selected traffic level and representative climate site, N_{ini}, N_{des}, and N_{max} are 8, 96, and 152, respectively, for the Superpave gyratory compactor. Specimens for the volumetric analysis were compacted to 152 gyrations (N_{max}).PG 64-22 was selected for these conditions using a 98 percent reliability level. Each one of the aggregate blends had a 19-mm nominal maximum size.

With a few exceptions, most of the Superpave design criteria were met. Voids in the mineral aggregates (VMA) at design gyrations for mixture design of natural sand and Blend 2 did not meet the Superpave minimum VMA requirements.

CHAPTER IV

RESULTS AND DISCUSSION

LABORATORY TEST RESULTS

FAA Test

Ninety-two fine aggregates were collected from 23 different state DOTs. Angularity and mineralogy of the samples varied widely. FAA was determined for 44 of the aggregates from 13 states. FAA values ranged from 37 to 50. According to ASTM C-1252, the results of two properly conducted FAA tests by the same operator on similar samples should not differ by more than 0.37 percentage point. Most of the samples followed this trend but a few samples did not. It is noteworthy that a difference in specific gravity of 0.05 can change the calculated uncompacted voids by approximately one percentage point. Table 2 contains the FAA test results.

FAA tests were also performed on the three fine aggregates used in the subsequent restricted zone analysis. According to subjective evaluations by state DOT representatives and aggregate suppliers, all three of these aggregates have demonstrated good field performance even though two of them have FAA values lower than 45. According to Superpave, these two aggregates do not qualify for use in a high traffic surface course mix.

ASTM C-1252 and AASHTO T-304 state that bulk dry specific gravity of the fine aggregate should be determined on the minus 4.75 (No. 4) material, implying that minus 4.75 mm as-received material should be used. The method further state that one should use this value in subsequent calculations unless the specific gravity of some size fractions differ by more than 0.05 from the specific gravity typical of the complete sample, in which case, the specific gravity of the fraction (or fractions) being tested must be determined. It appears that, in some cases, the

TABLE 2 Fine Aggregate Angularity Test Data

Sample ID	FAA Test 1	FAA Test 2	FAA Avg.	Sample ID	FAA Test 1	FAA Test 2	FAA Avg.
AR # 1	42.78	42.36	42.6	MS # 2	37.97	38.09	38.0
AR # 2	39.69	39.74	39.7	MS # 3	41.18	40.82	41.0
AR # 3	38.06	38.26	38.2	MS # 4	39.94	38.96	39.2
AR # 4	39.40	39.61	39.5	MT # 1	44.06	43.81	43.9
CT # 1	42.73	43.16	42.9	MT # 2	44.45	44.29	44.5
CT # 2	45.65	45.94	45.8	MT # 3	48.01	48.22	48.1
CT # 3	45.90	46.29	46.1	MT # 4	46.77	46.42	46.6
CT # 4	46.69	46.58	46.6	NC # 1	43.33	43.03	43.2
GA # 1	46.10	45.84	46.0	NC # 2	44.60	44.72	44.7
GA # 2	42.49	43.16	42.8	NC # 3	42.18	41.99	42.1
GA # 3	46.19	47.39	46.8	NC # 4	39.64	39.17	39.4
GA # 4	47.29	48.02	47.7	NE # 1	46.10	46.24	46.2
IA # 1	42.53	43.04	42.8	NE # 2	44.28	44.41	44.4
IA # 2	45.82	45.66	45.7	NE # 3	45.30	46.41	45.9
IA # 3	37.01	37.41	37.2	NE # 4	37.61	37.39	37.5
IA # 4	37.96	38.88	38.4	NM # 2	47.89	47.85	47.9
IN # 1	39.82	39.85	39.8	SC # 1	50.35	50.68	50.5
IN # 2	39.16	39.18	39.2	SC # 2	45.50	45.67	45.6
KY # 1	43.29	43.60	43.5	SC # 3	43.33	43.65	43.5
KY # 2	44.14	45.16	44.7	SC # 4	49.57	49.23	49.4
KY # 3	48.29	47.97	48.1	*GA # 5	47.88	48.09	48.0
KY # 4	47.50	47.64	47.6	*TX # 1	43.52	43.37	43.5
MD # 2	42.79	42.48	42.6	*TX # 2	44.29	44.25	44.3
MS # 1	40.41	40.16	40.3				

* These aggregates are also used in restricted zone study.

specific gravity of the minus 4.75 mm as-received material may differ from that for the Method A gradation by more than the amount allowed by these standards. (Recall, the Method A grading is required by Superpave.) If the specific gravity of the Method A grading is not measured, one would not know how much the values differed. If the specific gravity of the Method A grading is measured, clearly, it should be used in the calculation of uncompacted void content. For materials with borderline FAA values, it would probably be best to use the specific gravity of the fine aggregate grading used in the FAA test.

Direct Shear Test

Twenty-three fine aggregates were chosen based on the FAA test results for direct shear testing. The selected samples represent a wide range of FAA values. These materials included the fine aggregates used in the restricted zone analysis. Direct shear tests were conducted using air dry samples with the same gradation (ASTM C-1252, Method A) as that used in FAA testing. Three different normal loads (2399, 6804, and 11,260 kPa or 348, 987, and 1633 psi, respectively) were used in these tests. The rate of shear strain was 1.27 mm/min (0.05 inch/minute). Ultimate shearing stress versus corresponding normal stress was plotted and a best fit line was constructed. The slope of the trendline gives the angle of internal friction. Duplicate tests were performed on each sample, and the results were averaged. In some cases, considerable variation in two test results on similar samples was observed. Results of these tests are summarized in Table 3. The AIF values for the 23 aggregates ranged from 37.5 to 48.5 degrees. These values provide significant differences.

TABLE 3 Direct Shear Test Data

Sample ID	Angle of Internal Friction (Degree)			Sample ID	Angle of Internal Friction (Degree)		
	Test 1	Test 2	Average		Test 1	Test 2	Average
AR # 3	42.20	39.57	40.9	MS # 2	37.68	37.33	37.5
CT # 1	48.71	46.30	47.5	MT # 3	42.88	44.80	43.8
GA # 1	39.12	40.07	39.6	NC # 2	42.95	41.50	42.2
GA # 2	42.69	41.00	41.9	NC # 4	42.52	41.94	42.2
GA # 3	43.12	41.26	42.2	NE # 2	48.71	46.30	47.5
GA # 4	40.78	39.21	40.0	NM # 2	47.84	49.08	48.5
IA # 3	40.76	40.76	40.8	SC # 1	42.27	40.43	41.4
IN # 1	45.71	43.90	44.8	SC # 4	45.60	46.78	46.2
IN # 2	41.37	42.02	41.7	GA # 5	41.93	43.27	42.6
KY # 2	45.83	42.70	44.3	TX # 1	45.12	45.36	45.2
KY # 3	45.18	42.36	43.8	TX # 2	41.56	39.38	40.5
MD # 2	47.04	46.83	46.9				

Compacted Aggregate Resistance Test

CAR tests were performed on the 23 selected aggregates. Results of the tests on materials containing 1.75 percent moisture are shown in the Table 4. The CAR test method appears to be very sensitive to aggregate angularity. Most of the samples were tested using a conventional Marshall machine, however, the resistance value of some aggregates exceeded the limits of the machine (10,000 lb or 44480 N). Resistance value of those aggregates was measured using Instron machine. The resistance value of two aggregates (KY # 2 and KY # 3) even exceeded the limits of the Instron (22,500 lb or 100,080 N). The CAR value for those materials was reported as 22,500+ lb. For each of the aggregates, triplicate CAR tests were conducted and the average of the three values rounded to the nearest whole number was reported as CAR value. The rate of vertical deformation was 2.0 inches/minute (50.8 mm/min). The CAR value for these 23 aggregates varied from 202 lb (898 N) to 22,500+ lb (100,080 N), indicating this test offers much more sensitivity than either the FAA test or the direct shear test.

TABLE 4 Compacted Aggregate Resistance Test Data

Sample ID	Stability Value (lbs)				Sample ID	Stability Value (lbs)			
	Test 1	Test 2	Test 3	Avg.		Test 1	Test 2	Test 3	Avg.
AR # 3	400	250	325	325	MS # 2	211	415	--	313
CT # 1	1700	1330	1360	1463	MT # 3	3050	2800	3200	3017
GA # 1	280	200	225	235	NC # 2	1175	1340	1360	1292
GA # 2	200	275	130	202	NC # 4	500	650	675	608
GA # 3	780	860	915	852	NE # 2	20000	19560	19850	19803
GA # 4	430	450	500	460	NM # 2	5070	5095	6095	5420
IA # 3	260	325	275	287	SC # 1	1475	1325	1500	1433
IN # 1	925	1425	875	1075	SC # 4	6100	5600	6550	6083
IN # 2	750	715	825	763	GA # 5	2310	2151	--	2231
KY # 2	22500	22500	--	22500	TX # 1	19410	15590	17400	17467
KY # 3	22500	22500	--	22500	TX # 2	1452	1344	--	1398
MD # 2	15640	16950	12620	15070					

- - Data not available

Those aggregates containing relatively high amounts of minus No. 200 material exhibited the highest CAR values when graded (unwashed) in accordance with Method A. The researchers suspected this phenomenon may have been partially due to surface tension generated by the presence of water and the ultra fine particles. Further, it appears that effects of the water on CAR values may vary with the specific surface area and/or water absorption of the specimens. Therefore, two aggregates with a very high CAR values (KY # 2 and KY # 3) and two with a very low CAR values (GA # 1 and GA # 2) were selected for further CAR testing using different moisture contents. The objective of this testing was to determine the effect of moisture content on the CAR value and identify an optimum moisture content where the CAR value is least affected by moisture (such as dry or saturated).

Results of the moisture tests are plotted in Figure 15. Limited quantities of fine aggregates restricted the number of tests in this work element. The tests revealed a consistent relationship between the CAR value and moisture content for the two aggregates with very high

(A) Aggregate GA # 1

m/c %	CAR Stability (N)
1.00	1215
1.75	1046
2.50	1682
5.00	1558
6.00	1825
8.00	1780
10.00	2114
15.00	2336

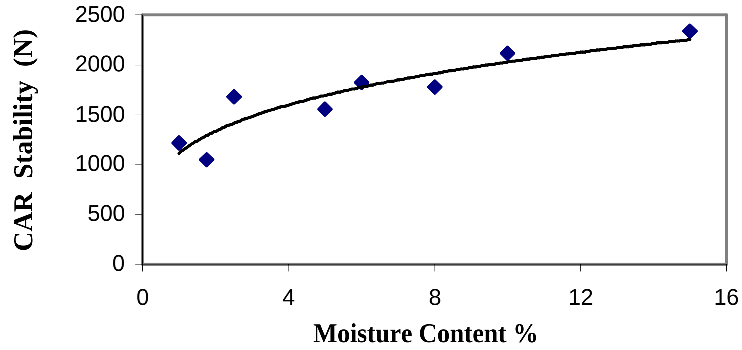

(B) Aggregate GA # 2

m/c %	CAR Stability (N)
1.00	1896
1.75	899
2.50	2234
8.00	2670
15.00	1669

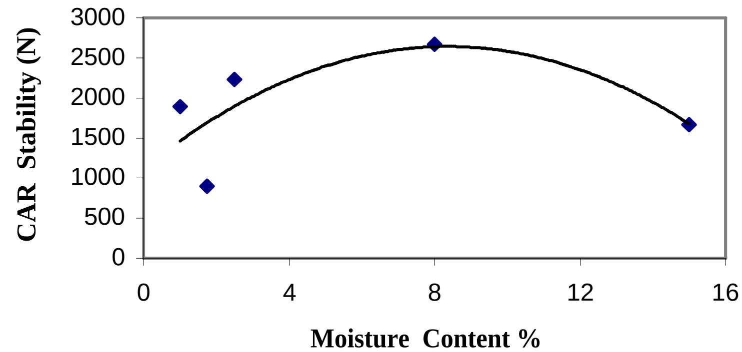

(C) Aggregate KY # 2

m/c %	CAR Stability (N)
0.00	17778
1.00	81012
1.75	100125
2.50	63168
6.00	52955

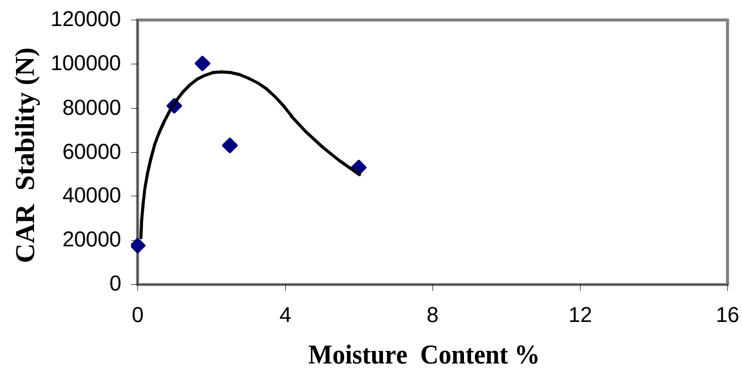

(D) Aggregate KY # 3

m/c %	CAR Stability (N)
0.00	30385
1.00	89000
1.75	100125
6.00	56159
7.00	70177

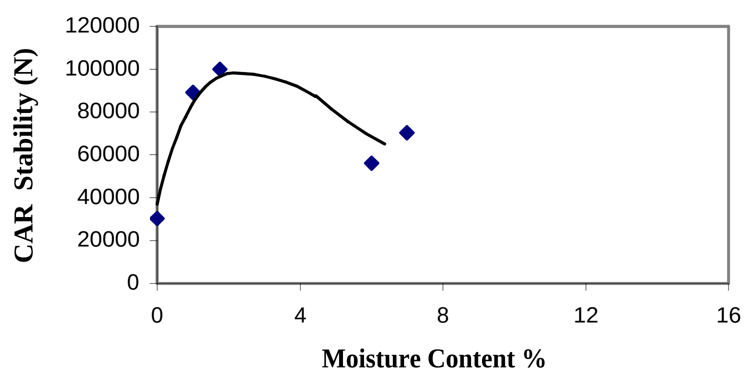

FIGURE 15 CAR Stability at Different Moisture Content

CAR values and relatively high filler contents. The peak CAR value is attained at about 2 percent moisture content for KY # 2 and KY # 3. The two samples with low CAR values also show fairly consistent pattern. However, they reach their peak value at much higher water content. Anyway, a significant effect of moisture is noticed. So, more work is needed.

In addition the results from this study, findings from CAR tests conducted at different places are included in Appendix C.

Hough Transform Method

Twenty-three fine aggregate samples were tested using the Automated Aggregate Shape Analysis technique (*8*) which incorporates a Hough Transform algorithm. Shape and texture of individual aggregate particles were quantified directly using a video-based, computer-controlled imaging system.

In this process, shape attributes are used by a neural network classifier to calculate a single number classification index termed K, which ranges from 0 to 1. The neural network has been "trained" by a panel of expert judges representing agencies from several states.

The K-index is computed for a two-dimensional image from a combination of several different indices: S, E, R, T, and several harmonic components of the S(q) function. The S-index is used to identify an outline with one or more long straight edges. R-index describes the roundness of the image. E-index denotes the elongation characteristics of the image. T-index refers to the surface texture of the image. Harmonic components are very similar to the slope density function of an image outline. The K-index was determined for approximately 500 particles of each aggregate to maximize statistical validity of the data. The median of K-index (for approximately 500 particles) is considered as the K-index for the particular aggregate sample. Table 5 contains the results of this test method.

The samples used for these tests were divided into two size classes: large and small. The large size consists of – No. 4 to + No. 16 and small size consists of – No. 16 to + No. 50 size particles. The large size particles of all 23 fine aggregates and small size particles from three aggregates (representing low to high angularity from natural and manufactured

TABLE 5 Hough Transform Results

Sample ID	K-Index	Sample ID	K-Index
AR # 3	0.45	MS # 2	0.47
CT # 1	0.53	MT # 3	0.64
GA # 1	0.65	NC # 2	0.51
GA # 2	0.59	NC # 4	0.48
GA # 3	0.66	NE # 2	0.62
GA # 4	0.63	NM # 2	0.62
IA # 3	0.48	SC # 1	0.64
IN # 1	0.48	SC # 4	0.64
IN # 2	0.43	GA # 5	0.61
KY # 2	0.59	TX # 1	0.60
KY # 3	0.66	TX # 2	0.63
MD # 2	0.61		

sources) were tested. It is noteworthy that there were no significant differences between the K-indices of large particles and small particles from the same aggregate. Table 5 contains the test results of larger particles only.

The Hough transformation technique for characterizing aggregate particle shape and texture is still in the developmental stage. Improvements are necessary to make it commercially viable for routine measurement of aggregate angularity and texture.

Image Analysis at WSU

Researchers sent 23 aggregates to WSU for testing using image analysis. The WSU technique calculates three different parameters of fine aggregates. They are: surface parameter, fractal length, and form factor. Results of this method are included in Table 6.

TABLE 6 WSU Image Analysis Test Result

Sample ID	Surface Parameter	Fractal Length	Form Factor	Sample ID	Surface Parameter	Fractal Length	Form Factor
AR # 3	1.70	0.04	0.82	MD # 2	2.74	0.13	0.47
CT # 1	3.10	0.17	0.42	MS # 2	1.80	0.06	0.59
GA # 1	3.60	0.10	0.60	MT # 3	4.32	0.12	0.15
GA # 2	1.84	0.12	0.53	NC # 2	1.78	0.11	0.57
GA # 3	3.80	0.15	0.57	NC # 4	1.18	0.09	0.64
GA # 4	2.90	0.16	0.55	NE # 2	2.34	0.22	0.36
GA # 5	4.48	0.21	0.33	NM # 2	3.30	0.17	0.47
IA # 3	1.50	0.07	0.76	SC # 1	3.90	0.16	0.44
IN # 1	2.10	0.10	0.74	SC # 4	4.04	0.17	0.45
IN # 2	0.97	0.02	0.69	TX # 1	2.88	0.14	0.48
KY # 2	3.50	0.13	0.48	TX # 2	3.60	0.14	0.52
KY # 3	3.28	0.19	0.45				

In this method, only one size of aggregate (- No.16 to + No. 30) was used, even though it is capable of using other sizes of particles. The surface parameter was calculated using the surface erosion-dilation technique. The values of the surface parameter range from 0.97 to 4.48. Higher surface parameter values indicate higher angularity. This range appears quite sensitive to the particle shape. In this case, a low level of magnification (38 X) was used to identify the shape attribute.

Fractal length is another parameter used to describe the shape attribute. Higher fractal length values indicate higher surface irregularity. FL was measured using a high level of magnification (312 X). The value of fractal length varies from 0.02 to 0.22. Fractal length is not as sensitive as surface parameter.

The form factor is derived from a mathematical equation. The measured value of FF ranges from 0.15 to 0.82. The FF of a perfect circular object is one. For all other cases, the value is less than one. Lower FF values indicate higher surface irregularity. Form factor measured at high resolution actually indicates surface texture property rather than shape property. In this case, low level resolution was used to identify the shape property.

These three parameters were compared with the results obtained from other test methods. Comparisons with FAA and the two other image analysis methods are described in two different subsections. Surface parameter, fractal length, and form factor are plotted against log of CAR values (Fig. 16, 17, and 18, respectively). These plots suggest poor to fair correlations with log of CAR stability. The coefficient of determination (R^2) value for SP, FL, and FF are 0.16, 0.35, and 0.32, respectively. Although no plots are shown, these three WSU parameters also exhibit poor to no correlation with the angle of internal friction, with R^2 of 0.05, 0.3, 0.2, for SP, FL, and FF, respectively.

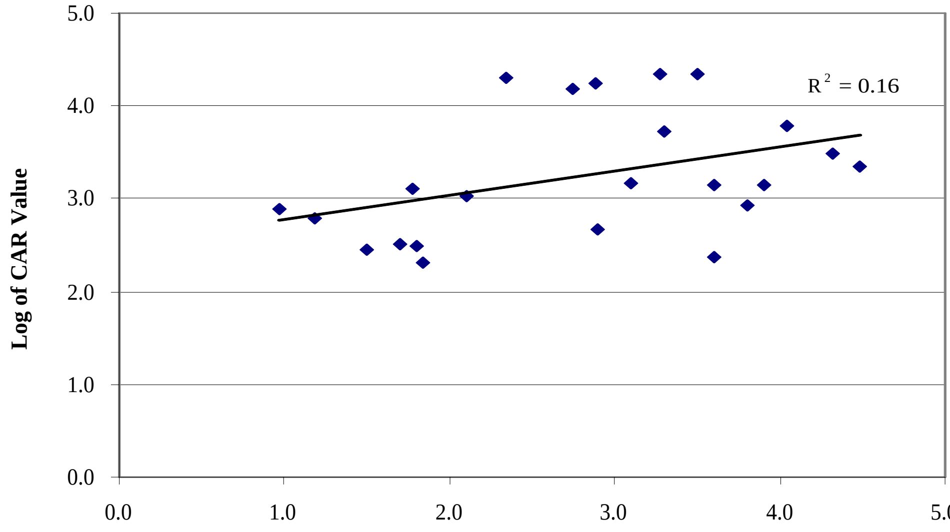

FIGURE 16 Log of CAR Value Versus Surface Parameter (WSU)

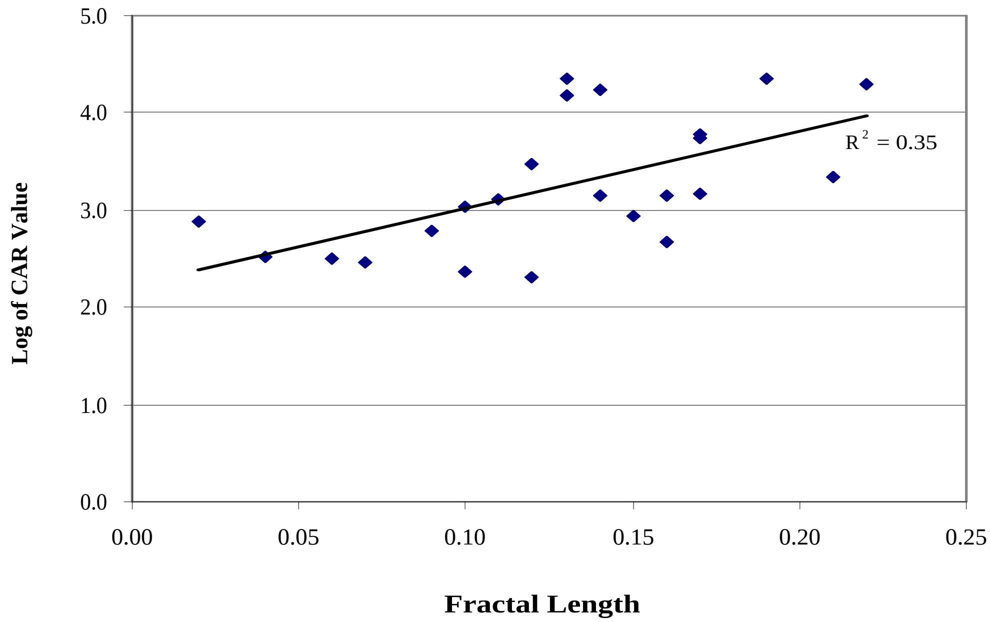

FIGURE 17 Relationship Between Log of CAR Value and Fractal Length (WSU)

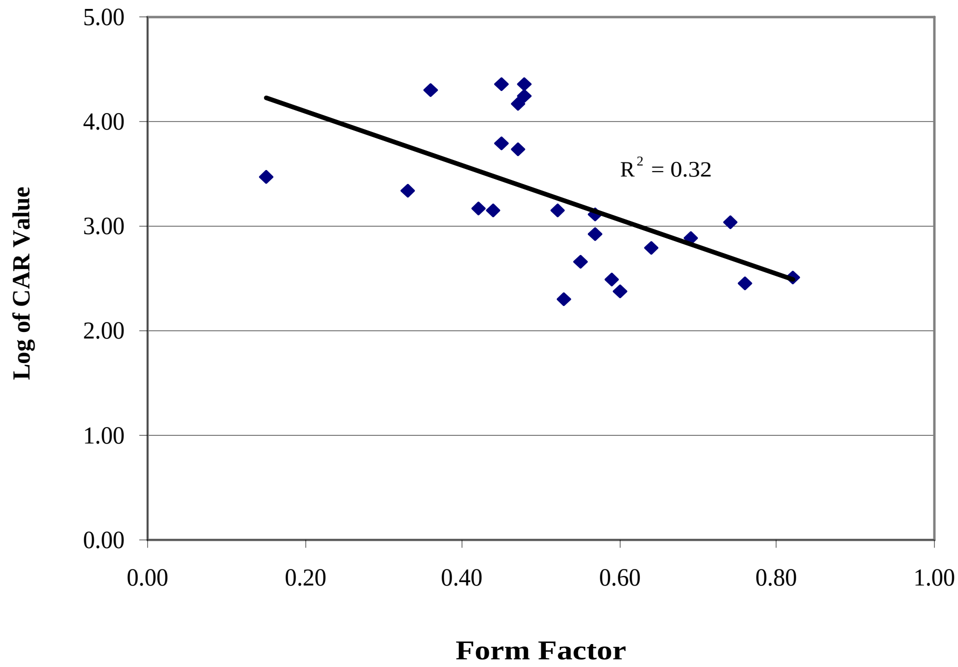

FIGURE 18 Relation Between Log of CAR Value and Form Factor (WSU)1

Image Analysis at VTRC Nineteen fine aggregate samples were sent to VTRC for testing with the VDG-40 video grader. This method yields two parameters termed slenderness ratio and flatness factor. The algorithms are designed particularly to identify elongated and/or flat particles. Results from this test are shown in the following Table 7. Typical outputs from this test are included in Appendix B.

TABLE 7 VTRC Image Analysis Test Results

Sample ID	Slenderness Ratio	Flatness Factor	Sample ID	Slenderness Ratio	Flatness Factor
AR # 3	1.390	0.940	MD # 2	1.585	1.285
CT # 1	1.440	0.955	MS # 2	1.410	0.905
GA # 1	1.450	0.600	MT # 3	1.595	1.040
GA # 2	1.435	0.680	NC # 4	1.405	0.805
GA # 3	1.475	0.700	NE # 2	1.565	1.070
GA # 4	1.485	0.820	NM # 2	1.490	0.995
IA # 3	1.400	1.005	SC # 1	1.515	0.990
IN # 1	1.445	0.855	SC # 4	1.575	1.020
IN # 2	1.445	0.790	TX # 1	1.520	0.875
KY # 2	1.600	1.075	TX # 2	1.510	0.895
KY # 3	1.645	1.125	GA # 5	1.550	1.005

The slenderness ratio values range from 1.390 to 1.645. Slenderness ratio increases with an increase of particle angularity. Flatness factor varies from 0.600 to 1.285. Higher flatness factors indicate higher surface irregularity. The results from the video grader are plotted against log of CAR value in Figures 19 and 20, respectively. These two graphs suggest that there is a strong correlation between CAR and VTRC image analysis method. When the log of CAR value is plotted with slenderness ratio and flatness factor, it has coefficient of determination (R^2) values of 0.78 and 0.60, respectively.

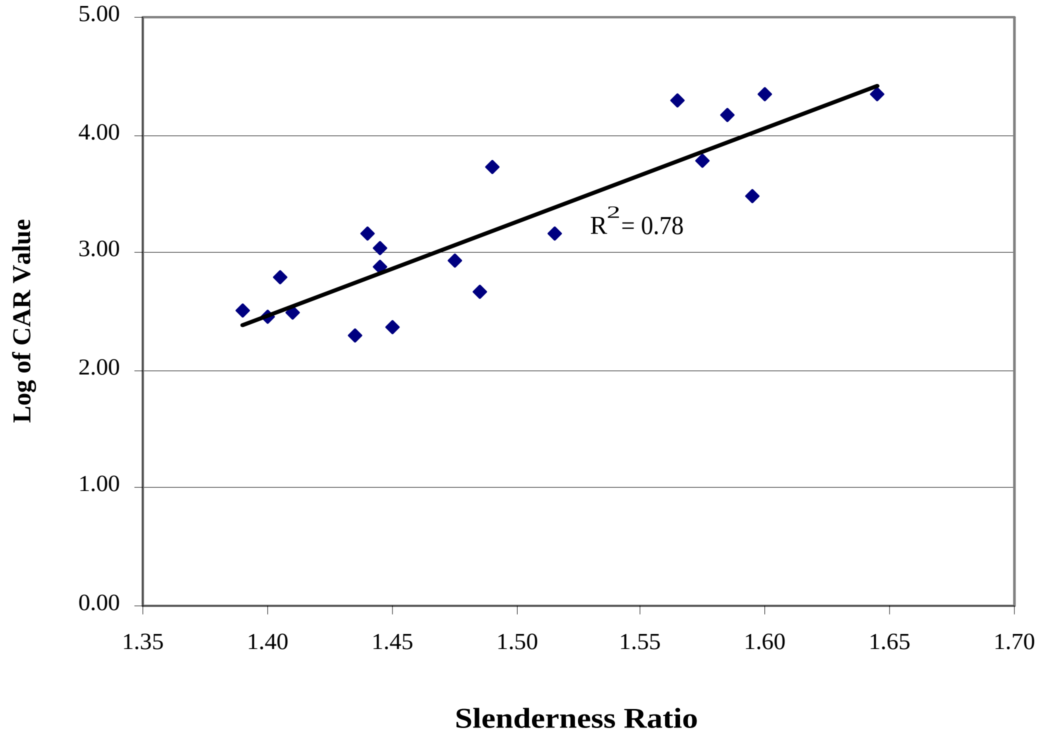

FIGURE 19 Log of CAR Value Versus Slenderness Ratio (VTRC)

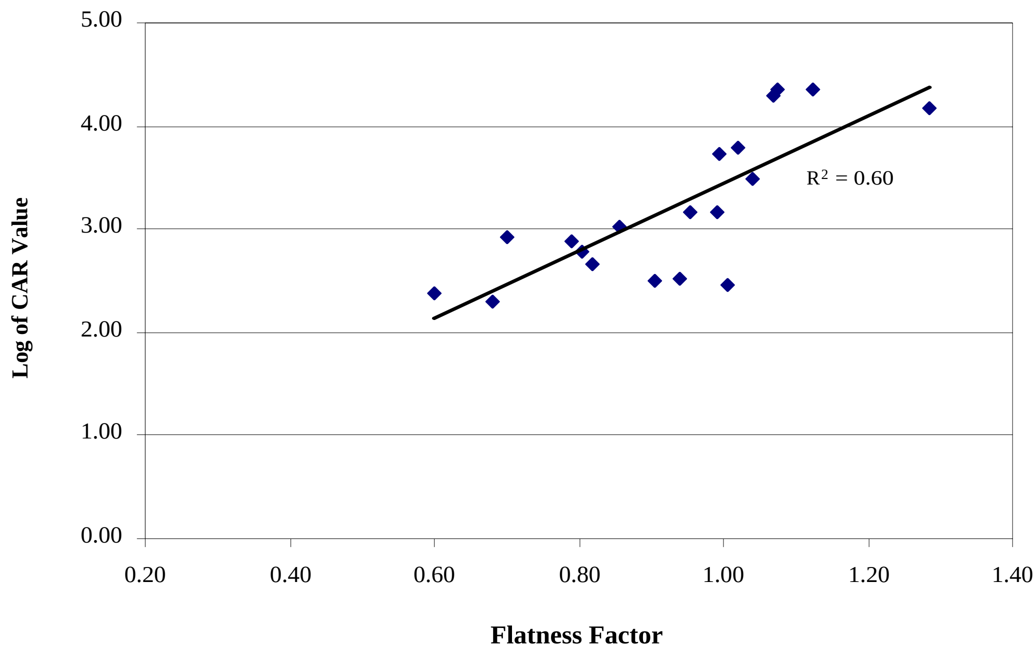

FIGURE 20 Log of CAR Value Versus Flatness Factor (VTRC)

Comparisons Between the Different Image Analyses

The K-index (Hough Transform) was compared with five different parameters from two other image analysis methods. Figures 21, 22, and 23 demonstrate the relationship between K-index and three different particle parameters from WSU method. K-index maintains a good correlation (R^2 = 0.71) with surface parameter (WSU). It also has fairly good correlations with fractal length (R^2 = 0.62) and form factor (R^2 = 0.48). This trend is quite similar to the relation between FAA and these parameters. Figure 24 also shows a good relation between K-index and slenderness ratio. Like FAA, K-index does not show any trend with flatness factor (VTRC).

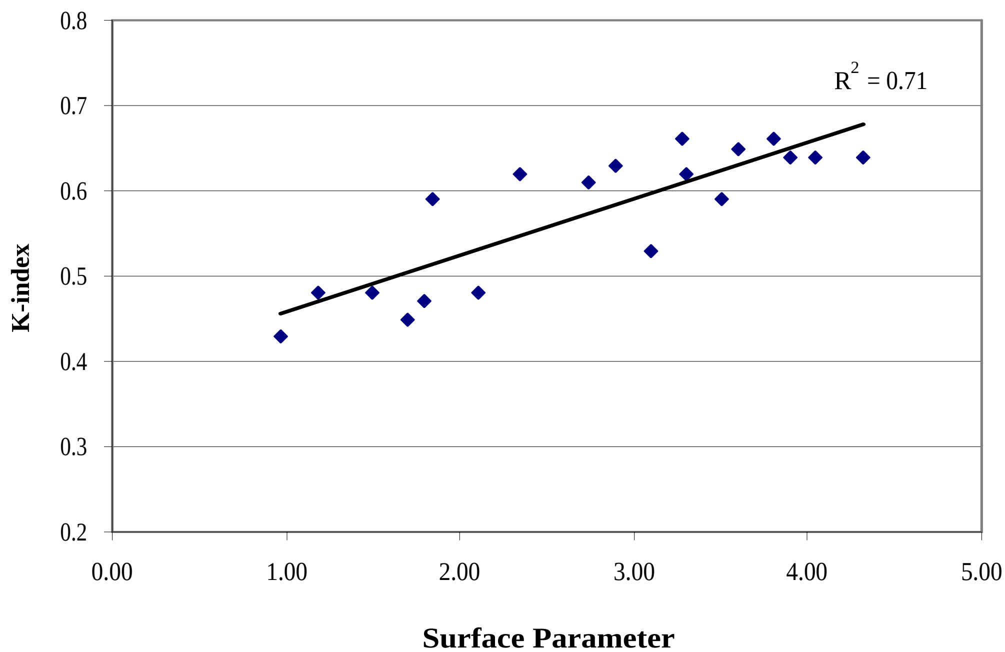

FIGURE 21 K-index (Hough Transform) Versus Surface Parameter (WSU)

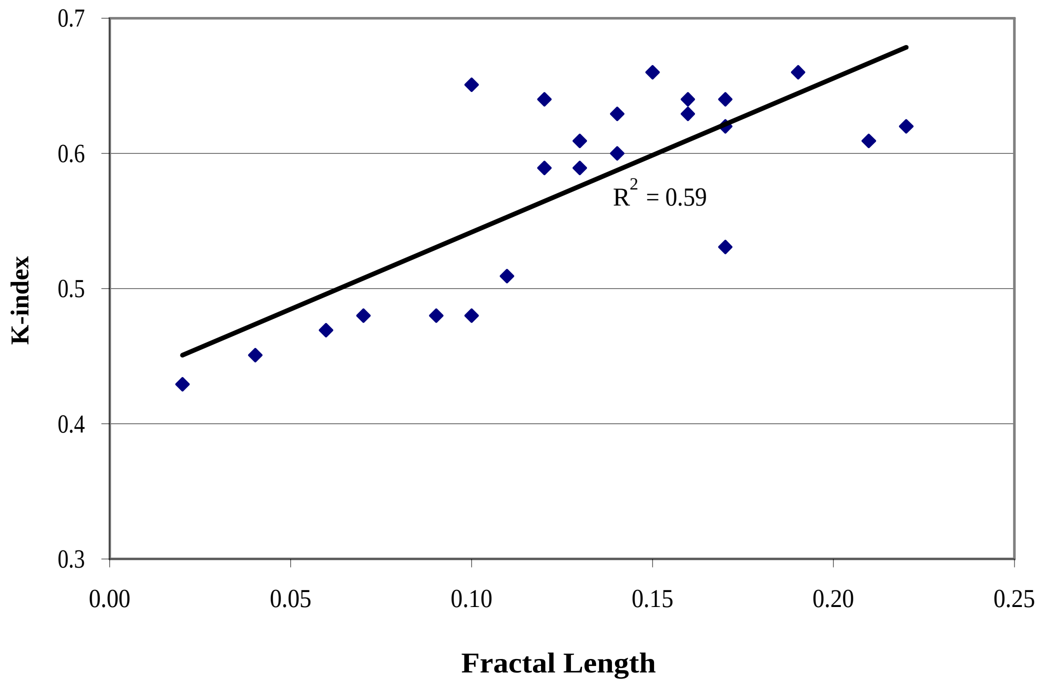

FIGURE 22 K-index (Hough Transform) Versus Fractal Length (WSU)

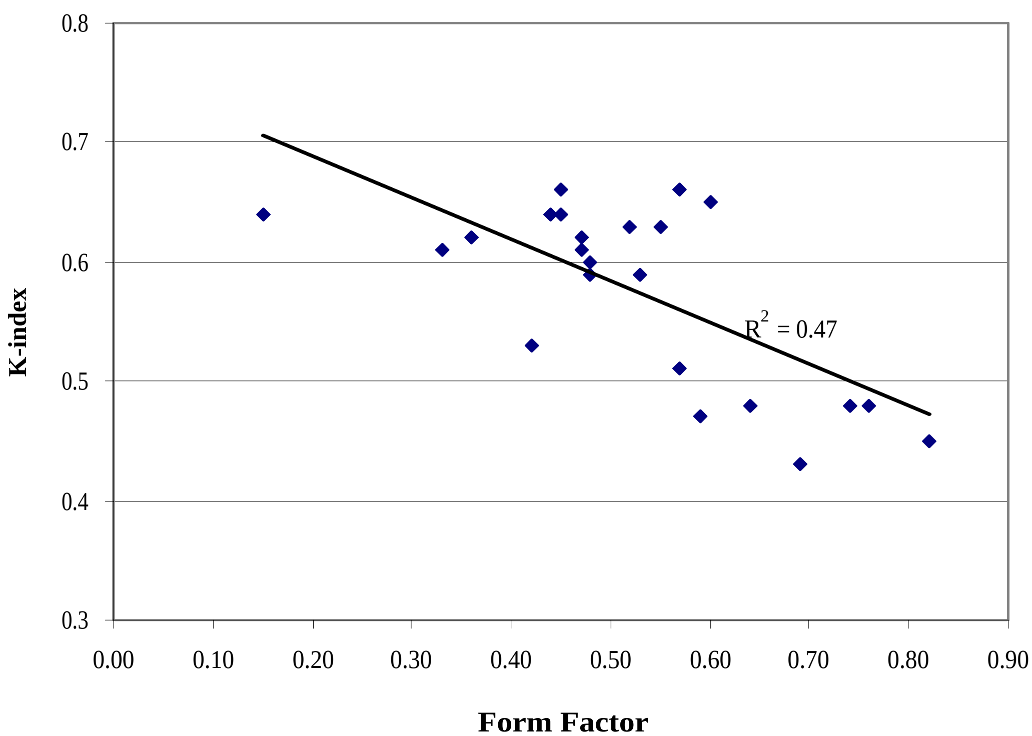

FIGURE 23 K-index (Hough Transform) Versus Form Factor (WSU)

Among the two parameters from VTRC analysis, slenderness ratio consistently shows good correlations with other image parameters and FAA values. But the slenderness ratio and flatness factor show good correlations with log of CAR value, indicating that shear strength of fine aggregate is enhanced by flat and elongated particles.

In most of the cases, the parameters from image techniques show good correlations among themselves. There are a few crushed cubical aggregates (KY # 2, MD # 2, NE # 2, and TX # 1) with FAA values less than 45 but exhibiting high values in all three image analysis methods. Incidentally, they also have good field performance history.

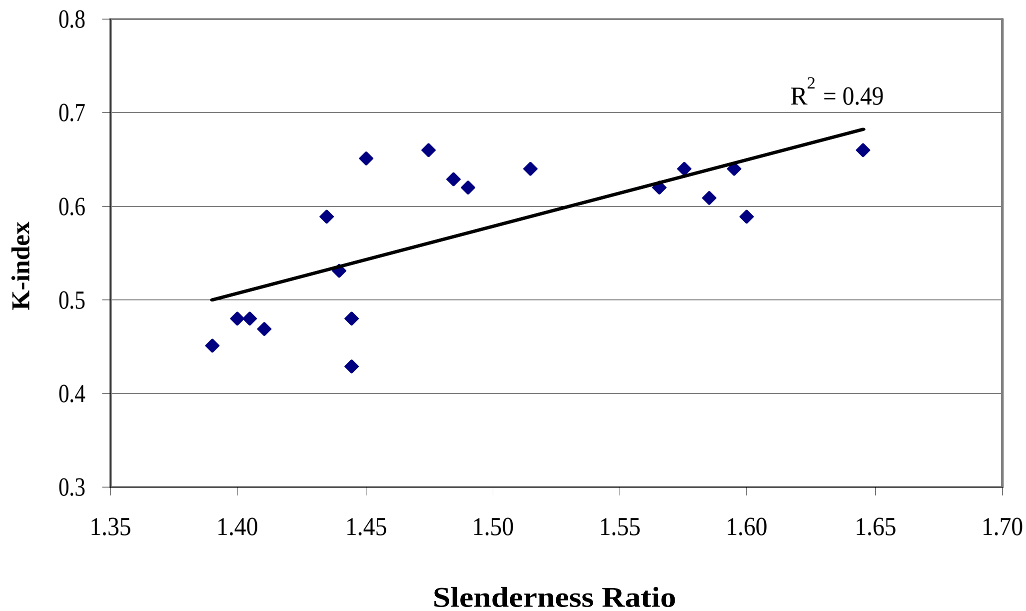

FIGURE 24 K-index (Hough Transform) Versus Slenderness Ratio (VTRC)

Comparison of FAA with Other Test Results

Results of CAR and direct shear tests are compared with FAA values in Figure 25 and Figure 26, respectively. These figures show little to no correlation between AIF and FAA or the logarithm of the CAR values and FAA. However, a fair correlation exists between the logarithm of the CAR values and AIF (Figure 27). A coefficient of determination (R^2) of 0.55 indicates a reasonably good correlation (*38*). These data indicate that direct shear and CAR are measuring similar material properties, but that FAA is influenced by different aggregate properties. The fair correlation between CAR and direct shear test can be attributed to the fact that the two tests evaluate the same type of failure, i.e., shear failure.

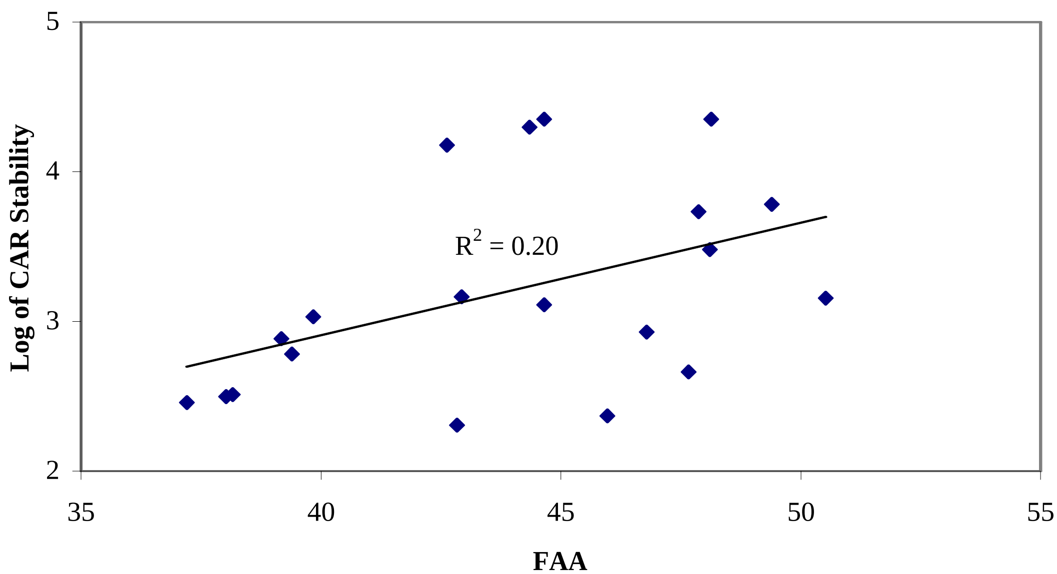

FIGURE 25 Relation Between Logarithmic Value of CAR Stability and FAA

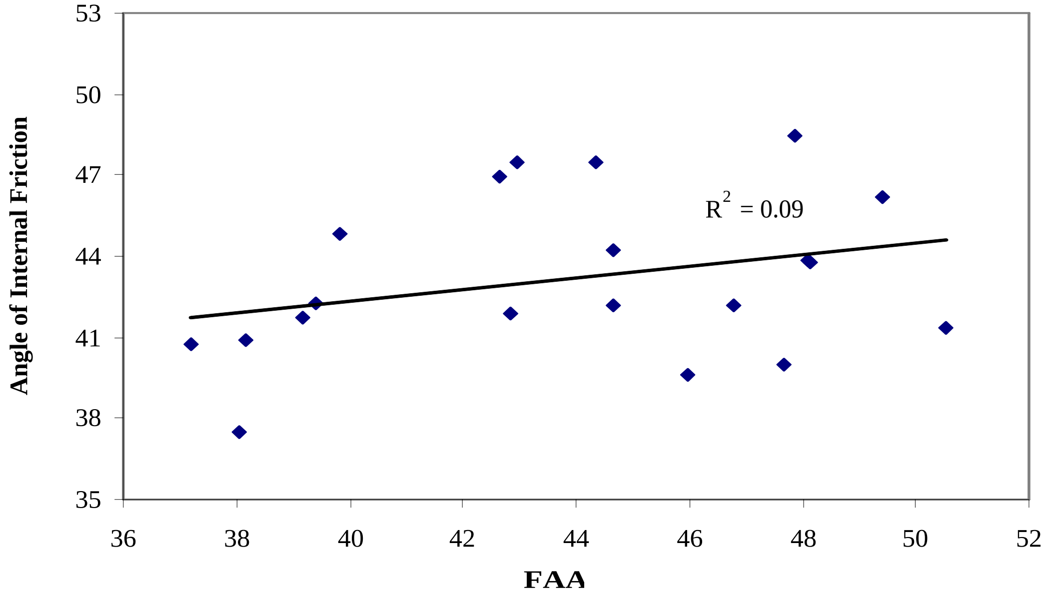

FIGURE 26 Relation Between Angle of Internal Friction and FAA

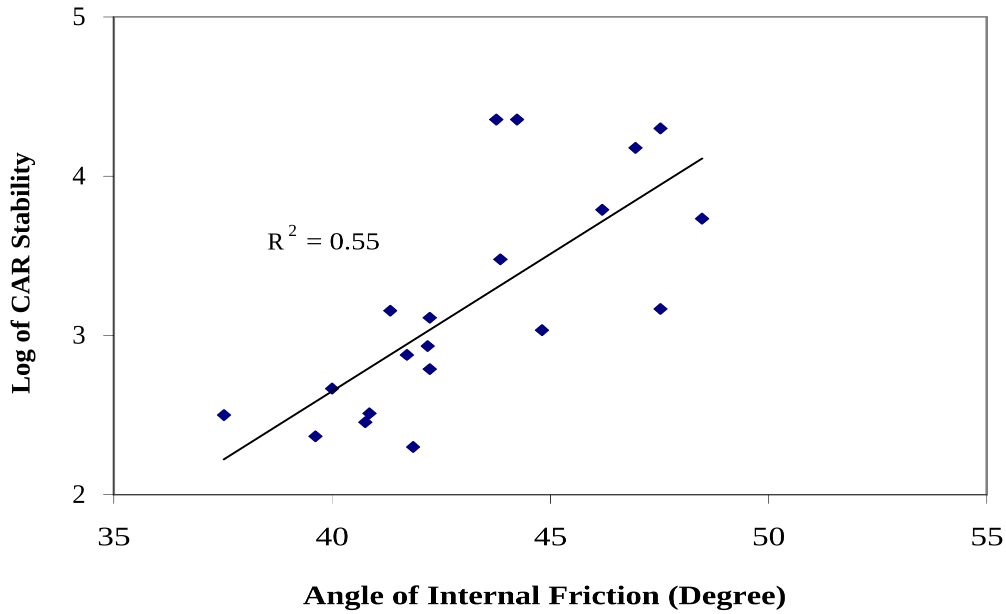

FIGURE 27 Relation Between Logarithmic Value of CAR Stability and Angle of Internal Friction

Tables 3 and 4 show that some aggregates (e.g., KY # 2, MD # 2, NE # 2, and TX # 1) have very high angles of internal friction and CAR values but they cannot meet the Superpave specification for a high volume surface course because their FAA values are less than 45 (43 - 44). According to state DOT personnel, all but one of these aggregates have exhibited good field performance history in HMA pavements. All of them appear as angular and cubical from visual observation with a microscope. Furthermore, all of these aggregates are from calcareous sources such as limestone.

Figure 28 is a bar chart showing CAR values for selected fine aggregates with FAA values between 42.6 and 46.0; all but one value is just below specified value for heavy traffic. Although the FAA values cover only a narrow range, the CAR values cover a very wide range, demonstrating its high sensitivity. The four aggregates with high CAR values are 100% crushed stone fines; whereas, the four of the aggregates with low CAR values are fairly clean natural sands and one is fairly clean partially crushed river gravel (chert/quartzite) fines. Three of the four aggregates with the highest CAR values are rated as good or very good by the state DOT supplying them. Ky #2, a highly angular rough textured product, was rated as bad due to poor soundness values. Based on these selected aggregates, the CAR test appears to separate uncrushed and crushed aggregates much better than the FAA test. This could be, in part, due to the higher filler content of the crushed materials as compared to the sands. Although the TX #2 aggregate contains mostly crushed particles (crushed river gravel and sand), it contains very little filler. Further, HMA made using the crushed river gravel (TX#2 plus its parent material) showed poor rutting performance in the APA and SST. More work is needed to study the effects of water content and filler content of fine aggregates on the very promising CAR test. The authors believe that, ideally, any test to measure angularity of fine aggregate should be performed on the fines in the job mix formula for the HMA. The authors further realize that this process would complicate the practice of qualifying fine aggregate from a given source.

Aggregate SC # 1 yielded the highest FAA value (50.5) of all the aggregates tested in this program but exhibited very low values of AIF and CAR. Its field performance was also rated as poor by the South Carolina DOT (Table 2). According to the SCDOT, the Los Angeles Abrasion value of SC # 1 is 58 percent.

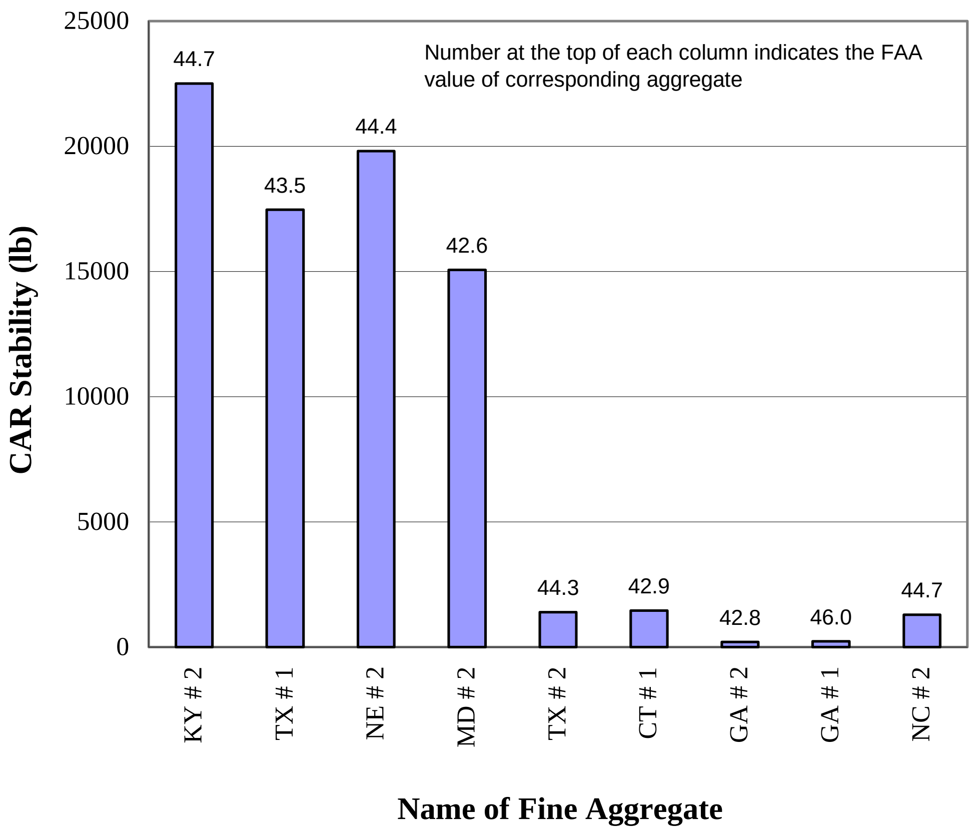

FIGURE 28 CAR Values of Selected Aggregates

K-index values (from Hough Transformation) are plotted against FAA (Figure 29), logarithm of CAR stability value (Figure 30), and angle of internal friction (Figure 31), respectively. No correlation was found between angle of internal friction and K-index. A poor correlation was found between. K-index and CAR stability value. However, a good correlation exists between K-index and FAA values (R^2 = 0.76). An exciting feature of this chart is that there are four crushed calcareous aggregates that are cubical, angular, and all but one have historically shown good performance aggregates which show high values of K-index, even though their FAA values range between 42.6 and 44.6. These same aggregates exhibited very high values of AIF and CAR stability.

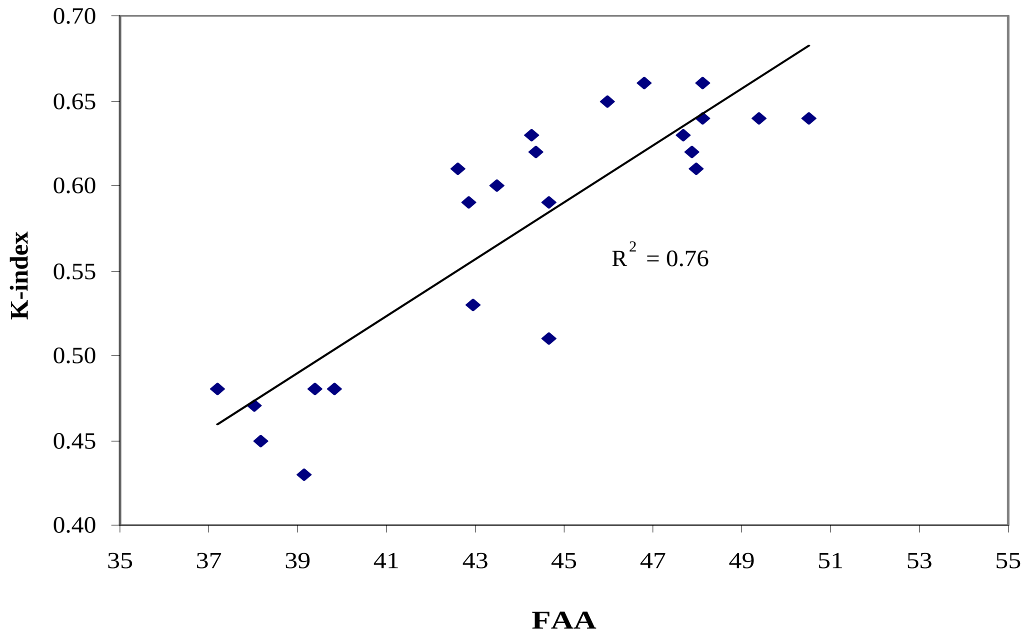

FIGURE 29 K-index Versus FAA Value

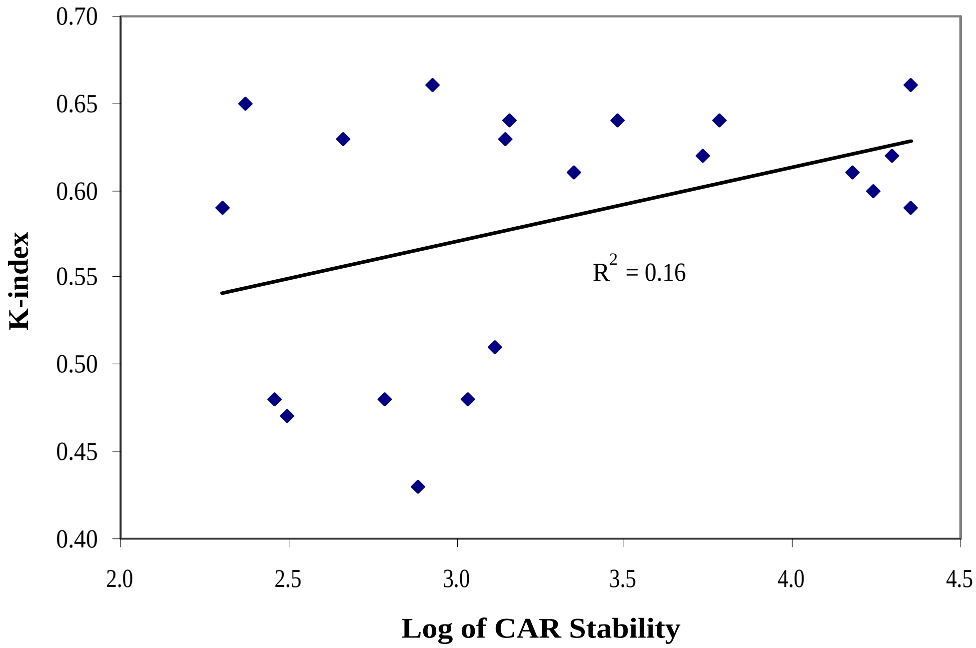

FIGURE 30 Relation Between K-index and Logarithmic Value of CAR Stability

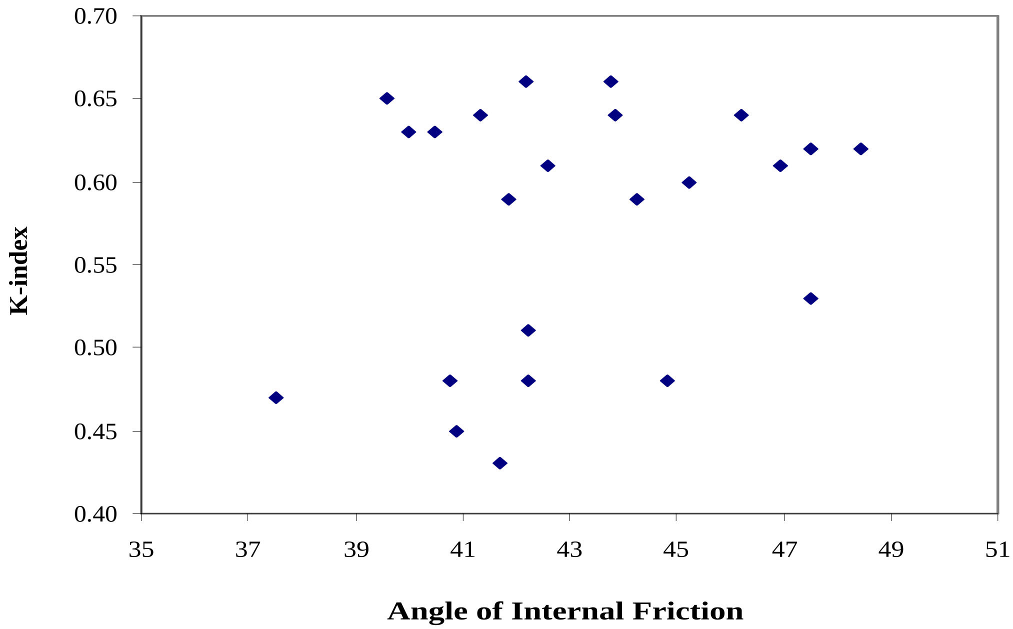

FIGURE 31 Relation Between K-index and Angle of Internal Friction

FAA values are plotted against the three parameters calculated from the WSU image analysis technique. There is good correlation (R^2 = 0.72) between FAA and SP (Figure 32). Fractal length (Figure 33) and form factor (Figure 34) also exhibited fair correlations (R^2 = 0.57 and 0.50, respectively) with FAA values. Surface parameter and fractal length increase with an increase of FAA values. Form factor decreases with an increase of FAA values.

The two parameters measured from the VTRC videograder analysis are also plotted against FAA values. FAA has fair correlation (R^2 = 0.46) with slenderness ratio (Figure 35). No correlation was found between FAA and flatness factor.

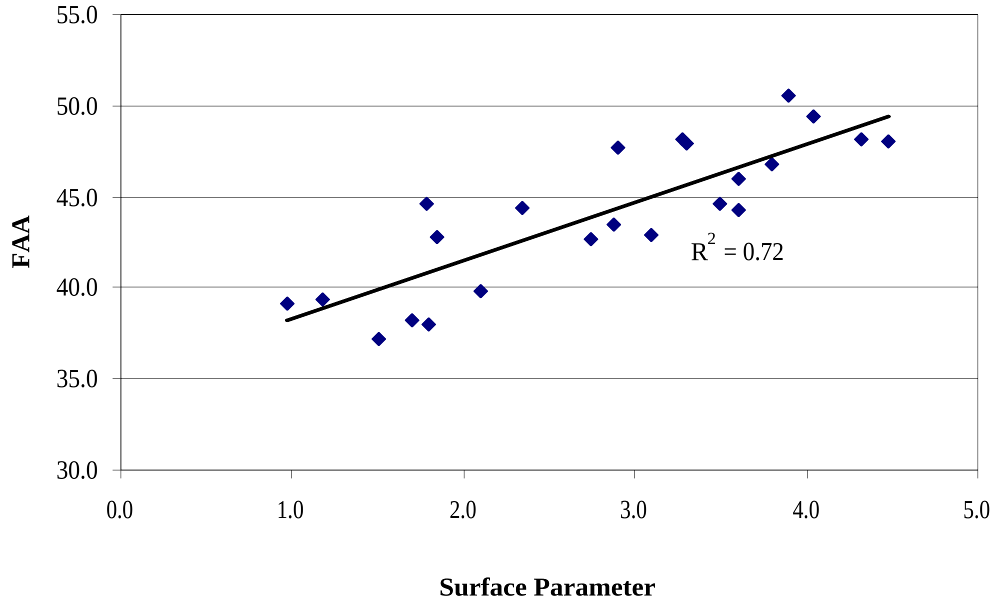

FIGURE 32   FAA Value Versus Surface Parameter (WSU)

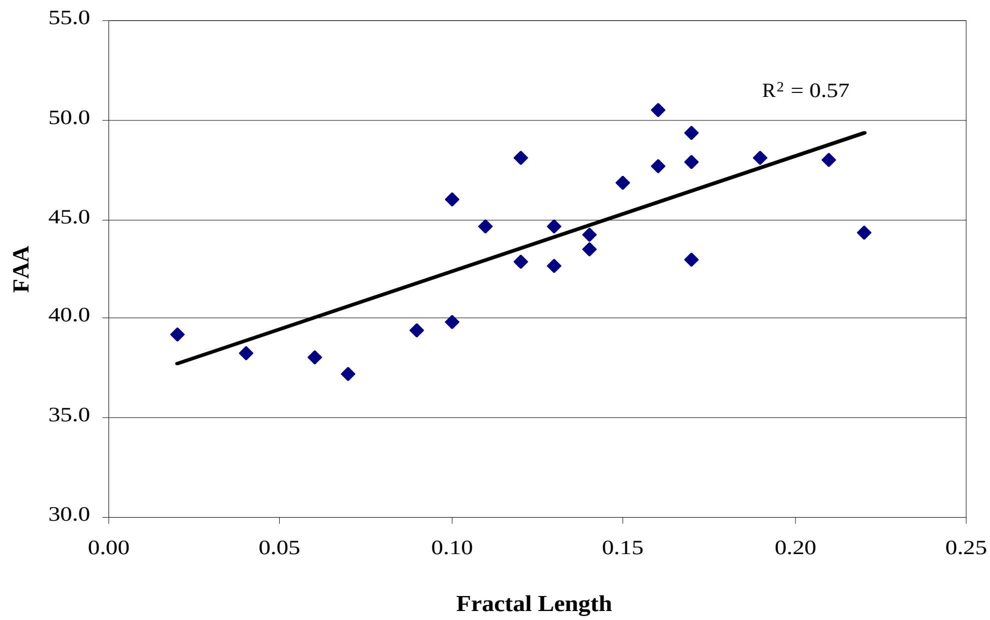

FIGURE 33   FAA Value Versus Fractal Length (WSU)

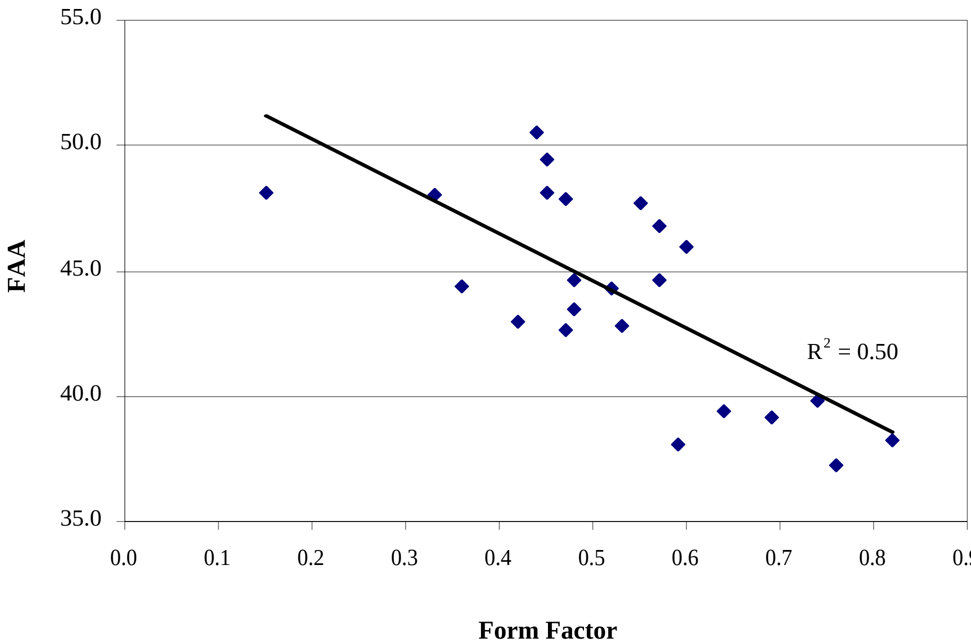

FIGURE 34 Relationship Between FAA Value and Form Factor (WSU)

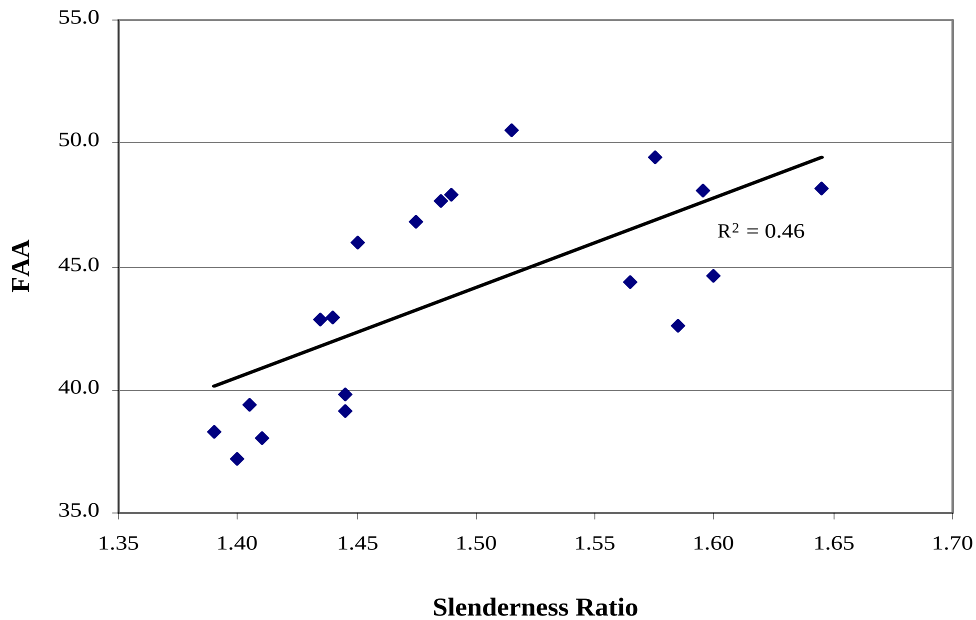

FIGURE 35 FAA Value Versus Slenderness Ratio (VTRC)

The 23 aggregates tested were ranked (Table 8) according to the test results obtained from the six test methods. Both the WSU and VTRC image analysis results provide multiple parameters. One parameter from each method (WSU and VTRC) was chosen for ranking

TABLE 8 Ranking of Each Sample in Descending Order

Aggregate ID	FAA	AIF	CAR	K-Index	Surface Parameter	Slenderness Ratio
SC # 1	1	17	11	5	4	9
SC # 4	2	5	6	6	3	5
KY # 3	3	10	2	2	9	1
MT #3	4	9	8	4	2	3
GA # 5	5	11	9	11	1	7
NM # 2	6	1	7	10	8	11
GA # 4	7	21	18	7	11	12
GA # 3	8	14	15	1	5	13
GA # 1	9	22	22	3	6	14
NC # 2	10	13	13	17	18	- -
KY # 2	11	8	1	15	7	2
NE # 2	12	3	3	9	14	6
TX # 2	13	20	12	8	6	10
TX # 1	14	6	4	13	12	8
CT # 1	15	2	10	16	10	17
GA # 2	16	15	23	14	16	18
MD # 2	17	4	5	12	13	4
IN # 1	18	7	14	19	15	15
NC # 4	19	12	17	20	21	20
IN # 2	20	16	16	23	22	16
AR # 3	21	18	19	22	19	22
MS # 2	22	23	20	21	17	19
IA # 3	23	19	21	18	20	21

- - Data not available

purposes. The parameter which is more closely related to angularity and has more sensitivity was selected for preparation of the ranking. A ranking of 1 in a given column means that the aggregate has the highest value of either FAA, AIF, CAR, K-index, surface parameter, or slenderness ratio. The relative rankings of AIF and CAR values correspond more closely than either of those two (AIF and CAR) correspond with FAA. With some exceptions, rankings by the three image analysis methods are relatively similar. The relative rankings of FAA and K-index correspond more closely than either AIF or CAR values correspond to K-index. Table 8 shows that the relative rankings of aggregates with lower values of FAA correspond more closely to the relative rankings of the other test methods. This observation suggests that the FAA test is less accurate for higher values of angularity.

Visual Inspection

A subjective evaluation for shape and texture for all 23 fine aggregates was performed using a microscope (Table 9). The samples used in this test were washed over a No. 200 (0.075 mm) sieve. Some of the washed aggregates were observed to have very fine filler adhered to larger particles. In most cases, these same aggregates showed very high values from the CAR test, indicating the fine dust may have enhanced shear strength. The samples were classified on the basis of observed shape (angularity) and texture. Four different classifications of shape were identified: angular, subangular, subrounded, or rounded. Texture was classified as smooth, rough, or very rough. Many of the samples were a mixture of particles with different shapes and textures. The subjective evaluation was made on the basis of the dominating type of aggregate particles.

TABLE 9 Visual Inspection Results

Sample ID	Visual Inspection		Sample ID	Visual Inspection	
	Shape	**Texture**		**Shape**	**Texture**
AR # 3	Subrounded	Rough	MS # 2	Subrounded	Smooth
CT # 1	Angular	Rough	MT # 3	Angular	Very Rough
GA # 1	Angular	Very Rough	NC # 2	Subangular	Rough
GA # 2	Subangular	Rough	NC # 4	Subangular	Smooth
GA # 3	Angular	Rough	NE # 2	Angular	Rough
GA # 4	Angular	Rough	NM # 2	Subangular	Clean Quartz
IA # 3	Subrounded	Smooth	SC # 1	Angular	Very Rough
IN # 1	Subangular	Clean Quartz	SC # 4	Angular	Rough (Filler)
IN # 2	Subrounded	Clean Quartz	GA # 5	Angular	Rough
KY # 2	Angular	Rough (Filler)	TX # 1	Subangular	Rough (Filler)
KY # 3	Angular	Rough (Filler)	TX # 2	Subangular	Rough
MD # 2	Ang & Rounded	Smooth & Rough			

The results of all test methods and performance history of the samples are summarized in Table 10.

TABLE 10 Summary of All Tests Results

Sample ID	FAA Value %	AIF Degree	CAR Stability, lb	K-Index	Visual Inspection		Performance History
					Shape	Texture	
AR # 3	38.26	40.88	325	0.45	Subrounded	Rough	Good
CT # 1	42.94	47.51	1463	0.53	Angular	Rough	Poor
GA # 1	45.97	39.60	235	0.65	Angular	Very Rough	- -
GA # 2	42.83	41.85	202	0.59	Subangular	Rough	- -
GA # 3	46.79	42.19	852	0.66	Angular	Rough	- -
GA # 4	47.66	40.00	460	0.63	Angular	Rough	- -
IA # 3	37.21	40.76	287	0.48	Subrounded	Smooth	Poor
IN # 1	39.84	44.81	1075	0.48	Subangular	Clean Quartz	- -
IN # 2	39.17	41.70	763	0.43	Subrounded	Clean Quartz	- -
KY # 2	44.65	44.26	22500	0.59	Angular	Rough (Filler)	Poor
KY # 3	48.13	43.77	22500	0.66	Angular	Rough (Filler)	Good
MD # 2	42.63	46.94	15070	0.61	Angular & Rounded	Smooth & Rough	Well in high vol. traffic
MS # 2	38.03	37.50	313	0.47	Subrounded	Smooth	- -
MT # 3	48.11	43.84	3017	0.64	Angular	Very Rough	- -
NC # 2	44.66	42.22	1292	0.51	Subangular	Rough	Good
NC # 4	39.40	42.23	608	0.48	Subangular	Smooth	Poor
NE # 2	44.35	47.51	19803	0.62	Angular	Rough	Very Good
NM # 2	47.87	48.46	5420	0.62	Subangular	Clean Quartz	Good
SC # 1	50.52	41.35	1433	0.64	Angular	Very Rough	Poor
SC # 4	49.40	46.19	6083	0.64	Angular	Rough (Filler)	Good
GA # 5	47.99	42.60	2231	0.61	Angular	Rough	Very Good
TX # 1	43.47	45.24	17467	0.60	Subangular	Rough (Filler)	Very Good
TX # 2	44.27	40.47	1398	0.63	Subangular	Rough	Good

- - Data not available

TABLE 10 Summary of All Tests Results (Continued)

Sample ID	WSU Method			VTRC Method	
	Surface Parameter	Fractal Length	Form Factor	Slenderness Ratio	Flatness Factor
AR # 3	1.70	0.04	0.82	1.390	0.940
CT # 1	3.10	0.17	0.42	1.440	0.955
GA # 1	3.60	0.10	0.60	1.450	0.600
GA # 2	1.84	0.12	0.53	1.435	0.680
GA # 3	3.80	0.15	0.57	1.475	0.700
GA # 4	2.90	0.16	0.55	1.485	0.820
IA # 3	1.50	0.07	0.76	1.400	1.005
IN # 1	2.10	0.10	0.74	1.445	0.855
IN # 2	0.97	0.02	0.69	1.445	0.790
KY # 2	3.50	0.13	0.48	1.600	1.075
KY # 3	3.28	0.19	0.45	1.645	1.125
MD # 2	2.74	0.13	0.47	1.585	1.285
MS # 2	1.80	0.06	0.59	1.410	0.905
MT # 3	4.32	0.12	0.15	1.595	1.040
NC # 2	1.78	0.11	0.57	- -	- -
NC # 4	1.18	0.09	0.64	1.405	0.805
NE # 2	2.34	0.22	0.36	1.565	1.070
NM # 2	3.30	0.17	0.47	1.490	0.995
SC # 1	3.90	0.16	0.44	1.515	0.990
SC # 4	4.04	0.17	0.45	1.575	1.020
GA # 5	4.48	0.21	0.33	1.550	1.005
TX # 1	2.88	0.14	0.48	1.520	0.875
TX # 2	3.60	0.14	0.52	1.510	0.895

- - Data not available

Surface Area Analysis

The researchers believed that specific surface area of the fine aggregates might be related to particle angularity and texture. Results of surface area measurements obtained using the Horiba Surface Area Analyzer for six aggregates are presented in Table 11. No correlation could be established between the surface area measured by this method with any of the angularity determination tests. One aggregate (KY # 2) exhibited a very large surface area (2.20 m^2/gm), which was almost 30 times higher than the surface area of SC # 1 even though the gradation of all the samples were the same. One possible reason for such high surface area for KY # 2 may be its relatively high porosity.

In this method, surface area is measured using nitrogen adsorption and desorption. Because of the small size of the N_2 molecule, it is reasonable to conclude that the N_2 could enter pores in certain types of fine aggregate particles, adsorb to the surface, and be falsely counted as particle surface area.

The water absorption values, measured during specific gravity testing, are included in Table 11. The Horiba surface area measurements and water absorption are plotted in Figure 36. A very good correlation exists between the surface area of the aggregate measured using this method and its water-absorption value (R^2 = 0.92). Although this procedure is unsuitable for measuring aggregate surface area, it may provide a quick method for estimating asphalt (or water) absorption. Additional testing using the Horiba device was not pursued in this study.

TABLE 11 Surface Area and Water Absorption Data

Sample ID	Surface Area, m^2/gm			Water Absorption, %		
	Run # 1	**Run # 2**	**Average**	**Run # 1**	**Run # 2**	**Average**
AR # 3	0.44	0.47	0.46	0.38	0.34	0.36
GA # 2	0.08	0.09	0.09	0.26	0.26	0.26
IA # 3	0.53	0.51	0.52	0.42	0.50	0.46
KY # 2	2.18	2.21	2.20	4.21	4.12	4.17
KY # 3	0.56	0.60	0.58	1.71	1.79	1.75
SC # 1	0.07	0.07	0.07	0.32	0.30	0.31

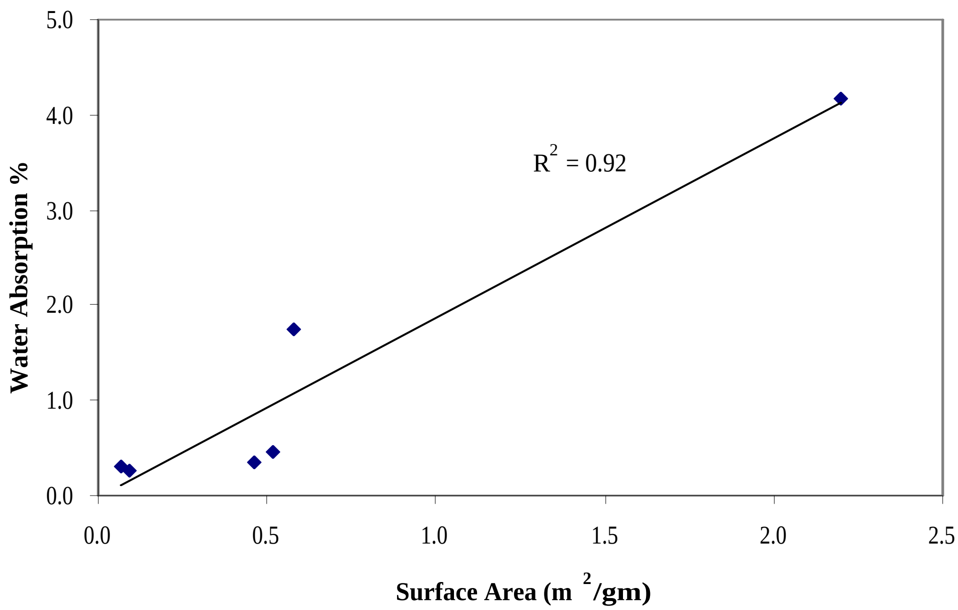

FIGURE 36 Correlation Between Water Absorption and Surface Area

FAA VERSUS PERFORMANCE IN THE SHRP LTPP DATABASE

A statistical analysis of the SHRP LTPP database was conducted to determine if a relationship between FAA and rutting in HMA pavements could be detected. It was very difficult to establish such a relationship, since the rutting is also a function of many other variables such as asphalt content, traffic loading, environment, aggregate gradation, etc. which were not controlled in the data set. The files from the database were imported into Microsoft Excel for further analysis. The important files for this study imported from DataPave contain rut depths in millimeters and the FAA data.

At the time of the analysis, the LTPP database contained 441 observations for FAA and 4677 observations for rut depths; however, only 160 rutting observations also had corresponding values of FAA. Corresponding asphalt content, air void content, aggregate gradation, and stability (Marshall and/or Hveem) were also available, but for fewer than the 160 observations.

The LTPP database provides rut depth data for both right and left wheelpaths. Averages of these two readings for each qualifying pavement were used in the statistical analysis. Figure 37 shows the data points for average rut depth as a function of FAA. These points are rather scattered and do not show any obvious pattern. The coefficient of correlation which is the identifier of any linearity, for the data is quite low as -0.15. This value is obviously not sufficient to conclude any strong correlation between the FAA and HMA rutting. The regression statistics for this result are given in Table 12.

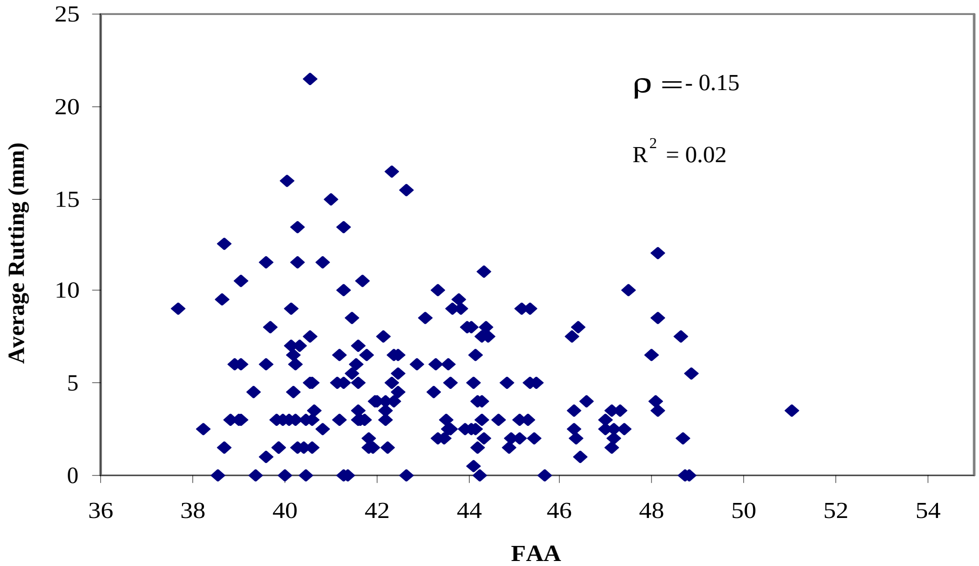

FIGURE 37Average Rutting of All 160 Points and Corresponding FAA Value

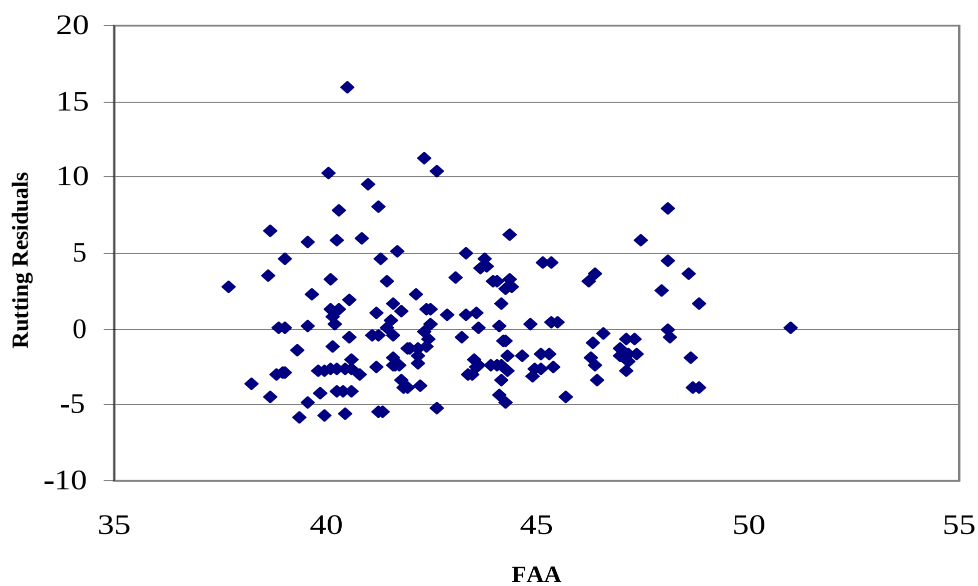

FIGURE 38 Residual Plot for Rutting Versus FAA

TABLE 12 ANOVA for All Rutting and FAA Data Points

	DF	SS	MS	F	Significance F
Regression	1	29.45	29.45	3.86	0.051
Residual	158	1207.00	7.64		
Total	159	1236.46			

Here the hypotheses are:

H_0 : the linear regression model is appropriate
H_1 : the linear regression model is not appropriate

Testing this regression value at $\alpha = 0.1$ significance level, we can reject H_0 (ρ value < α) and conclude that the linear regression model is not appropriate.

The residual plot (Figure 38) of the overall data does not show any pattern that would encourage use of a transformation. Also, the spread of the residuals is not even and the assumption that the residuals have the same mean zero does not hold true. The normal quintal plot of these data has heavy tails with too many outliers to exclude. These indicators suggest that the data are not normally distributed.

Since asphalt content is a major factor affecting the rutting, the rutting data were plotted separately for low (< 5.5 percent) and high (> 5.5 percent) asphalt contents (Figures 39 and Figure 40). Interestingly, the data for asphalt contents greater than 5.5 percent yields a coefficient of correlation (ρ) of - 0.27 (Figure 40), while the data for asphalt contents less than 5.5 percent gives a coefficient of correlation of - 0.0036 (Figure 39). The regression line for the data(Figure 40) gives a very high intercept(13.28) and very low slope (-0.19), which are not characteristic of a good model. A coefficient of determination (R^2) of 0.02 (Figure 37) is not sufficient to conclude linearity between FAA and pavement rutting. Tables 13 and 14 describe the ANOVA of these data for asphalt content less than or equal to 5.5 percent and greater than

5.5 percent, respectively. The F-statistic values for asphalt content less than or equal to 5.5 percent supports the earlier rejection of H_o (linear regression model is appropriate); but for asphalt content greater than 5.5 percent, the F-statistic values are significant even at level as high as 0.10. Hence, the null hypothesis can be accepted for the asphalt content greater than 5.5 percent. The following simple linear regression is suggested by SAS:

Rutting, mm = 43.6 – 0.17 $\times$ FAA (for asphalt content > 5.5 percent)

This model has a very high intercept and a low slope value. These are not characteristics of a good model.

TABLE 13 ANOVA of FAA versus Rutting Data for Asphalt Content Less than or Equal to 5.5%

	DF	SS	MS	F	Significance F
Regression	1	0.00549	0.00549	0.00062	0.98018
Residual	48	422.84065	8.80918		
Total	49	422.84065			

TABLE 14 ANOVA of FAA versus Rutting Data for Asphalt Content Greater than 5.5%

	DF	SS	MS	F	Significance F
Regression	1	24.19713	24.19713	2.82460	0.10149
Residual	36	308.39640	8.56656		
Total	37	332.59353			

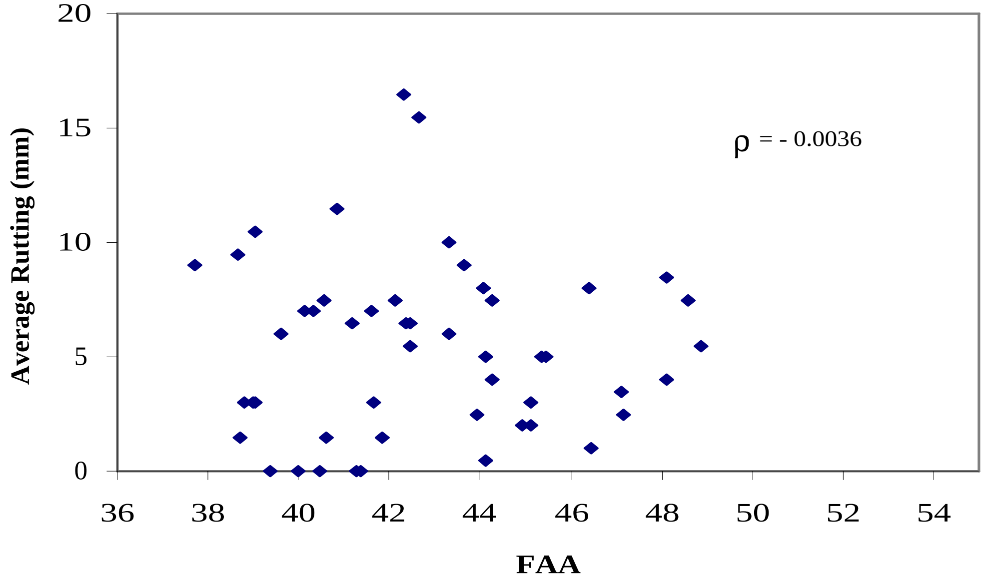

Figure 39. Average Rutting Depth Versus FAA for Asphalt Content Less than or Equal to 5.5%

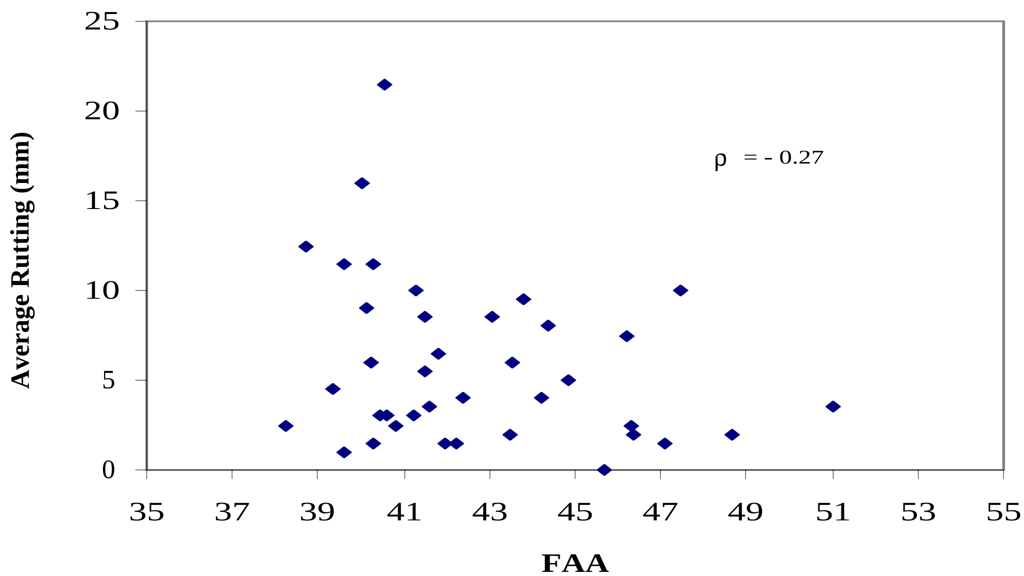

Figure 40. Average Rutting Depth Versus FAA for Asphalt Content Greater than 5.5%

The rutting versus FAA data were again plotted separately for low (<4 percent) and high (>4 percent) - No. 200 filler (Figures 41 and 42) and for low (<56 percent) and high (>56 percent) - No. 4 size aggregate (Figures 43 and 44). The values of 4 percent and 56 percent were chosen as they are approximately median values. The data for filler contents lower than 4 percent yield a coefficient of correlation of -0.34 (Figure 41), indicating that rutting decreases with an increase in FAA values. In the other three cases, there was no correlation between rutting and FAA.

The statistical studies generally show that there is no significant relationship between FAA and rutting. This study suffers from a too few data points for a good statistical analysis. To find definite conclusions, more than 160 data points are required.

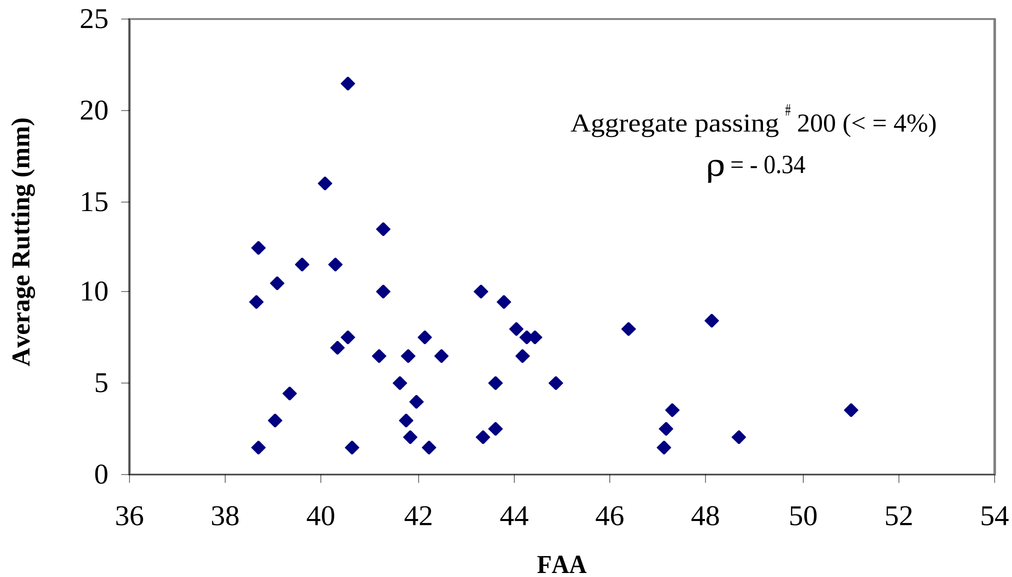

FIGURE 41 Average Rutting for Aggregate Passing #200 Sieve is Equal to or Less than 4%

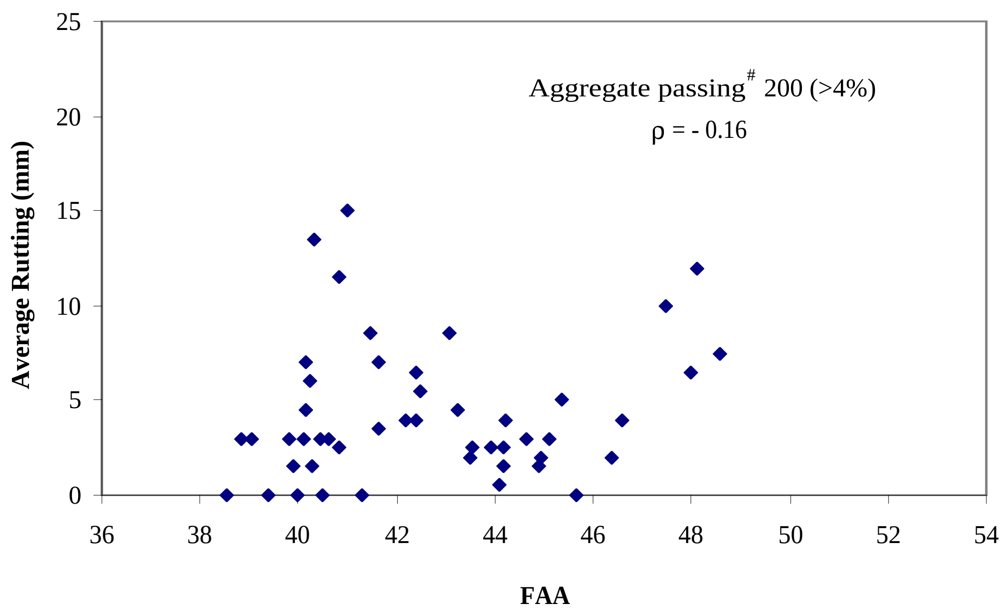

FIGURE 42Average Rutting for Aggregate Passing #200 Sieve is Greater than 4%

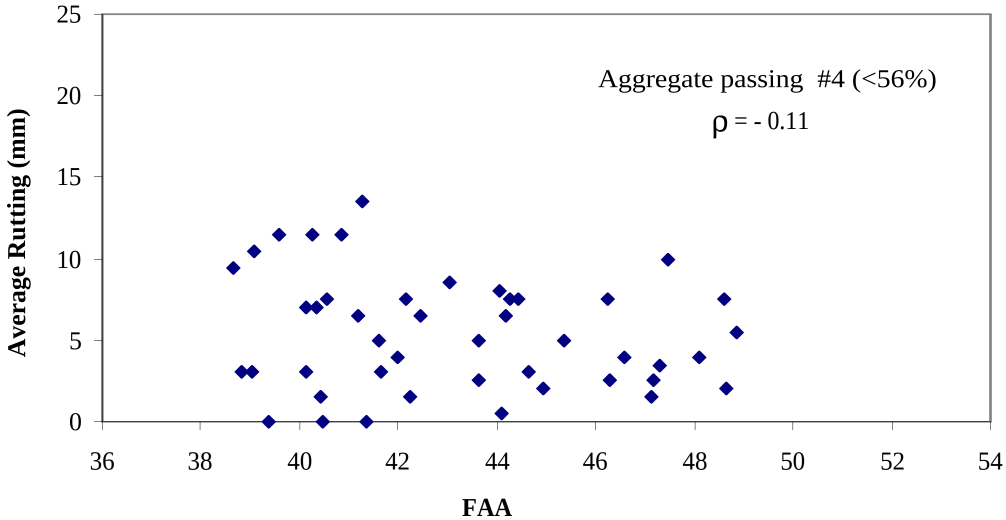

FIGURE 43Average Rutting for Aggregate Passing #4 Sieve is Equal to or Less than 56%

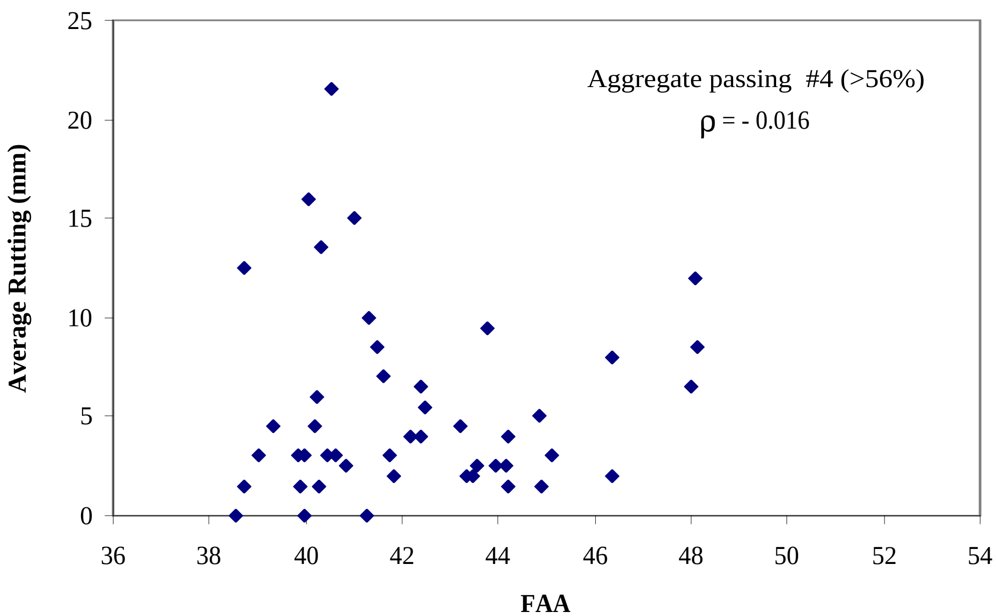

FIGURE 44 Average Rutting for Aggregate Passing #4 Sieve is Greater than 56%

RUTTING RESISTANCE EVALUATION WITH APA

Six fine aggregates selected for this part of the study were tested with FAA test, direct shear test, CAR test, Image analysis using WSU and VTRC methods. All other methods used previously could not be used due to unavailability of the equipment during that time. The results of the tests are mentioned in Table 15. Recall that Blend 1 is the mixture of 85 percent of GA # 5 & 15 percent of natural sand (NS) and Blend 2 is mixture of 70 percent of TX # 1 & 30 percent of natural sand.

TABLE 15 Aggregate Angularity Measurements of Fine Aggregates

Fine Aggregate	FAA Value (%)	Angle of Friction (degree)	CAR Value (lb)	Image Analysis at WSU			Slenderness Ratio (SR) at VTRC
				SP	FL	FF	
TX # 1	43.5	45.2	17467	2.88	0.14	0.48	1.52
TX # 2	44.3	40.5	1398	3.60	0.14	0.52	1.51
GA # 5	48.0	42.6	2231	4.48	0.21	0.33	1.55
Natural Sand	39.0	39.0	480	0.61	0.05	0.85	1.44
Blend 1	46.0	45.2	1460	1.45	0.18	0.80	1.49
Blend 2	42.2	45.2	2350	0.89	0.17	0.83	1.49

Superpave mix designs were performed using these six fine aggregates. For all mixtures, only one type of coarse aggregate (limestone) was used to keep the number of variables to a minimum. During the mix design procedure, meeting all Superpave specifications for all mixtures was not possible. Mix design summaries of each mixture are described in Table 16. Each mixture was prepared using the same overall aggregate gradation (Figure 45). This gradation passes below the restricted zone.

TABLE 16 Mixture Design Properties for Different Mixtures

Mix Property	TX # 1	TX # 2	GA # 5	NS	Blend 1	Blend 2	Criteria
Optimum Asphalt %	4.8	5.6	5.2	3.8	5.6	4.2	N/A
% Air Void at N_{design}	4.0	4.0	4.0	4.0	4.0	4.0	4.0
% VMA at N_{design}	14.8	14.7	14.8	11.4*	14.8	11.9*	13.0 min.
% VFA at N_{design}	74.8	72.6	74.8	61.7*	74.3	66.4	65-75
Dust Proportion	0.8	0.6	0.6	0.8	0.6	0.7	0.6-1.2
% G_{mm} at $N_{initial}$	85.4	87.2	87.7	89.0	89.2*	87.7	≤ 89
% G_{mm} at $N_{maximum}$	97.4	97.2	95.6	96.3	97.3	97.3	≤ 98

* did not meet the Superpave criteria

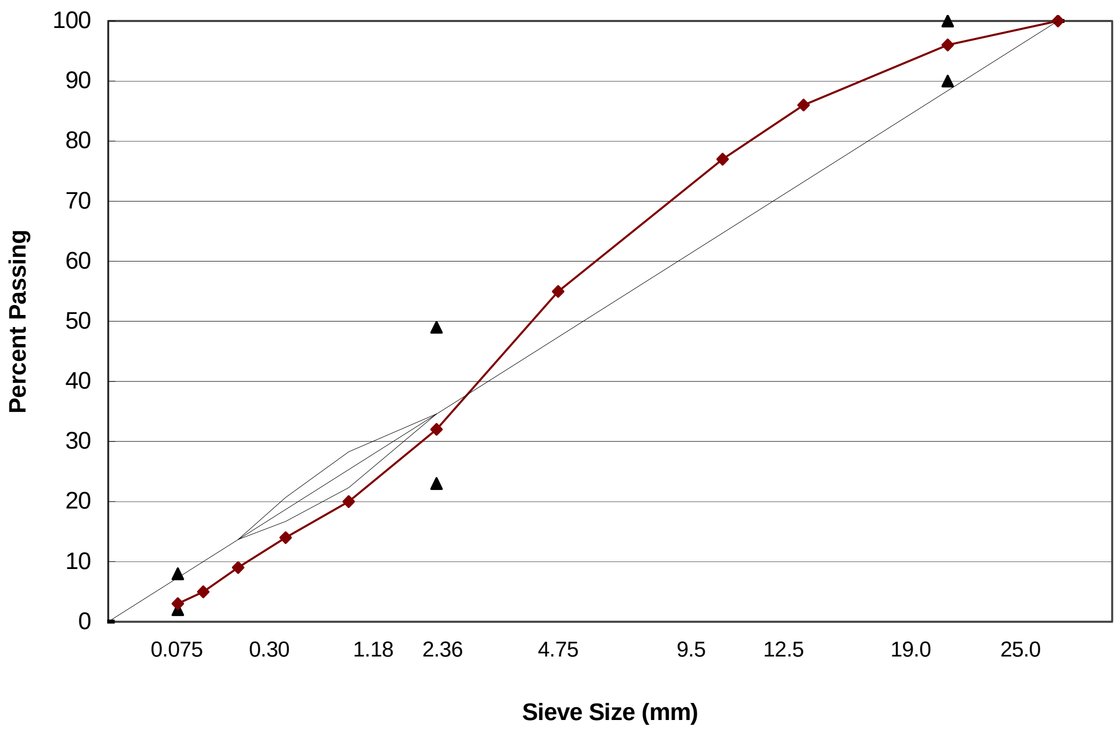

FIGURE 45 Aggregate Gradation Used in Mix Design

Specimen Preparation and Testing

All uncompacted mixtures were subjected to four hours of short-term aging at 135 ^{O}C before compaction. Specimens were compacted at 4$\pm$1 percent air voids using the Superpave gyratory compactor. Six cylindrical specimens from each mixtures with 6-inch (150-mm) diameter and 2.5-inch (50-mm) height were prepared for APA testing. APA testing was performed using 8,000 cycles at 64 ^{O}C using 100-lb (445 N) of wheel load and 100-psi (694-KPa) hose pressure. Specimens were preconditioned for 6-10 days at 25 ^{O}C and 5 hours at 64 ^{O}C just before the testing. Rut depths were measured after 8,000 load cycles (passes). Figure 46 shows the rut depth measured for each mixture after 8,000 cycles. Measured rut depths are shown in millimeter rather than inch.

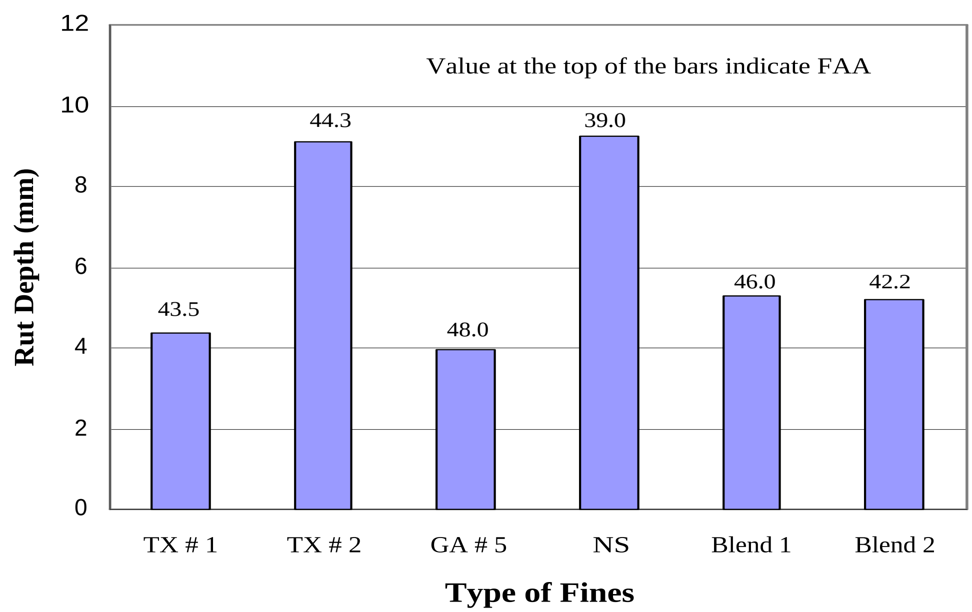

FIGURE 46 Rut Depth Measured by APA for Different Mixtures

APA Rut Depth and Different Measures of Angularity

Rut depth measured by APA are compared with different fine aggregate angularity measures. Researchers are aware that this rut depth is also a function of other variables like asphalt content and VMA. Researchers tried to keep the number of variable minimum. But some variables cannot be eliminated.

Mixtures containing natural sand with a FAA of 39 exhibited the highest rut depth (9.2 mm). Mixtures containing river gravel fines with a FAA of 44.3 had a statistically equivalent rut depth (9.1 mm). Granite fines mixture with the highest FAA of 48 showed the lowest rut depth (4.0 mm). Limestone fines mixture with a FAA of 43.5 showed the second lowest rut depth (4.4 mm), statistically equivalent to the measured rut depth of the granite mixtures. Mixtures containing the blend of 85 percent granite fines and 15 percent natural

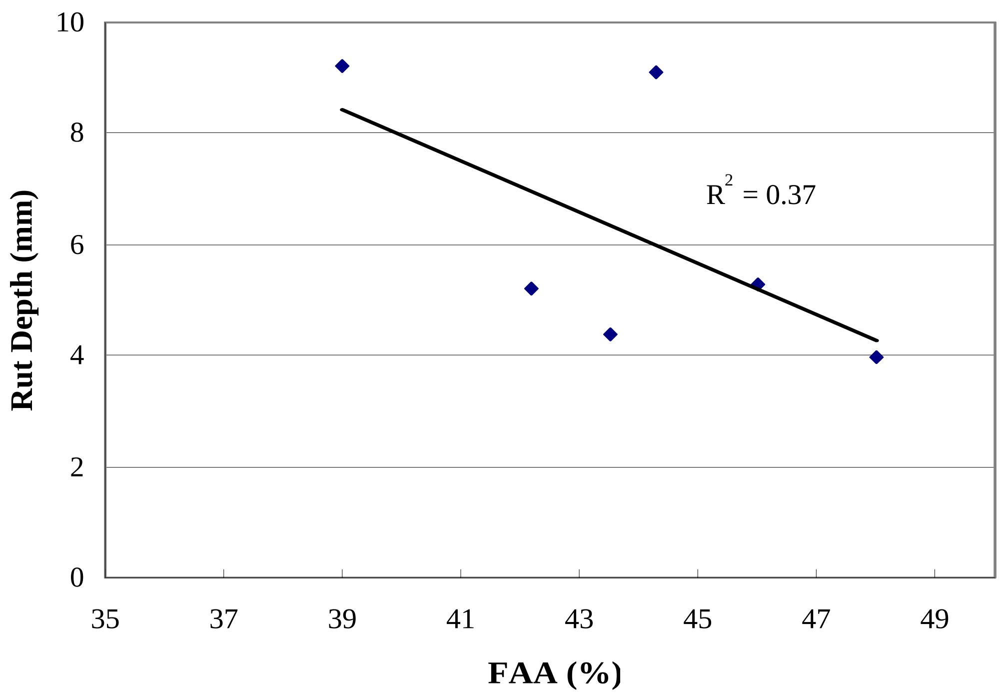

FIGURE 47 APA Rut Depth versus FAA

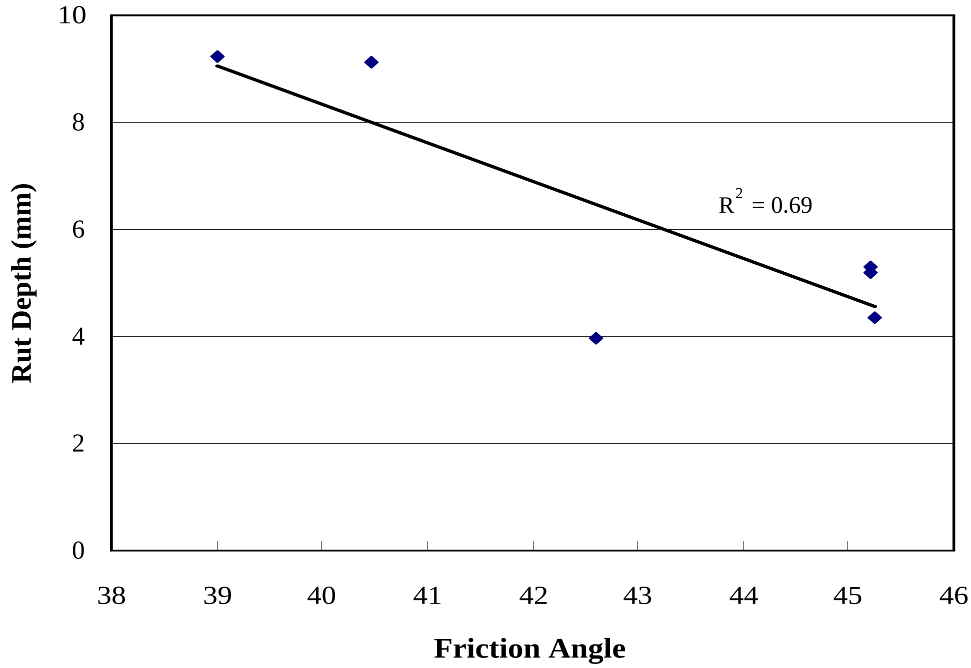

FIGURE 48 APA Rut Depth Versus Angle of Internal Friction

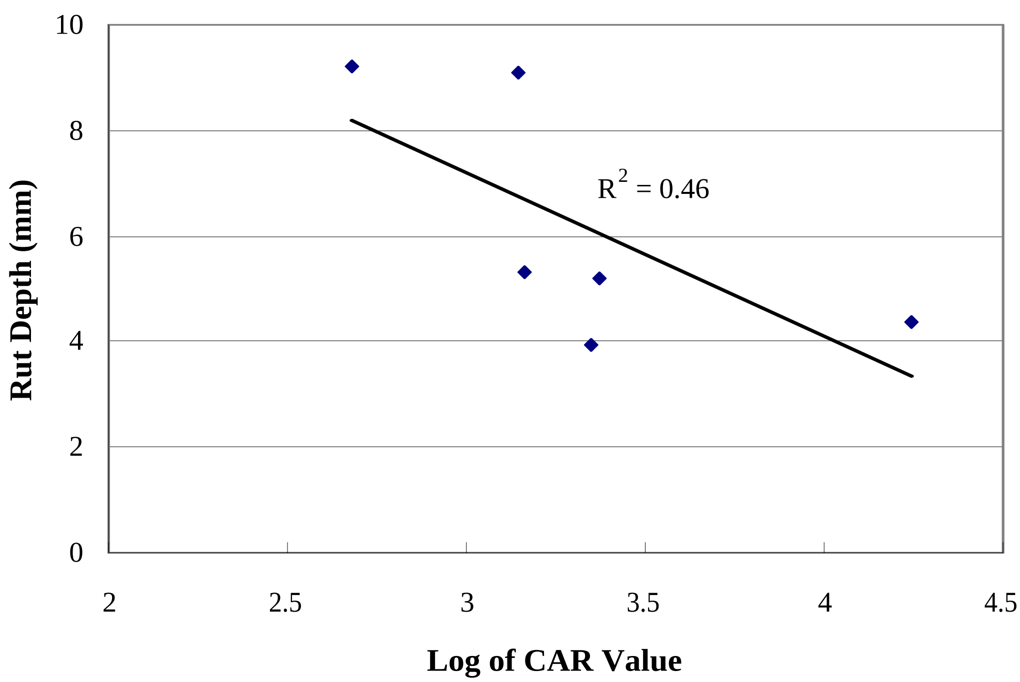

FIGURE 49 APA Rut Depth versus Logarithm of CAR Value

sand with a FAA of 46 exhibited a 5.3-mm rut depth. Mixture containing 70 percent limestone fines and 30 percent natural sand with a FAA 42 showed a 5.2-mm rut depth. FAA shows a fair correlation (R^2 = 0.37) with APA rut depth (Figure 47).

Rut depths were compared with angle of internal friction as measured by the direct shear test. The Direct shear test shows (Figure 48) a fairly good correlation with rut depth. In fact, this correlation (R^2 = 0.69) is the best among the correlations of rut depth and angularity measures. Logarithm of CAR value showed a fair correlation with rut depth (Figure 49). Even though limestone (TX # 1) had a very high CAR value, it produced a statistically similar rut depth as granite (GA # 5). Natural sand had the lowest CAR value and yielded the highest rut depth.

Granite fines exhibited the highest surface parameter, fractal length, and lowest form factor, indicating it has more surface irregularity and angularity. The HMA mixture containing granite fines exhibited the lowest rut depth. Even though river gravel fines gave the same or similar results in the image analysis, rut depths of their resulting mixtures were significantly different. Recall that form factor decreases with increasing particle surface irregularity. Among the three parameters from WSU imaging method only fractal length shows a good correlation (R^2 = 0.58) with rut depth (Figure 50). Figure 51 exhibits a fair correlation (R^2 = 0.42) between the rut depth and slenderness ratio measured by VTRC imaging method.

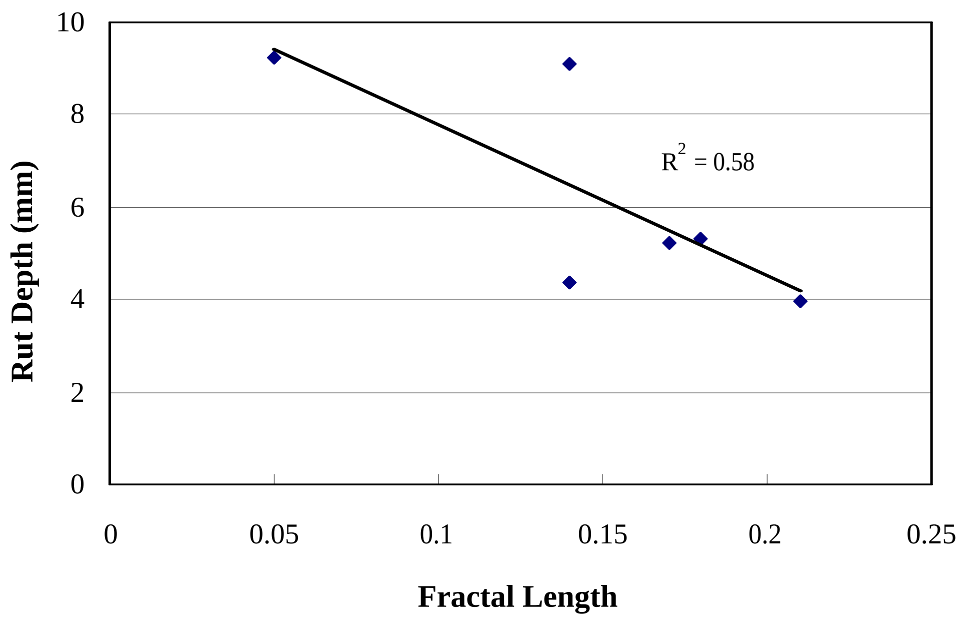

FIGURE 50APA Rut Depth Versus WSU Fractal Length

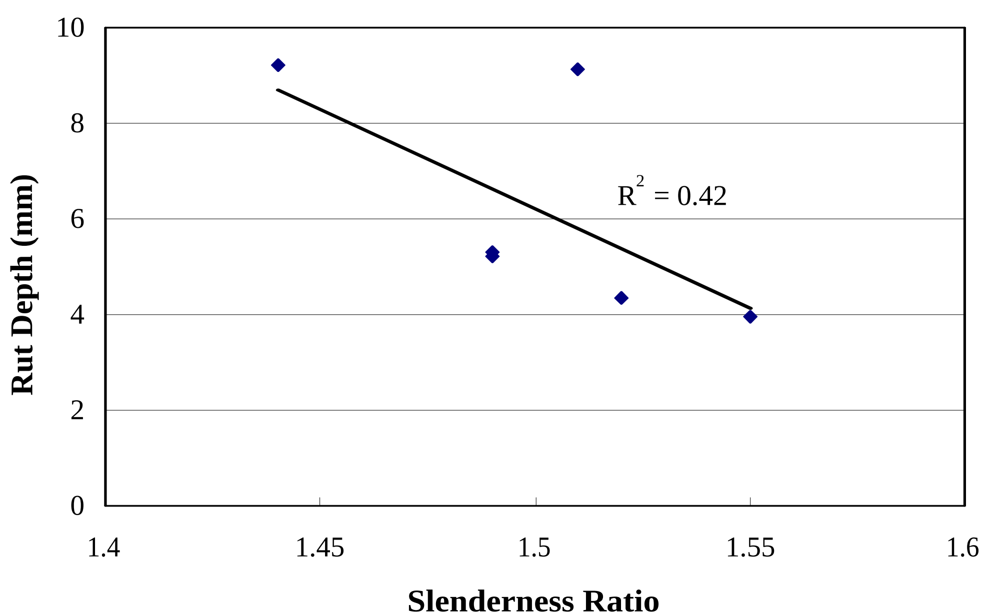

FIGURE 51 APA Rut Depth Versus VTRC Slenderness Ratio

CHAPTER V

CONCLUSIONS AND RECOMMENDATIONS

Laboratory experiments were performed to evaluate various procedures for measuring fine aggregate angularity. The research focused on seven methods of measuring angularity: FAA test (ASTM C-1252, Method A), direct shear test, compacted aggregate resistance test, specific surface area, and three image analysis techniques. Image analysis was performed at three different laboratories. Visual inspection was employed to examine fine aggregate angularity. Results from these tests were compared with subjective performance history (provided by some state DOTs) of fine aggregate samples. Results from the laboratory tests were compared.

A statistical analysis of the SHRP LTPP database was also conducted to determine if there was a relationship between FAA and rutting in HMA pavements. It was very difficult to establish such a relationship, since the rutting is also a function of many other variables such as asphalt content, traffic loading, environment, aggregate gradation, which were not controlled in the data set.

Superpave mix design was performed using six different fine aggregates with the same coarse aggregate and asphalt and their rutting resistance was evaluated using APA machine. Results from the APA were compared with several different measures of fine aggregate angularity.

Based on the findings of these tests the following conclusions and recommendations are given:

CONCLUSIONS

- # The FAA test method does not consistently identify angular, cubical aggregates as high quality-materials. FAA values of some cubical crushed limestones fell below 45. Some high-quality fine aggregates with good field performance history did not meet the Superpave criteria for the FAA for a surface course under heavy traffic.
- # There was a fair correlation between the compacted aggregate resistance (CAR) value and the angle of internal friction from the direct shear tests. One reason for this correlation could be that both tests involve shear failure of the as-received sample.
- # No correlation was found between FAA and CAR stability or between FAA and angle of internal friction (AIF).
- # Some cubical, crushed, calcareous aggregates with FAA values from 42.6 to 44.6 gave high values of CAR stability, AIF, and K-index (from Hough Transform image analysis).
- # One fine aggregate with a poor field performance history was identified that exhibited a very high FAA value (50.5) but low values of CAR stability and AIF.
- # Measurement of specific surface area of fine aggregate using nitrogen gas was shown to be ineffective for measuring angularity. Incidentally, however, there was an excellent correlation between this test and water absorption.
- # The three image analysis techniques appear to be very promising for directly quantifying fine aggregate particle shape. The Hough Transform and WSU methods also provide useful information about texture. The VDG-40 methodology concentrates on the flat and elongated characteristics of the particles. Current image analysis methods are capable of measuring several characteristics of a 2-D (or 3-D, in some cases) image and using these

characteristics in a mathematical model to compute a single value or index. One apparent advantage of the image methods is that the models can be adjusted to maximize the sensitivity to those fine and/or coarse aggregate properties that affect HMA performance.

The Hough Transform and WSU imaging methods currently consider a two-dimensional image of a particle lying on a flat surface. The measured shape is influenced by the fact that the particle is lying on a flat surface. The VTRC imaging method also considers a two-dimensional image, but since the image is captured while the particle is falling, the particle orientation is more random in nature.

Both parameters from VTRC analysis exhibited fair correlations with logarithm value of CAR stability.

From the data available in SHRP-LTPP database, there was no evidence of any good linear relationship between FAA and pavement rutting. For asphalt content greater than 5.5 percent and filler (- No. 200) content less than 4 percent, there appeared to be a trend between FAA and rutting, where rutting decreased with an increase in FAA value.

An abbreviated study was conducted wherein six HMA specimens were prepared using the same crushed limestone coarse aggregate but varying the fine aggregate. The asphalt pavement analyzer (APA) was used to estimate relative rut depth of the resulting mixtures. Findings are as follows:

! HMA mixtures with natural sand (FAA 39.0) and crushed river gravel fines (FAA 44.3) yielded statistically equivalent rut depths.

! HMA mixtures with crushed limestone fines (FAA 43.5) and crushed granite fines (FAA 48.0) yielded statistically equivalent rut depths.

- HMA mixtures containing crushed limestone fines (FAA 43.5) yielded significantly lower rut depth than the mixture containing crushed river gravel fines (FAA 44.3).
- HMA mixtures containing blends of aggregate fines with FAA 42.0 and 46.0 yielded statistically equivalent rut depths.
- These limited findings indicate that FAA does not correlate well with rut resistance of HMA mixtures. Further, certain fine aggregates with a FAA value lower than 45 (limestone), or even lower than 43 (blend 2), but with relatively high particle surface texture, can produce mixtures with relatively good rut resistance.
- Angle of internal friction from the direct shear test showed the best correlation (R^2 = 0.69) with rut depth when compared to FAA, CAR and parameters from the image analysis methods.

RECOMMENDATIONS

- ASTM C 1252 and AASHTO T 304 would provide more accurate FAA results if the specific gravity of the fine aggregate grading used in the FAA test was used to compute uncompacted voids. For Superpave evaluations of fine aggregates with borderline FAA values, the gradation of the aggregate for specific gravity determination should be the same as that used for ASTM C 1252, Method A.
- It appears that ASTM C 1252, Method A, loses accuracy above an FAA value of 43, and there is no good relationship between FAA and rutting. Some angular, cubical fine aggregates in this study demonstrated good field performance but did not meet the Superpave FAA criteria for heavy traffic. Their FAA values were between 43 and 45.

These limited data suggest that the FAA criteria for a Superpave surface course for heavy traffic could be decreased to 43. One hundred percent crushed fine aggregate with FAA value greater than 43 should not be rejected for use in HMA.

Image analysis appears to be a very promising methodology for directly measuring fine aggregate angularity. The methods evaluated herein capture two-dimensional images. A 3-D image analysis technique may offer significant advantages. Hough Transform and WSU methods require further development to be commercially marketable.

Several image analysis methods have been developed for measuring characteristics of aggregate particles related to overall shape or form, angularity, and surface texture. Only three methods were studied herein. Most methods analyze 2-dimensional images but a few are capable of characterizing 3-dimensional images. Algorithms need to be developed that can use the different measured particle parameters in a mathematical model that will compute a single value that is highly correlated with permanent deformation in HMA mixtures. Permanent deformation in HMA may react differently to the different aggregate characteristics, for example, permanent deformation may be more sensitive to particle texture than to angularity, if so, texture would be weighted more heavily in the model. The next step would be to develop acceptance criteria or specifications for coarse and fine aggregates based on the image analyses.

The data available for analysis of FAA versus rutting from SHRP-LTPP database were insufficient for a sound statistical analysis. The FAA vs. rutting analysis should be attempted again after the LTPP program collects more FAA values on fine aggregates and associated rutting data.

- Establish a study to develop a laboratory test for fine aggregate that is related to shear strength or rut resistance of HMA. The test apparently should be sensitive to aggregate particle texture.
- Gradation plays an important role in the shear strength of fine aggregates. This was clearly demonstrated by results from the CAR tests. Since the Superpave FAA test (ASTM C 1252/AASHTO T 304, Method A) uses a specified arbitrary gradation, the results are unaffected by gradation of the source fine material tested or the gradation in the job mix formula of the HMA. It appears that the most critical fine aggregate quality test should be performed on the gradation actually used in the HMA.

REFERENCES

1. Jahn, D. W. *A Closer Look at Superpave Aggregate Specification*. 4th Annual Symposium Proceedings, ICAR, Atlanta, Georgia, 1996.
2. McGennis, R. B., R. M. Anderson, T. W. Kennedy, and M. Solaimanian. *Background Of Superpave Asphalt Mixture Design and Analysis*. Report SA-95-003. FHWA, U.S. Department of Transportation, 1994.
3. Cross, S. A., B. J. Smith, and K. A. Clowers. "Evaluation of Fine Aggregate Angularity Using National Aggregate Association Flow Test." In *Transportation Research Record 1437*, TRB, National Research Council, Washington D.C., 1994.
4. Barksdale, R. D., M. A. Kemp, W. J. Sheffield, and J. L. Hubbard. "Measurement of Aggregate Shape, Surface Area, and Roughness." In *Transportation Research Record 1301*, TRB, National Research Council, Washington D.C., 1991.
5. White, T. D., C. J. Lee, and J. E. Haddock. *Fine Aggregate Angularity*. 6th Annual Symposium Proceedings, ICAR, St. Louis, Missouri, 1998.
6. Fernandes, J. L., R. Rouque, M. Tia, and L. Casanova. *Evaluation of Uncompacted Void Content of Fine Aggregate as a Quality Indicator of Materials Used in Superpave Mixtures.* Paper prepared for presentation and publication at the 79th Annual meeting of the Transportation Research Board, Washington, D.C., January 2000.
7. Haddock, J. E., T. D. White, and B. J. Coree. *Validation of SHRP Asphalt Mixture Specifications Using Accelerated Testing*. 6th Annual Symposium Proceedings, ICAR, St. Louis, Missouri, 1998.
8. Wilson, J. D., L. D. Koltz, and C. Nagaraj. *Automated Measurement of Aggregate Indices of Shape*. Report FHWA-RD-95-116. FHWA, U.S. Department of Transportation, 1995.

9. Cross, S. A., and E. R. Brown. "Selection of Aggregate Properties to Minimize Rutting of Heavy Duty Pavements." *Effects of Aggregate and Mineral Fillers on Asphalt Mixture Performance*, ASTM STP 1147, Richard C. Meininger, Ed., American Society for Testing and Materials, Philadelphia, PA, 1992.

10. Hudson, S. W., and S. B. Seeds. "Evaluation of Increased Pavement Loading and Tire Pressures." *In Transportation Research Record 1207*, Transportation Research Board, Washington, D.C., 1988.

11. Roberts, et. al. *Hot Mix Asphalt Materials, Mixture Design, and Construction.* 2nd Ed. NAPA Education Foundation, Lanham, Maryland, 1996.

12. Button, J.W., M. Yeggoni, and D. G. Zollinger . *Influence of Coarse Aggregate Shape and Surface Texture on Rutting of Hot Mix Asphalt Concrete.* Technical Report FHWA/TX-94/1244-6. Texas Transportation Institute, 1994.

13. Button, J.W., and D. Perdomo. *Identifying and Correcting Rut-Susceptible Asphalt Mixtures*. Technical Report FHWA/TX-91/1121-2F. Texas Transportation Institute, 1991.

14. Kandhal, P. S., and P. Frazier, Jr. *Aggregate Tests Related to Asphalt Concrete Performance in Pavements*. NCHRP Report 405, Transportation Research Board, National Research Council, Washington, D.C., 1998.

15. Bayomy, F. M. S., H. R. Guirguis. *An Upgrading technique for AC Pavement Materials*. Roads and Developments, Vol. 2, Roads and Development Center, Kuwait.

16. Kalcheff, I.V., and D. G. Tunicliff. *Effects of Crushed Stone Aggregate Size and Shape on Properties of Asphalt Concrete*. Proc. Association of Asphalt Paving Technologists, Vol. 51, 1982, pp. 453-483.

17. Ahlrich, R. C. "Influence of Aggregate Properties on Performance of Heavy-Duty Hot-Mix Asphalt Pavements." In *Transportation Research Record 1547*, TRB, National Research Council, Washington D.C., 1996.

18. Butcher, M. *The Effect of Particle Shape on Asphalt Compaction and Mechanical Properties*. 10th AAPA International Flexible Pavement Conference Proceedings, Vol 2, 1997, Sidney, Australia.

19. Kandhal, P. S., J. B. Motter, and M. A. Khatri. "Evaluation of Particle Shape and Texture: Manufactured Versus Natural Sands." In *Transportation Research Record 1301*, TRB, National Research Council, Washington D.C., 1991, pp. 48-56.

20. U.S. Department of Transportation, Federal Highway Administration, Technical Advisory T5040.27, Subject: Asphalt Concrete Mix Design and Field Control, March, 10, 1988.

21. Standard Test Method for Uncompacted Void Content for Fine Aggregate (as Influenced by Particle Shape, Surface Texture, and Grading). ASTM C 1252-93. *Annual Book of ASTM Standards, Vol. 04.02*, ASTM, Philadelphia, Pennsylvania, 1996.

22. Aschenbrener, T. *Implementation of a Fine Angularity Test*. Report CDOT-DTD-94-6, Colorado Department of Transportation, Denver, Colorado, 1994.

23. Stuart, K. D., W. S. Mogawer. *Evaluation of Natural Sands Used in Asphalt Mixtures*. In Report FHWA-RD-93-070. FHWA, U. S. Department of Transportation, 1993.

24. Wilson, J. D., and L. D. Koltz. "Quantitative Analysis of Aggregate Based on Hough Transformation." In *Transportation Research Record 1530,* TRB, National Research Council, Washington D.C., 1996.

25. Masad, E., J. W. Button, and T. Papagiannakis. *Fine Aggregate Angularity: Automated Image Analysis Approach.* A paper submitted for publication in the TRB, 79th Annual Meeting, January 2000.

26. Masad, E., and J. W. Button. "Unified Imaging Approach for Measuring Aggregate Angularity and Texture." A paper submitted for publication in Computer-Aided Civil Infrastructure Engineering. *Advanced Computer Technologies in Transportation Engineering*. 1999.

27. Weingart, R. L., and B. D. Prowell. *Flat and Elongated Aggregate Tests: Can the VDG-40 Videograder Deliver the Needed Precision and be Economically Viable*. 6th Annual Symposium Proceedings, ICAR, St. Louis, Missouri, 1998.

28. Marez, N. H. *Aggregate Sizing and Shape Determination Using Digital Image Processing*. 6th Annual Symposium Proceedings, ICAR, St. Louis, Missouri, 1998.

29. Yudhbir, and R. Abedinzadeh. "Quantification of Particle Shape and Angularity Using the Image Analyzer." *Geotechnical Testing Journal, GTJODJ, Vol. 14, No. 3*, September 1991, pp. 296-308.

30. Lambe, T. W. *Soil Testings for Engineers*. Wiley, New York, 1951.

30. Monismith, C. L. *Asphalt Paving Mixtures- Properties, Design, and Performance.* Prepared for the Short Course in Asphalt Paving Technology, 1961-62. University of California, Berkeley, CA

31. Klotz, L. D. *Measuring Fine Aggregate Shape by Digital Imaging*. Doctoral Dissertation. Department of Applied Science. University of Arkansas at Little Rock, 1998.

32. Li, L., P. Chan, D. G. Zollinger, and R. L. Lytton. "Quantitative Analysis of Aggregate Based on Fractals." *ACI Materials Journal, Vol. 90, No. 4*, July-August, 1993.

33. Wilson, J. D., and L. D. Klotz. *Automated Aggregate Shape Analysis and Rutting /Stripping Performance*. A Report Sponsored by Mack-Blackwell Transportation Center, University of Arkansas, Fayetteville, Arkansas, April, 1998.

34. Kung, S. Y. *Digital Neural Networks*. PTR Prentice Hall, Englewood Cliffs, New Jersey, 1993.

35. Young, I. T., R. L. Peverini, P. W. Verbeek, and P. J. Van Otterloo. "A new Implementation for the Binary and Minkowski Operators." *Computer Graphics And Image Proceedings*. 1981, pp 189-210.

36. "Granulometric Analysis, Flattening and Elongation Video-granulometer Test." Translation of French Norm P 18-566, May 1994, LCPC, France

37. *Long-Term Pavement Performance DataPave Demonstration Workshop- Participant's Notebook*. FHWA .Texas A&M University, September, 1998. A. Chowdhury, Private collection.

38. Milton, J. S., and J. C. Arnold. Introduction to Probability and Statistics: Principles and Applications for Engineering and the Computing Sciences. Third Edition, Irwin McGraw-Hill, 1995, pp 432-433.

APPENDIX A

FINE AGGREGATE DATABASE

TABLE A1 Description of All Fine Aggregates Collected

Aggregate ID	Description (Supplier / Manufacturer, Location)	Additional Properties	Performance History[1]
AR # 1	Mc Mellow Sand & Gravel, Black Spring, AR	--	Poor
AR # 2	Gifford Hill, Delight, AR	--	Good
AR # 3	Jeffery SA Co, North Little Rock, AR	--	Good
AR # 4	Cosattot, Locksburg, AR	--	Poor
AZ # 1	Pit 6610	--	--
AZ # 2	Pit 8268	--	--
AZ # 3	Pit 8372	--	--
AZ # 4	Pit 2342	--	--
CO # 1	Monk’s Pit, CO	--	Poor
CO # 2	Ralston Quarry Fines	--	Good
CO # 3	McAtee Natural fines	--	Poor
CO # 4	Holly Crushed Fines	--	Good
CT # 1	American Sand & Gravel	--	Poor
CT # 2	O&G Industries, Dover Plains	--	Poor
CT # 3	O&G Industries, Torrington	--	Good
CT # 4	Tilcon, Walingford	75% stone sand and 25% natural sand	Good
DE # 1	Tilcon Concrete Sand	Gradation, Sp Gr., Abs.	Good
DE # 2	Tarburton Mason Sand	Grad., Sp. Gr., Abs.	Good
DE # 3	Md Materials	Grad., Sp. Gr., Abs.	Good
DE # 4	Dyer Sand	Grad., Sp. Gr., Abs.	Good

TABLE A1 (Continued)

Aggregate ID	Description (Supplier / Manufacturer, Location)	Additional Properties	Performance History[1]
GA # 1	Butler Sand, No. 7F, GA	Sp. Gr., Abs., Sand Eqv., Durability factor	Excellent with Concrete
GA # 2	Cox Sand, Cox, 149F, GA	Same	Same
GA # 3	Watkinsville, L.C. Curtis, GA	Same	Fair with Concrete
GA # 4	Cumming, Blue Circle, GA	Same	Same
IA # 1	Moore Quarry, Gilmore City	FAA, Sp. Gr., Grad.	Poor (soft)
IA # 2	Ferguson Quary, M. Marietta	Same	Good
IA # 3	Lyman Richy, Oreapolis Plant	Same	Poor, low stability
IA # 4	Sackton, Lakeview	Same	Good
IL # 1	Channahon Mat, #51970-27	FAA, Sp. Gr., Abs.	--
IL # 2	Rockford Sand & Gravel, #52012-77, Crushed dolomite	Same	--
IL # 3	Chrleston Stone, #50292-02, Crushed Lime Stone	Same	--
IL # 4	Cape Girardeau, #52300-17	Same	--
IN # 1	US Agg. Inc., Richmond , IN, Natural Sand, Code 2331	Sp. Gr., Abs., SS Loss, FT Loss, Gradation	Quality Rating A5
IN # 2	Martin Marietta, Waverly, IN, Natural Sand, Code 2522	Same	Same
IN # 3	Evansville Materials, Griffin, IN,Nat. Sand, Code 2631	Same	Same
IN # 4	Evansville Materials, Griffin, IN,Nat. Sand, Code 2632	Same	Same
KS # 1	Quartzite, CS-2 Sec12 T12S R8W, Lincoln County, KS	--	Very Good
KS # 2	Bingham S & G, Sec 22 T29N R23E, Ottawa County,	--	Very Good

TABLE A1 (Continued)

Aggregate ID	Description (Supplier / Manufacturer, Location)	Additional Properties	Performance History[1]
KS # 3	Martin Marietta, CS-2A, Greenwood County, KS	--	Fails Lottman AASHTO T283
KS # 4	Kleiwer Loc#2 Sec34 T10S R28W, Sheridan County, KS	--	Stripping Problem
KY # 1	Ken Mor ‘A’, Grassy, Ky	Specific Gravity	Marginal
KY # 2	Vulcan Mat, Ft Knox, Ky	Sp Gr, Absorption	Poor
KY # 3	Vulcan Mat, Lake City, KY	Specific Gravity	Good
KY # 4	Kentucky Stone, Canton, KY	Sp Gr, Gradation	Good
MD # 1	Redland / Genstar Texas, Calcitic Marble	Sp Gr, Abs, LA Wear, ASR, Unit Wt	Well (used in low vol. Traffic road)
MD # 2	Arundel Corp., Havre De Grace, MD, Greenstone	Same	Well (used in high vol. traffic road)
MD # 3	Redland/Genstar, Churchville, MD, Layered Gneiss	Same	Well (used in high vol. traffic road)
MD # 4	Rockville Crushed Stone, Travilah, MD	Same	Poor (Used in low vol. rural roads)
MO # 1	St. Louis Limestone, Fred Weber # 1, Maryland Hts, MO	Gradation, Specific Gravity, LA loss	Good
MO # 2	Ceder Valley Limestone, Capital Quarries # 1A, Holts Summit, MO	Same	Good
MO # 3	Gasconade Dolomite, Lake Quarry # 1, Linn Creek, MO	Same	Poor, significant breakage in plant
MO # 4	Burlington Limestone, Hilty Quarries # 1, Tightwad, MO	Same	Poor
MN # 1	BA97-0399	Absorption, Specific Gravity, Gradation	–

TABLE A1 (Continued)

Aggregate ID	Description (Supplier / Manufacturer, Location)	Additional Properties	Performance History[1]
MN # 2	BA 97-0434, Ramsey, MN	Absorption, Specific Gravity, Gradation	--
MN # 3	BA97-0441, Sherburne, MN	Same	--
MN # 4	CA97-0450, Anoka	Same	--
MS # 1	Memphis S&G, Batesville, MS	--	--
MS # 2	American Sand & Gravel, MS	--	--
MS # 3	R & S Haulers, MS	--	--
MS # 4	Blain Sand & Gravel, MS	--	--
MT # 1	North Part of State, Project STPS 213-1(6)0, 746492	FAA, Specific Gravity	--
MT # 2	East Part of State, Hillside, RTF 18-3(13) 43, 745396	Same	--
MT # 3	Middle of Sate, Project 90-8(138)298, 746141	Same	--
MT # 4	Middle of State, Bighorn Project BR 9002(11), 746139	Same	--
NC # 1	Ft Williams Pit, Pageland, SC	FAA, Sand Eqv, Sp Gr	Good
NC # 2	Piedmont Sand, Pageland, SC	Same	Good
NC # 3	Rambeaut Pit, Sanford, NC	Same	Poor
NC # 4	Angus Pit, Elizabeth City, NC	Same	Poor
ND # 1	Mandon, ND	Gradation	Good
ND # 2	Minnesota	Gradation	Good
ND # 3	10 miles south of I-94 on Hwy 8 & 4 miles west, ND	Gradation	Poor
ND # 4	Benson City, ND	Gradation	Poor

TABLE A1 (Continued)

Aggregate ID	Description (Supplier / Manufacturer, Location)	Additional Properties	Performance History[1]
NE # 1	Quartizite Manufactured Sand, LG Everist, Soux Falls, SD	FAA	Very Good
NE # 2	Mfg Limestone, Martin Marietta, Weeping Water, NE	FAA	Very Good
NE # 3	Biba Co, SW 1/4, Sec 33, Township 29N, Range 54W, NE	Gradation, Specific Gravity, LA Loss, Absorption	Very Poor
NE # 4	Central Sand & Gravel, Ashland, NE	Specific Gravity, Absorption	--
NM # 1	Shakespeare Pit, NM	--	Good
NM # 2	Contractor's Pit, NM	--	Good
NM # 3	Price Pit, NM	--	Poor
NM # 4	San Antonio, NM	--	Poor
SC # 1	Lyman regular screenings, crushed granite	LA loss	Poor
SC # 2	Marlboro sand, very clean quartzite	--	Good for lower vol. traffic
SC # 3	Lanier sand, high clay content	--	Poor
SC # 4	Cayce regular screenings, crushed granite	LA loss	Good
TN # 1	Burns Stone, Dickson, TN	Gradation, FAA	Excellent
TN # 2	American Limestone, Springfield, TN	Same	Excellent
TN # 3	Vulcan Mat, Harmitage, TN	Same	Poor
TN # 4	Vulcan Mat, River Road, TN	Same	Poor

TABLE A1 (Continued)

Aggregate ID	Description (Supplier / Manufacturer, Location)	Additional Properties	Performance History[1]
WY # 1	Pete Lien & Son Quarry, WY	Gradation, Absorption, Specific Gravity, FAA	--
WY # 2	Dry Creek Pit, WY	Same	--
WY # 3	North Rawlings Quarry & Pass Creek Filler, WY	Same	--
WY # 4	Mummy Pit, WY	Same	--
GA # 5[2]	Crushed granite, Forsyth Quarry, Ga	Gradation, Sp. Gravity, Sand Eq.	Excellent
TX # 1[2]	Crushed Limestone, Vulcan Mat, Brownwood, TX	Same	Excellent
TX # 2[2]	Crushed River Gravel, Fordyce, McAllen, TX	Same	Good

1 Performance histories are subjective evaluations supplied by the state DOT person who supplied the aggregate.

2 These three aggregates were subsequently used for restricted zone analysis.

- - Information not available.

APPENDIX B

TYPICAL TEST OUTPUT

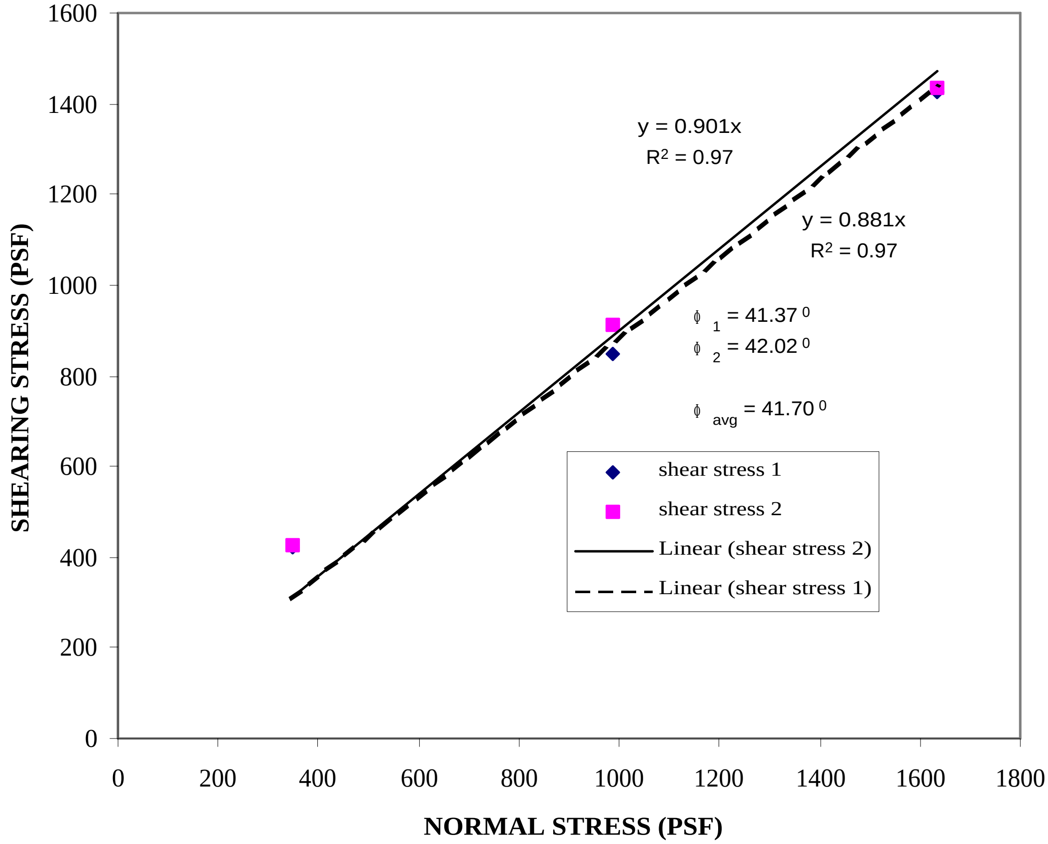

FIGURE B1 A Typical Shearing Stress versus Normal Stress Chart for Angle of Internal Friction Calculation

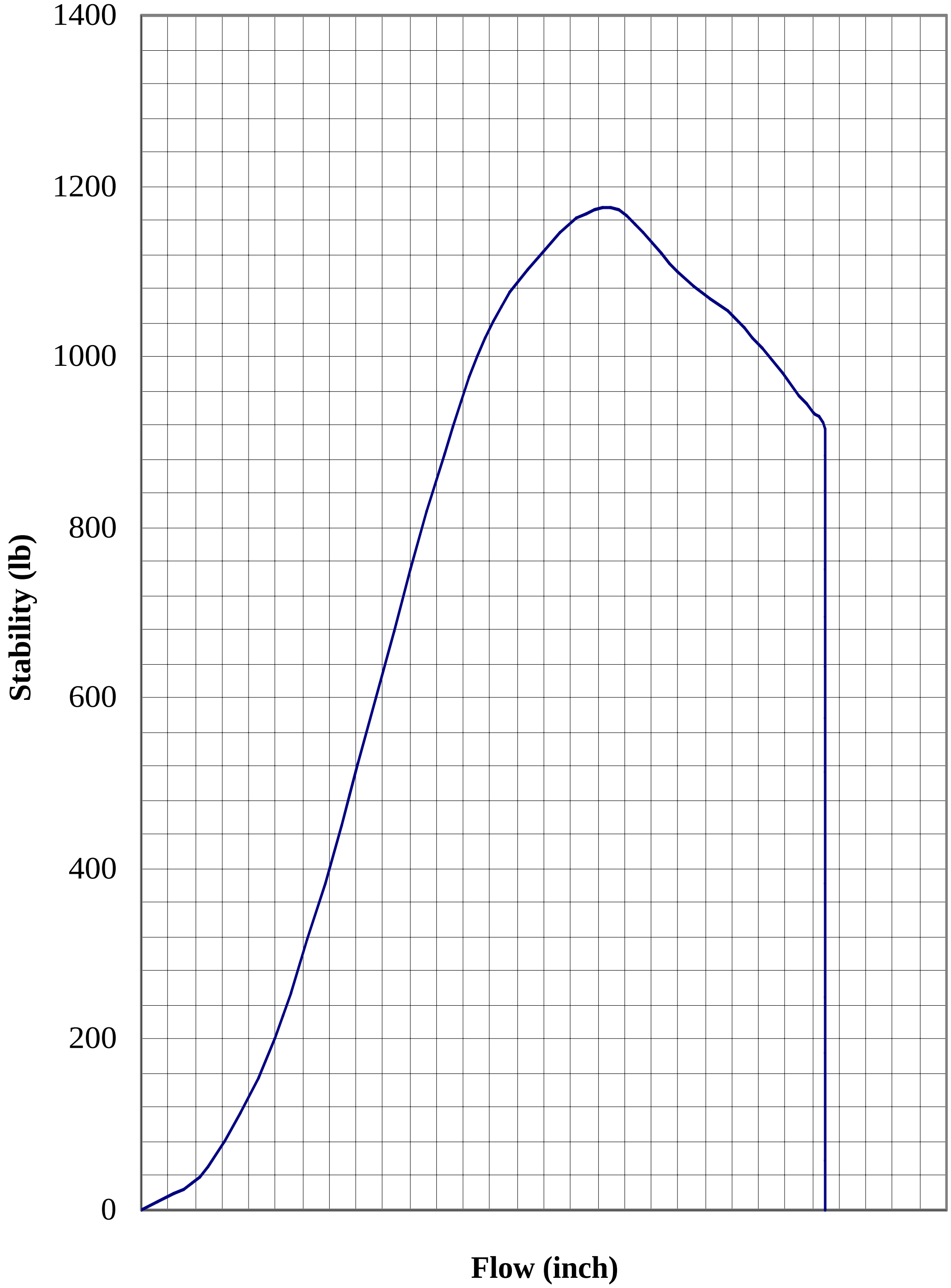

FIGURE B2 A Typical CAR Test Output

TABLE B1 A Typical Hough Transform Output for K-index Calculation

Particle#	Perim Pix	E Index	R Index	T Index	S Index	FFT2	FFT3	FFT4	FFT5	FFT6	FFT7
1	204	0.5979	0.4844	0.0378	0.6878	0.1032	0.1975	0.1541	0.1697	0.0695	0.1315
2	438	0.7497	0.6016	0.1954	0.5294	0.0944	0.1648	0.0919	0.0515	0.0393	0.0455
3	222	0.5976	0.4688	0.0362	0.6646	0.0994	0.1714	0.1213	0.1489	0.0569	0.1252
4	427	0.7407	0.6094	0.1973	0.5058	0.0963	0.1485	0.0899	0.0610	0.0439	0.0342
5	306	0.5034	0.4375	0.0653	0.5988	0.2054	0.0421	0.0956	0.1144	0.0449	0.1095
6	210	0.7454	0.6172	0.0507	0.4226	0.1018	0.1427	0.0457	0.0718	0.0456	0.0142
7	235	0.7931	0.5938	0.0462	0.6390	0.0545	0.1655	0.0261	0.0994	0.1115	0.1209
8	248	0.6300	0.5469	0.0407	0.6907	0.1528	0.1120	0.2209	0.1592	0.1766	0.0829
9	202	0.7643	0.5234	0.0703	0.5315	0.0760	0.1219	0.0171	0.1321	0.0333	0.0449
10	410	0.7592	0.5469	0.0792	0.6604	0.1335	0.2855	0.0730	0.0898	0.0516	0.1362
11	399	0.7463	0.5313	0.0864	0.6535	0.1209	0.2941	0.0860	0.0962	0.0475	0.1405
12	286	0.6718	0.5156	0.0894	0.5527	0.0369	0.1288	0.0939	0.0628	0.1058	0.0577
13	439	0.4730	0.2813	0.1029	0.6386	0.1812	0.2189	0.1286	0.1210	0.1026	0.0406
14	249	0.5742	0.6094	0.0716	0.4862	0.1678	0.0918	0.0654	0.0964	0.0376	0.0368
15	239	0.9034	0.7578	0.0435	0.5698	0.0871	0.0091	0.1814	0.0963	0.1094	0.0596
16	433	0.7672	0.3438	0.2250	0.4687	0.0766	0.1248	0.1463	0.0630	0.0457	0.0436
17	241	0.7124	0.6953	0.0398	0.5639	0.1679	0.1718	0.1196	0.0421	0.1065	0.0980
18	533	0.5420	0.4375	0.1184	0.5242	0.1182	0.1352	0.0843	0.0155	0.0413	0.1014
19	302	0.4897	0.4609	0.0449	0.7030	0.1861	0.1524	0.1429	0.1143	0.0928	0.0790
20	206	0.7286	0.6563	0.0373	0.4745	0.1267	0.0591	0.0739	0.0742	0.0946	0.0689
21	208	0.6159	0.3672	0.1056	0.6810	0.1679	0.2135	0.0721	0.2661	0.0189	0.0818
22	237	0.5853	0.5000	0.0701	0.5625	0.1564	0.1011	0.0679	0.0862	0.0423	0.0821
23	215	0.6224	0.3750	0.1118	0.6656	0.1508	0.1955	0.0740	0.2736	0.0194	0.0709
24	206	0.5468	0.5078	0.0580	0.5990	0.1971	0.0503	0.0657	0.1650	0.0616	0.0291
25	437	0.6351	0.4297	0.0893	0.6713	0.1337	0.2280	0.1942	0.0867	0.0603	0.1320
26	437	0.6480	0.1172	0.2579	0.5874	0.0873	0.1169	0.1402	0.0488	0.0402	0.0522
27	559	0.5718	0.2109	0.1825	0.5302	0.0565	0.0338	0.1810	0.0569	0.1182	0.0438
28	265	0.6620	0.4453	0.0752	0.6432	0.0837	0.2895	0.0957	0.1330	0.0742	0.1096
29	941	0.5369	0.3516	0.2275	0.3890	0.0783	0.0924	0.0268	0.0370	0.0481	0.0212
30	342	0.6187	0.0781	0.2733	0.4564	0.1709	0.0565	0.0971	0.0262	0.0427	0.1063
31	212	0.5415	0.4922	0.0506	0.5777	0.1876	0.0577	0.0642	0.1568	0.0620	0.0127
32	218	0.7572	0.6484	0.0417	0.4984	0.1186	0.0527	0.0582	0.0777	0.0773	0.0395
33	300	0.5765	0.5469	0.0445	0.5626	0.2296	0.2505	0.0420	0.1215	0.0918	0.0915
34	283	0.5742	0.5547	0.0401	0.5757	0.2237	0.2659	0.0196	0.1318	0.1020	0.0741
35	314	0.9347	0.8594	0.0466	0.4885	0.0346	0.0369	0.1126	0.0895	0.0183	0.1203
36	240	0.7128	0.6953	0.0356	0.5928	0.1770	0.1790	0.1276	0.0346	0.1110	0.0927
37	418	0.7690	0.3125	0.2298	0.5301	0.0716	0.1303	0.1587	0.0667	0.0618	0.0522
38	472	0.3336	0.2422	0.0677	0.6827	0.3105	0.0745	0.2809	0.0405	0.1092	0.0353
39	252	0.5796	0.6328	0.0702	0.4859	0.1492	0.0710	0.0704	0.1168	0.0446	0.0158
40	293	0.7996	0.7656	0.0393	0.4986	0.0463	0.0695	0.0830	0.0348	0.0902	0.0644
41	329	0.7360	0.5781	0.0421	0.5300	0.1051	0.2426	0.0872	0.0353	0.0065	0.0347
42	296	0.6659	0.5000	0.0902	0.5466	0.0388	0.1338	0.0758	0.0451	0.1090	0.0525
43	216	0.8669	0.6328	0.0478	0.5975	0.0134	0.1919	0.0800	0.1283	0.0454	0.0605
44	209	0.6088	0.5469	0.0672	0.5114	0.1569	0.0942	0.0828	0.0652	0.0844	0.0132
45	227	0.7801	0.6016	0.0353	0.6720	0.0641	0.1650	0.0133	0.1094	0.1482	0.1429
46	298	0.7128	0.5469	0.0809	0.6262	0.1537	0.3097	0.0936	0.0913	0.0954	0.0947
47	332	0.7388	0.6328	0.0887	0.6953	0.0816	0.3120	0.0727	0.1706	0.0573	0.0582
48	360	0.4244	0.3828	0.0548	0.6557	0.2754	0.0609	0.1574	0.0155	0.0475	0.0827
49	330	0.7486	0.6406	0.0906	0.6747	0.0762	0.3064	0.0674	0.1669	0.0415	0.0359
50	354	0.4202	0.3672	0.0488	0.6625	0.2832	0.0772	0.1490	0.0235	0.0653	0.0715

TABLE B1 (Continued)

Particle#	FFT8	FFT9	FFT10	FFT11	FFT12	FFT13	FFT14	FFT15	FFT16	K-index
1	0.0663	0.1090	0.0634	0.1223	0.0203	0.0545	0.0341	0.0547	0.0645	0.64
2	0.0518	0.0438	0.0524	0.0235	0.0165	0.0303	0.0288	0.0170	0.0159	1.00
3	0.0530	0.0923	0.0452	0.1166	0.0187	0.0591	0.0521	0.0594	0.0696	0.58
4	0.0537	0.0436	0.0518	0.0096	0.0276	0.0423	0.0211	0.0108	0.0153	1.00
5	0.0899	0.0479	0.0141	0.0474	0.0301	0.0303	0.0391	0.0262	0.0133	0.60
6	0.0246	0.0667	0.0153	0.0570	0.0278	0.0206	0.0050	0.0144	0.0110	0.51
7	0.1236	0.0614	0.0212	0.0543	0.0103	0.0309	0.0734	0.0406	0.0333	0.70
8	0.0686	0.1317	0.0804	0.0618	0.0839	0.0535	0.0440	0.0802	0.0135	0.69
9	0.1389	0.0283	0.0121	0.0082	0.0735	0.0354	0.0306	0.0180	0.0180	0.72
10	0.0769	0.0150	0.0753	0.0828	0.0196	0.0305	0.0552	0.0153	0.0705	0.83
11	0.0620	0.0182	0.0607	0.0657	0.0160	0.0401	0.0496	0.0083	0.0648	0.87
12	0.0319	0.0434	0.0179	0.0883	0.0539	0.0354	0.0488	0.0375	0.0274	0.75
13	0.0513	0.0371	0.0262	0.0614	0.0488	0.0532	0.0544	0.0148	0.0742	-1.00
14	0.0903	0.0404	0.0684	0.0118	0.0630	0.0244	0.0325	0.0169	0.0507	0.66
15	0.0545	0.0497	0.0543	0.0286	0.0214	0.0309	0.0195	0.0456	0.0242	0.54
16	0.0234	0.0436	0.0453	0.0398	0.0506	0.0571	0.0234	0.0119	0.0320	1.00
17	0.0396	0.0532	0.0231	0.0764	0.0342	0.0179	0.0155	0.0547	0.0174	0.53
18	0.0224	0.0698	0.0330	0.0180	0.0270	0.0381	0.0150	0.0252	0.0372	0.87
19	0.1592	0.1134	0.0656	0.0948	0.0711	0.0489	0.0384	0.0457	0.0316	0.61
20	0.0309	0.0075	0.0584	0.0199	0.0416	0.0429	0.0249	0.0597	0.0322	0.39
21	0.0462	0.1451	0.0751	0.0384	0.0700	0.0384	0.0900	0.0296	0.0273	0.94
22	0.0277	0.0913	0.0559	0.0352	0.0482	0.0311	0.0391	0.0147	0.0385	0.70
23	0.0323	0.1392	0.0666	0.0237	0.0720	0.0099	0.0910	0.0218	0.0055	0.98
24	0.0527	0.0924	0.0315	0.0666	0.0030	0.0087	0.0484	0.0473	0.0454	0.58
25	0.0624	0.0851	0.0316	0.0776	0.0405	0.0495	0.0537	0.0340	0.0458	0.83
26	0.0602	0.0217	0.0643	0.0331	0.0472	0.0314	0.0362	0.0566	0.0281	-1.00
27	0.0043	0.0195	0.0337	0.0663	0.0386	0.0528	0.0454	0.0275	0.0336	-1.00
28	0.0471	0.0514	0.0317	0.0279	0.0581	0.0364	0.0046	0.0246	0.0566	0.80
29	0.0224	0.0140	0.0145	0.0174	0.0301	0.0197	0.0166	0.0105	0.0280	1.00
30	0.0208	0.0028	0.0357	0.0488	0.0236	0.0583	0.0207	0.0220	0.0166	-1.00
31	0.0438	0.0744	0.0403	0.0622	0.0148	0.0266	0.0474	0.0373	0.0348	0.52
32	0.0358	0.0058	0.0483	0.0550	0.0312	0.0336	0.0138	0.0464	0.0364	0.36
33	0.0428	0.0194	0.0303	0.0300	0.0320	0.0251	0.0451	0.0055	0.0326	0.64
34	0.0295	0.0098	0.0409	0.0304	0.0430	0.0274	0.0581	0.0098	0.0366	0.61
35	0.0767	0.0381	0.0074	0.0530	0.0617	0.0212	0.0411	0.0445	0.0327	0.51
36	0.0559	0.0435	0.0214	0.0654	0.0422	0.0223	0.0154	0.0390	0.0146	0.51
37	0.0081	0.0450	0.0569	0.0504	0.0430	0.0632	0.0499	0.0176	0.0444	1.00
38	0.0939	0.0820	0.0901	0.0515	0.0860	0.0343	0.0661	0.0300	0.0452	-1.00
39	0.1078	0.0477	0.0475	0.0237	0.0285	0.0377	0.0395	0.0190	0.0534	0.65
40	0.1120	0.0619	0.0175	0.0571	0.0532	0.0214	0.0328	0.0230	0.0526	0.43
41	0.0593	0.0475	0.0516	0.0403	0.0585	0.0432	0.0414	0.0207	0.0061	0.54
42	0.0751	0.0450	0.0302	0.0897	0.0363	0.0250	0.0421	0.0195	0.0318	0.76
43	0.0734	0.0266	0.0335	0.0257	0.0494	0.0481	0.0352	0.0255	0.0380	0.64
44	0.0854	0.0289	0.0270	0.0578	0.0389	0.0522	0.0248	0.0377	0.0282	0.57
45	0.1250	0.0763	0.0420	0.0689	0.0256	0.0351	0.0597	0.0294	0.0387	0.67
46	0.0892	0.0235	0.0196	0.0879	0.0129	0.0232	0.0661	0.0294	0.0244	0.83
47	0.1335	0.0785	0.0168	0.0751	0.0580	0.0116	0.0219	0.0435	0.0587	0.85
48	0.0889	0.0723	0.0446	0.0805	0.0374	0.0549	0.0168	0.0691	0.0118	0.45
49	0.1500	0.0653	0.0179	0.0758	0.0591	0.0088	0.0358	0.0340	0.0477	0.86
50	0.0715	0.0712	0.0371	0.0837	0.0248	0.0719	0.0159	0.0706	0.0229	0.41

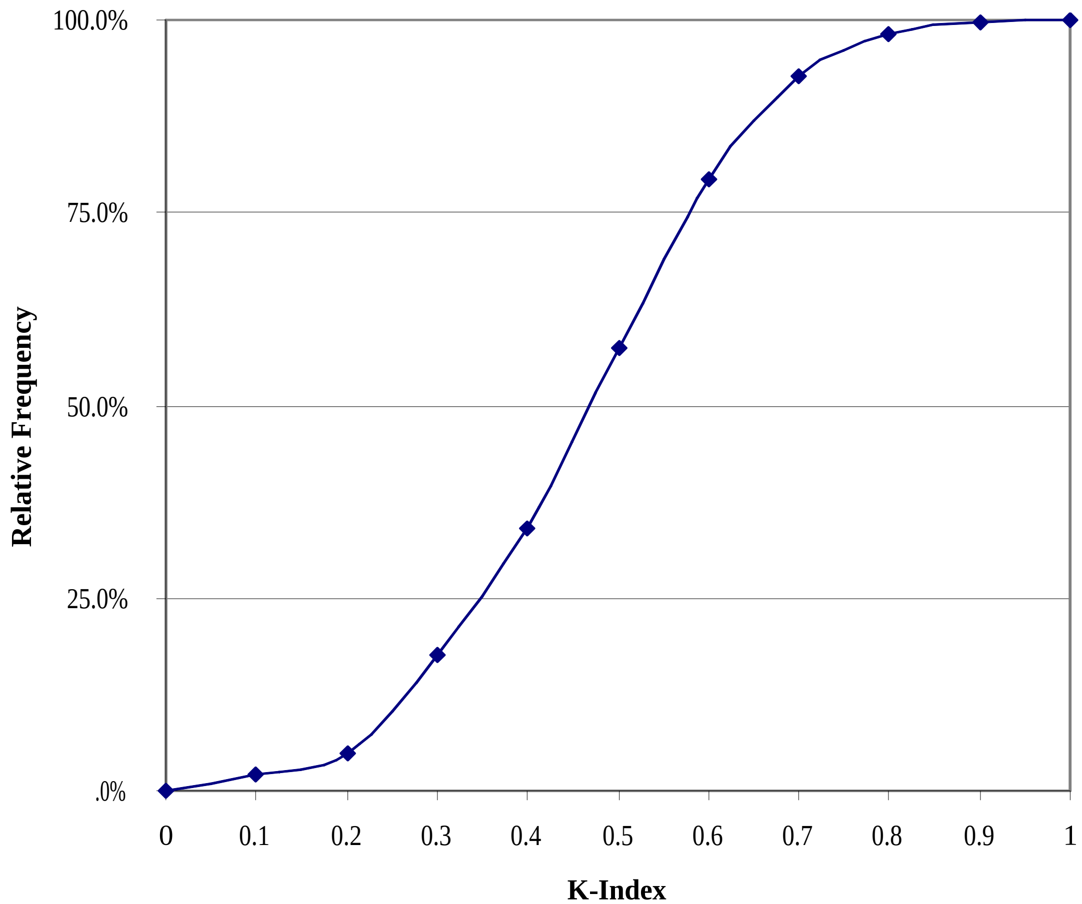

FIGURE B3 A Typical Chart for Calculating Median of K-indices

Flat & Elongated Worksheet

Reference : CONNETICUT #1	Quality :
Site : TTI	Spl. date :
Origin :	Cleanness: 0
Name :	Sample n°: 1
Test date : 06/10/1999 11:19	

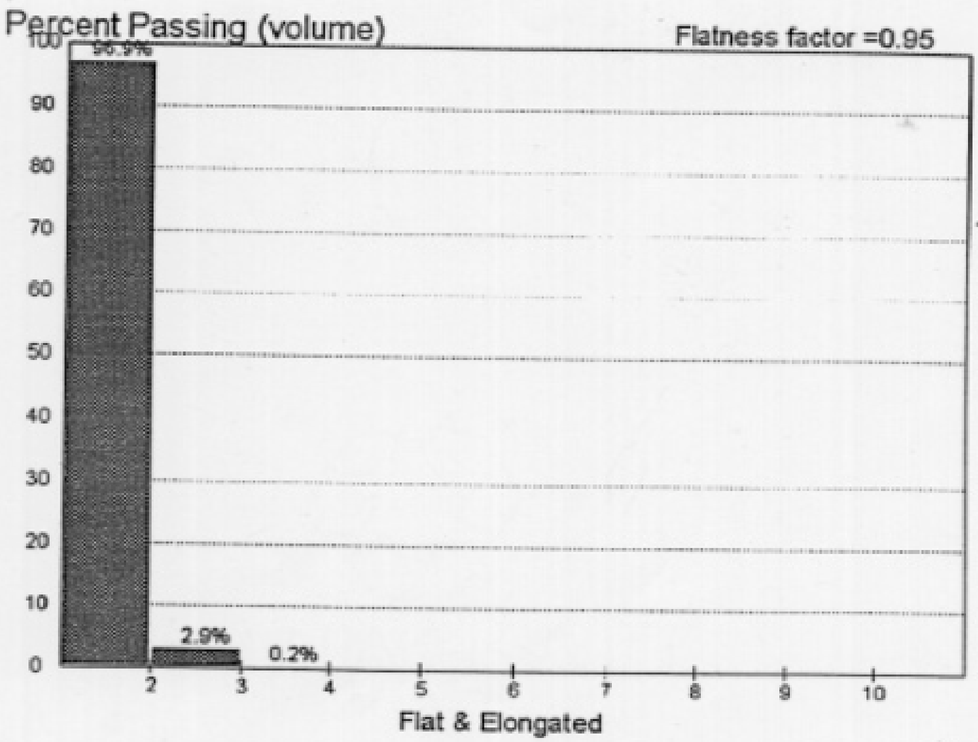

Operator's observations

C:\VDG\TRAVAIL\TTISAM~1\CONNETIC#1A.VDG VDG v4.02b
Operator :Brad

FIGURE B4 A Typical Output: VDG-40 Flat & Elongated Worksheet

Coarse Aggregate Gradation Worksheet

Reference : CONNETICUT #1	Quality :
Source : TTI	Spl. date :
Mine :	Cleanness : 0
Product :	Sample n°: 1
Test date : 06/10/1999 11:19	

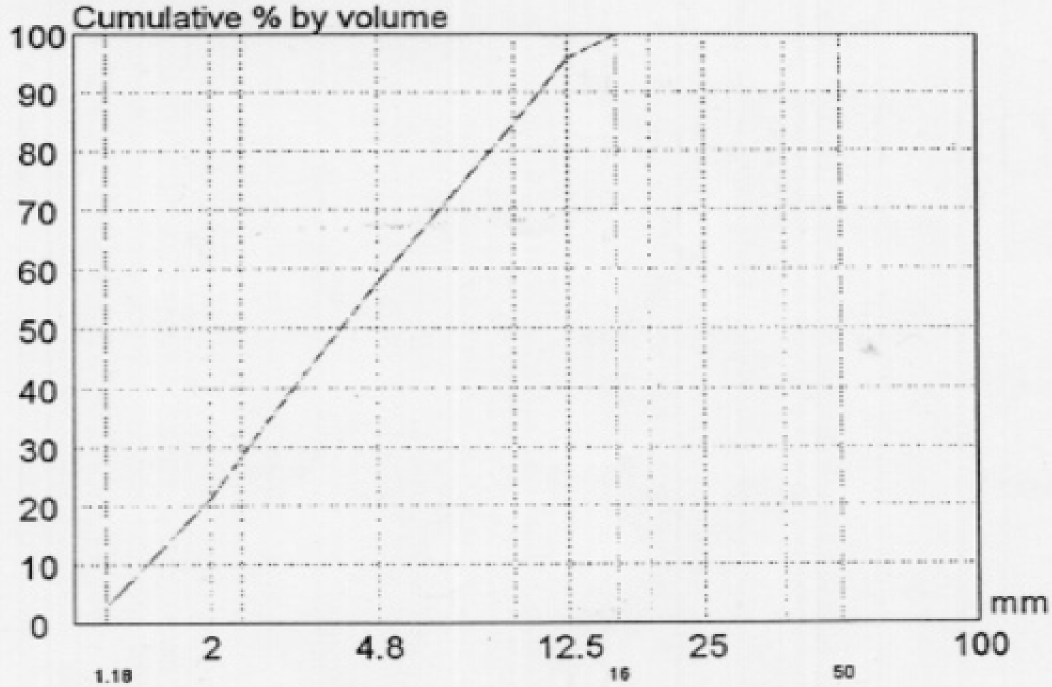

Tabulated results by size fraction

Size	% Volume	Slend-R.	Number	Size	% Volume	Slend-R.	Number
< 1.18	2.79	1.57	3681	16.00	100.00	1.23	3
2.00	21.14	1.42	9066	19.00	100.00	0.00	0
2.36	28.33	1.34	1216	25.00	100.00	0.00	0
4.75	57.86	1.31	1618	37.50	100.00	0.00	0
9.50	84.49	1.26	176	50.00	100.00	0.00	0
12.50	95.83	1.25	18	100.00	100.00	0.00	0
Sample weight	:		298.5 g	Mean slenderness ratio		:	1.44
Cubic mass	:		2.665 kg/dm³	Flatness factor		:	0.95

Operator's observations

C:\VDG\TRAVAIL\TTISAM~1\CONNETIC\#1A.VDG VDG v4.02b

Operator :Brad

FIGURE B5 A Typical Output: VDG-40 Aggregate Gradation Worksheet

APPENDIX C

CAR TEST PROCEDURE AND SUPPLEMENTAL CAR TEST RESULTS

Compacted Aggregate Resistance (CAR) Test

The Compacted Aggregate Resistance test is a test for evaluating the shear resistance of compacted fine aggregate materials in their “as-received” condition.

The CAR procedure is intended for use on the combined fine aggregate materials to be used in HMA paving mixtures. The performance of individual fine aggregate components can be estimated provided engineering judgement is used. For example, a high fines component will likely give a high stability value but could not represent 100 percent of the fine aggregate material in the mixture.

Equipment

The simple and inexpensive equipment includes a Marshall mold with base plate attached (welded or secured in a permanent manner), Marshall mold collar, Marshall compaction hammer, mixing bowl & utensils, riffle splitter, screen shaker, 2.36-mm (# 8) sieve, drying oven, balance (at least 8,000 gm capacity with accuracy of 0.1 gm), Marshall flow machine with graph recorder, 38-mm diameter by 38-mm high steel cylinder with smooth, flat face.

Procedure

Secure a representative 5,000 to 6,000-gm sample by riffle splitting. Splitting should be performed at or just below the saturated surface dry condition to prevent loss of fines. Then, sieve this portion over a 2.36-mm sieve. Oven dry the material finer than the 2.36-mm sieve to a constant weight at 110 ± 5 °C. Remove form oven and cool the material to ambient temperature. Weigh the material to the nearest 0.1 gm.

Add 1.75 percent water by dry weight of the sample and mix thoroughly. Reduce material by riffle splitting or quartering to approximately 1,100 gm as quickly as possible to minimize moisture loss. Record the weight. The remaining prepared material may be used within one hour if kept in a sealed container. Secondary absorption after a period of time may require that the drying procedure be repeated.

Cover the Marshall compaction hammer striking face with cellophane or aluminum foil. This cover will prevent particles from adhering to the striking face surface and produce a smooth bearing surface on the compacted specimen.

Place material in 100-mm Marshall mold meeting the requirements of ASTM D 1559. Spade the material with a spatula 15 times around the perimeter and 10 times over the interior of the mold. Remove the collar and smooth the surface with the spatula to a slightly rounded shape.

Replace the collar and place mold assembly with specimen in the compaction pedestal. Compact specimen with 50 blows from the Marshall hammer. Unlike the Marshall method of compacting bituminous mixture, only one surface of the specimen is compacted. After compaction is completed, carefully remove mold assembly from compaction pedestal. Remove collar and measure distance from top of the mold to top of the specimen. Calculate specimen height. The specimen should be 63.5 ± 3.18 mm in height. If the specimen does not meet the height requirement, discard the specimen and compact again with less or more loose aggregate.

Place compacted sample, with base plate and mold still in the upright, vertical position (compacted face up) along with appropriate spacers (to minimize travel) on the Marshall Stability machine. Place the 38-mm diameter by 38-mm high steel cylinder on the center of the compacted specimen, and align vertically under the load cell. Apply load with the Marshall Stability machine over the flat face of the cylinder at a rate of 50 mm/minute. The stability value at a flow of 25 or highest value achieved prior to a flow of 25 should be reported. The average of three specimens should be reported as the CAR value of a fine aggregate blend. Precision and bias for this test has not yet determined.

Findings from CAR Tests on Selected Materials

The fine aggregates used in the tests discussed below were specially selected to illustrate the sensitivity of the CAR stability test to aggregate particle angularity and gradation. Some of the materials tested are individual fine aggregates. Ideally, the CAR test should be performed on the combined fine aggregates as used in the job mix formula for the HMA paving mixture under consideration.

Figure C1 demonstrates that 100% crushed materials with high angularity and surface texture (crushed limestone) will yield high CAR stability values even though the FAA is borderline at a value 45. Although the granite material is 100% crushed and has high angularity and surface texture, it does not contain as much fine dust as the crushed limestone. This and other testing described in the text of this report indicates that a significant quantity of fine dust (-75 μm) will increase the CAR value. The CAR test shows a much greater difference in shear strength between the two aggregates (natural sand and limestone) with FAA values of 43 and 45 than one may expect from the FAA values alone. There appears to be a break between angular materials and rounded materials at a CAR value in the range of 1500 to 2000.

Figure C2 depicts the sensitivity of the CAR test to varying amounts of rounded natural sand blended with crushed limestone. As the concentration of natural sand increases both FAA and CAR value decrease. However, FAA decreases only three points; whereas, CAR value decreases by almost 1500 pounds.

Figure C3 shows that CAR stability is significantly affected by gradation while FAA (as measured using ASTM C 1252, Method A) is insensitive to the gradation used in the HMA mixture. Aggregate particles from the same source (granite) were tested in the as received gradation from the crushing/screening operations and in a specially prepared gradation simulating that of natural sand. The natural sand, used in this study exhibited a “humped” gradation with a preponderance of material near the 425-μm sieve with little material passing the 75-μm sieve. The CAR test clearly demonstrates significant differences in shear strength as a function of gradation.

Figure C4, again, illustrates sensitivity of the CAR test to gradation. In this case, however, natural sand has been reblended to the gradation that of the granite material shown in Figure C3. The change in gradation of the natural sand notably improves the CAR stability but, of course, has no effect on the FAA (as measured using ASTM C 1252, Method A). This figure, once again, shows that shear resistance is influenced by gradation.

Figure C5 was plotted to demonstrate that fine aggregates with similar values of FAA may exhibit widely different values of shear strength. Note that both the limestone and the 50/50 blend of granite and natural sand yielded FAA values of 44; however, the two materials show vastly different values of CAR stability.

The authors believe that the CAR test is a viable alternative for the FAA test. It is very sensitive, quick and easy to perform, and utilizes inexpensive, often existing equipment. The test appears to be performance-related because the compacted specimen is subjected to a shearing load similar to HMA mixtures in pavements. More work is needed to determine if 1.75% moisture is the appropriate amount for all fine aggregate materials, to determine the significance of the peak and slope of the shear curve, and to develop acceptance criteria for different materials types, combinations, and traffic levels.

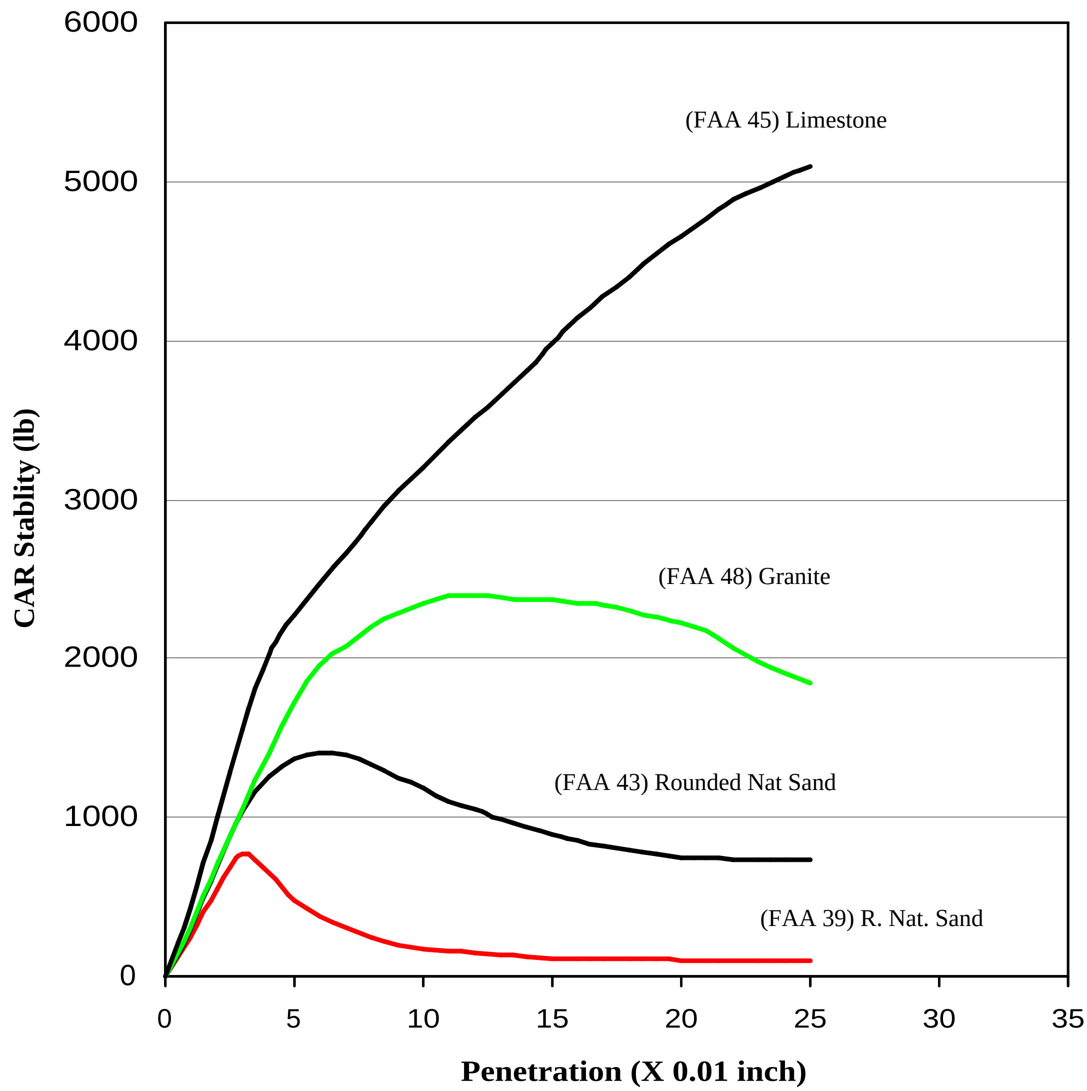

Figure C1 CAR Values of Different Fine Aggregate Materials

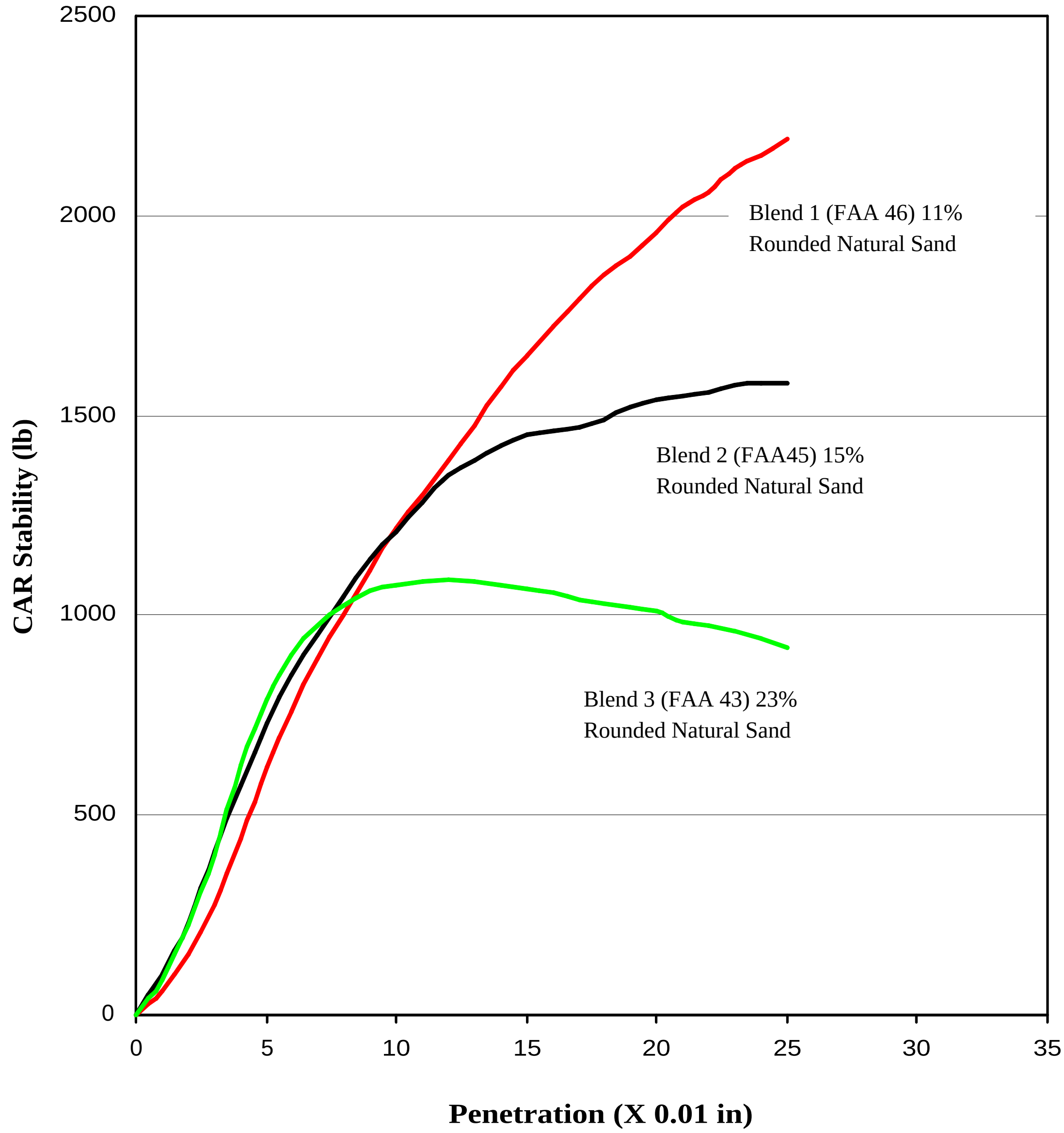

Figure C2 Sensitivity of CAR Stability to Varying Amounts of Natural Round Sand

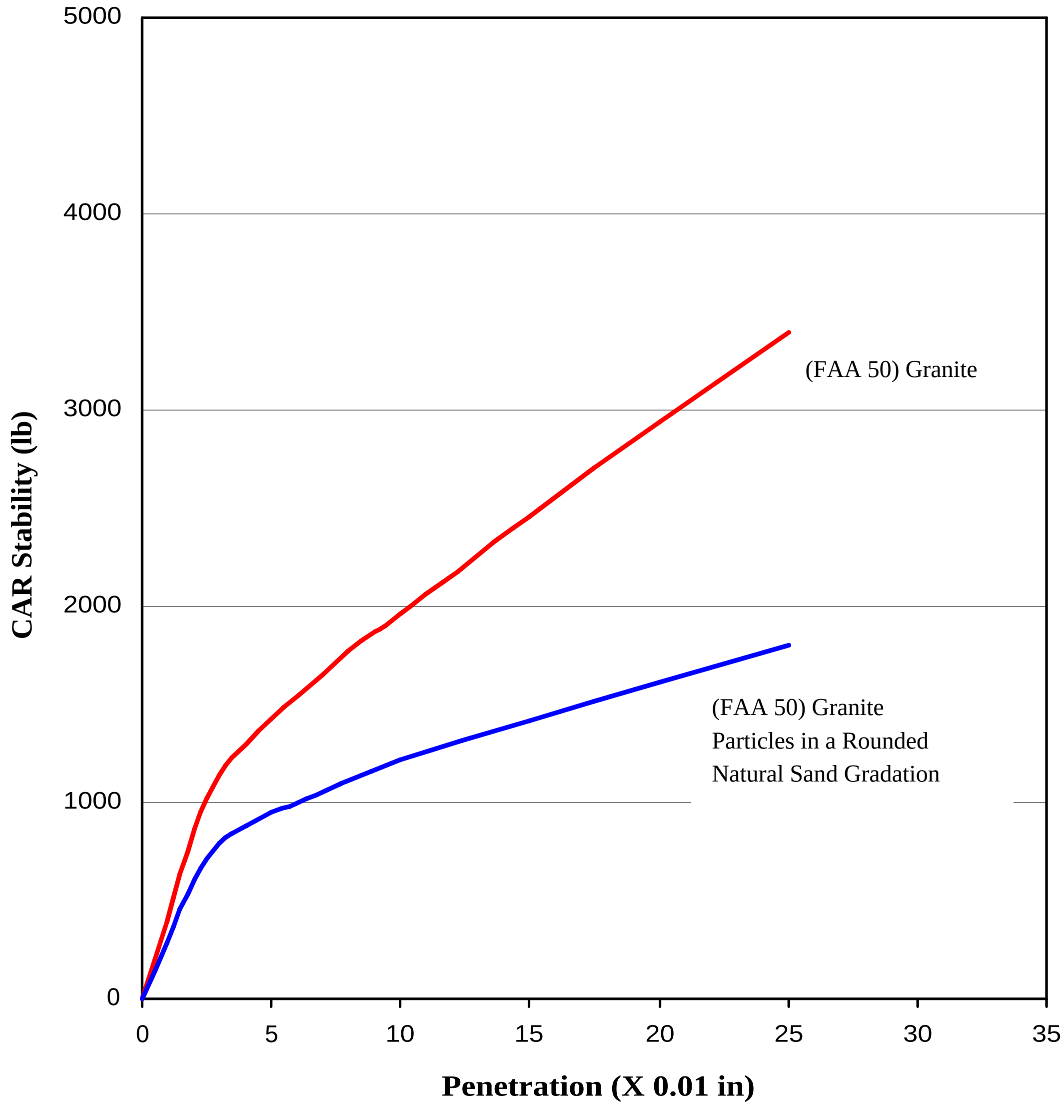

Figure C3 Sensitivity of CAR Stability to Changes in Gradation

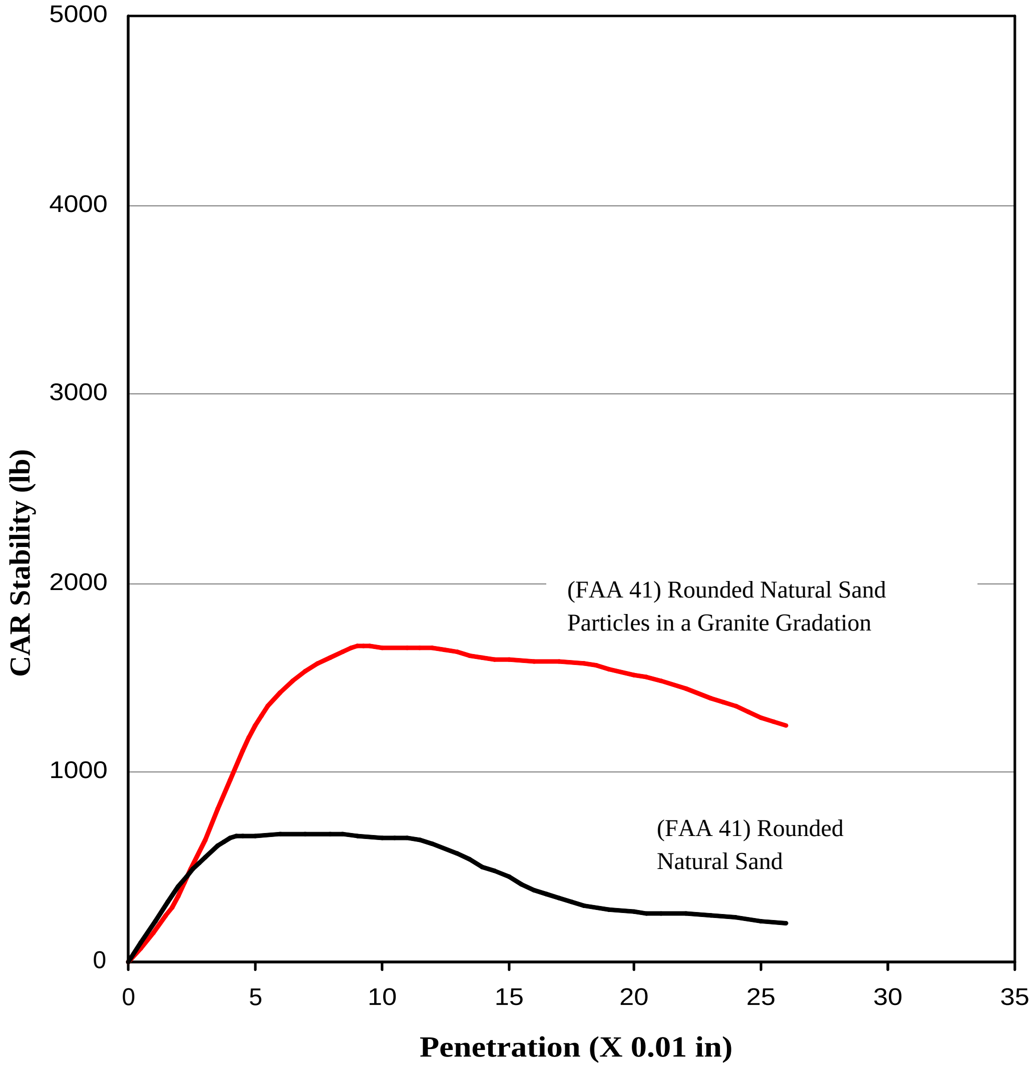

Figure C4 Sensitivity of CAR Stability to Changes in Gradation

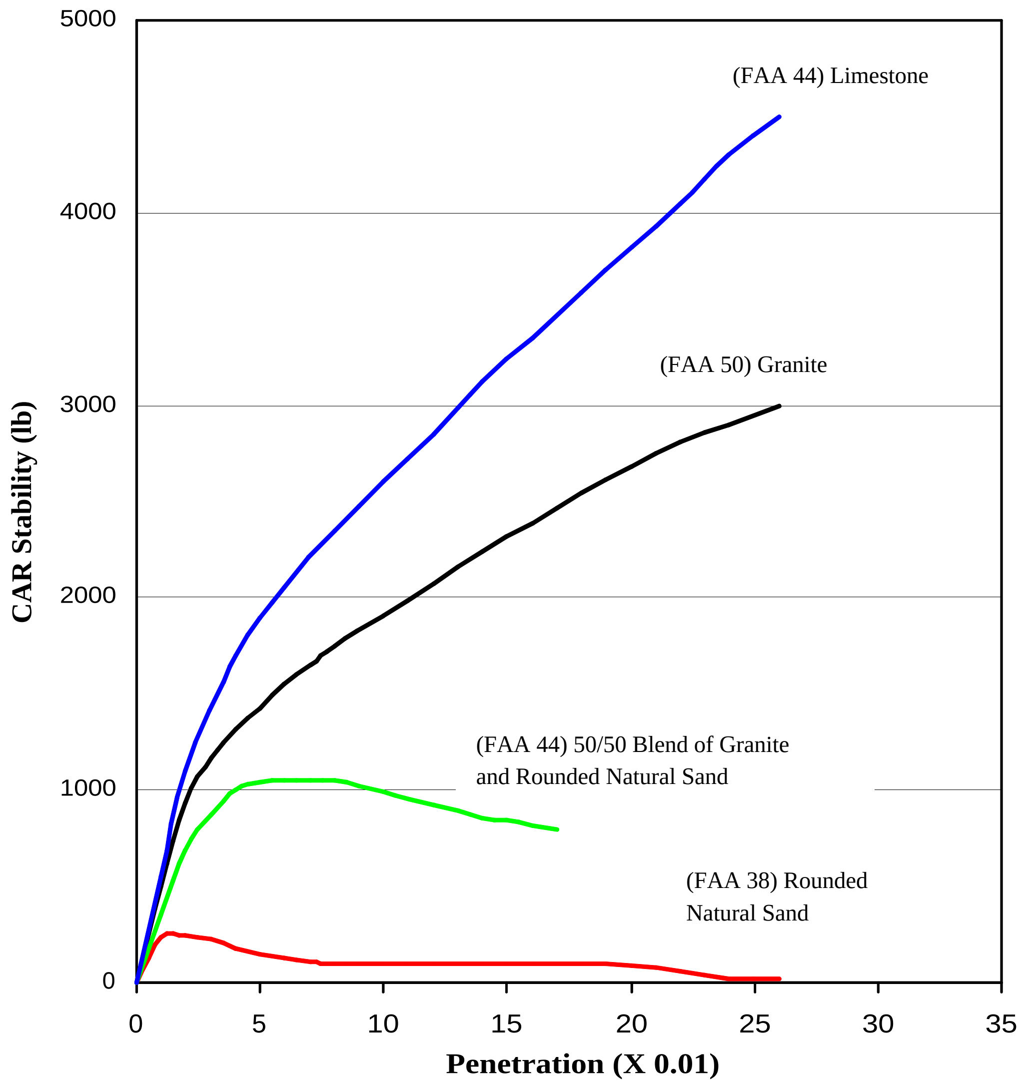

Figure C5 The Car Test Can Differentiate Between like FAA Values